How can the James Webb Space Telescope Measure First Light, Reionization, & Galaxy Assembly?

Rogier Windhorst (Arizona State University)

Collaborators: S. Cohen, R. Jansen, N. Hathi (ASU), C. Conselice & H. Yan (Caltech)

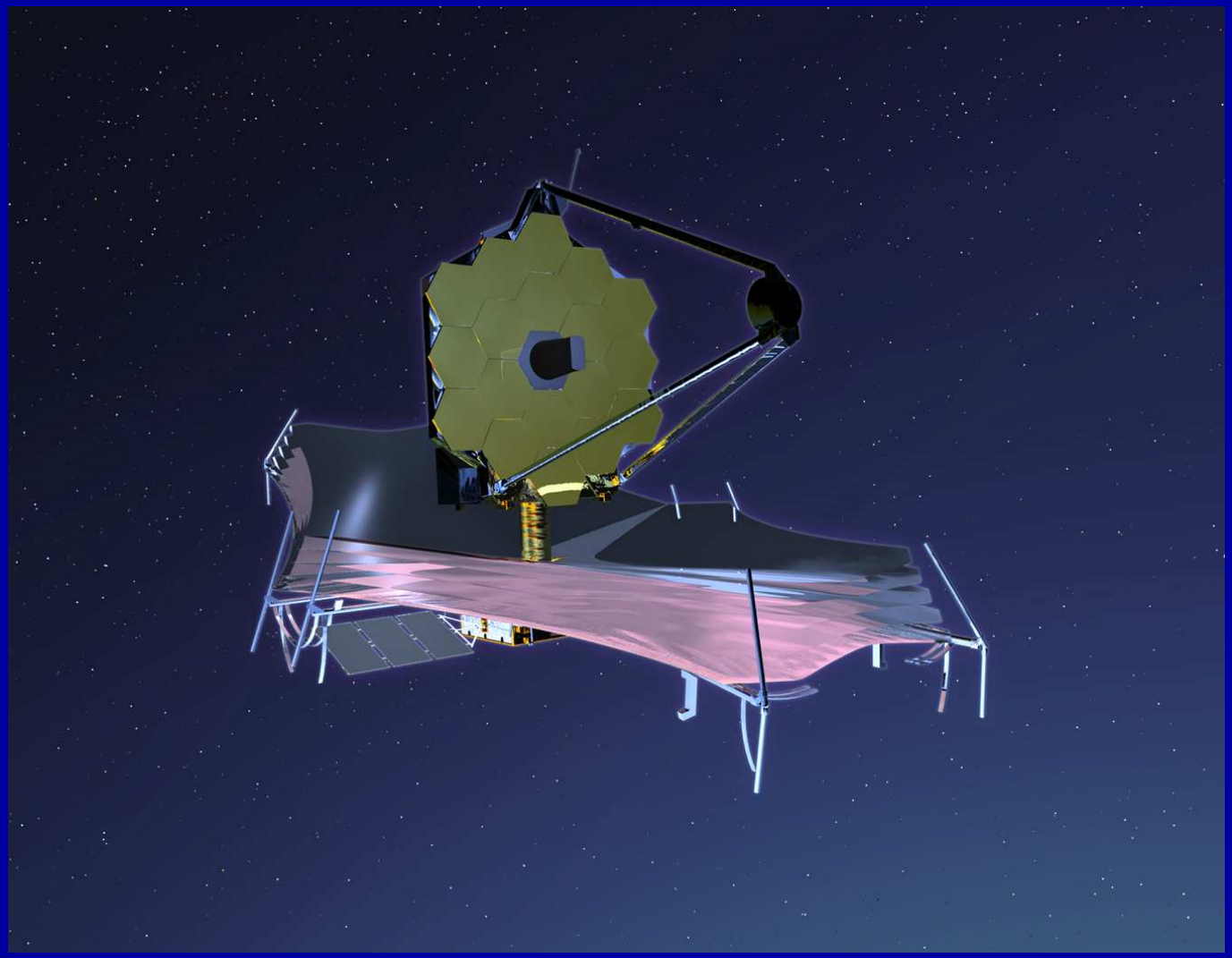

Colloquium at UC Davis, CA, Nov. 16, 2006

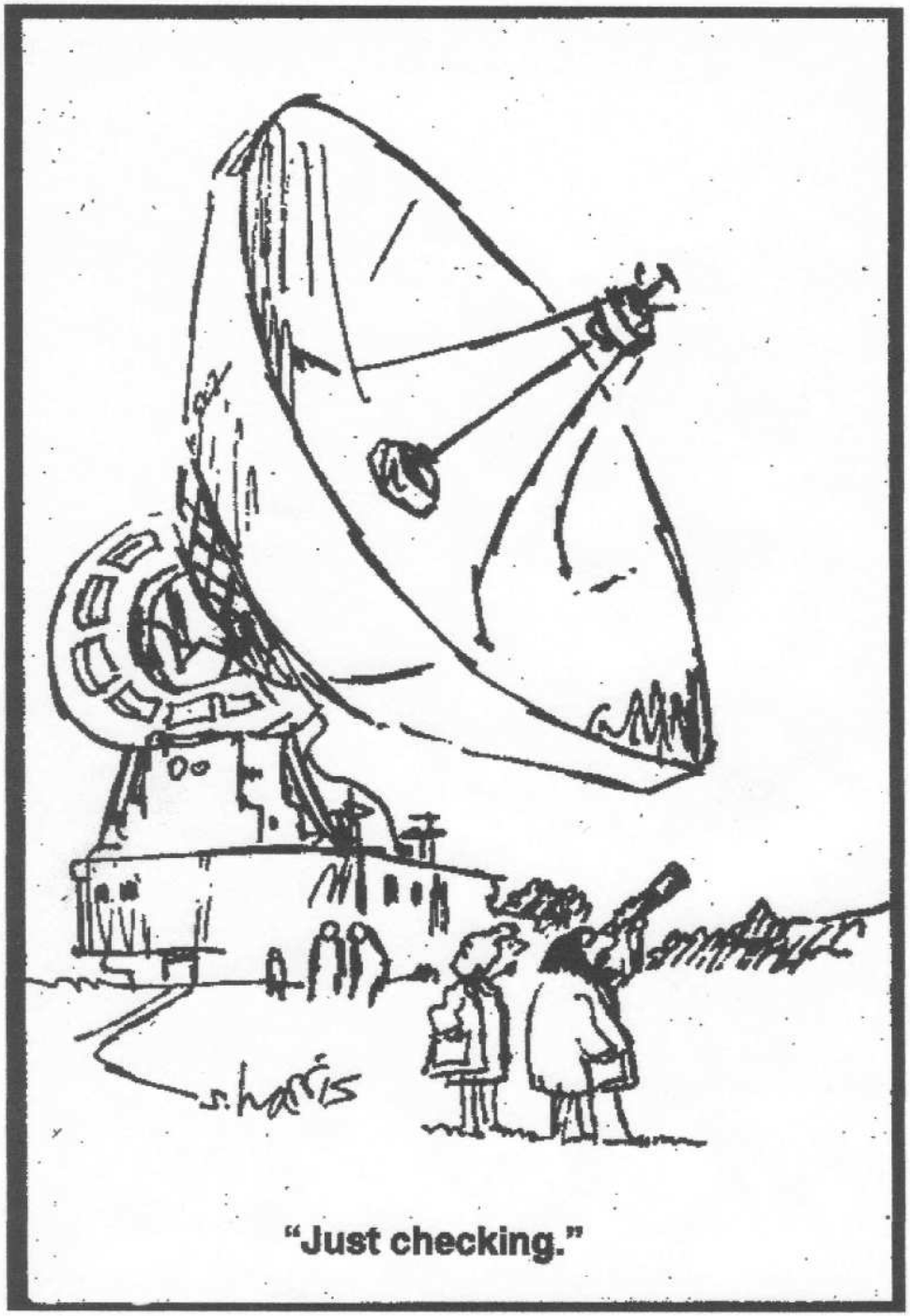

HST and JWST changed the career of this radio astronomer, but ...

Outline

- (1) What is JWST and how will it be deployed?
- (2) What instruments and sensitivity will JWST have?
- (3) How JWST can measure First Light and Reionization
- (4) How JWST can measure Galaxy Assembly
- (5) Predicted Galaxy Appearance for JWST at z$\simeq$1–15
- (6) Summary and Conclusions
- (7) Appendix: will JWST & SKA reach the Natural Confusion Limit?

Sponsored by NASA/JWST

ASU Arizona State University

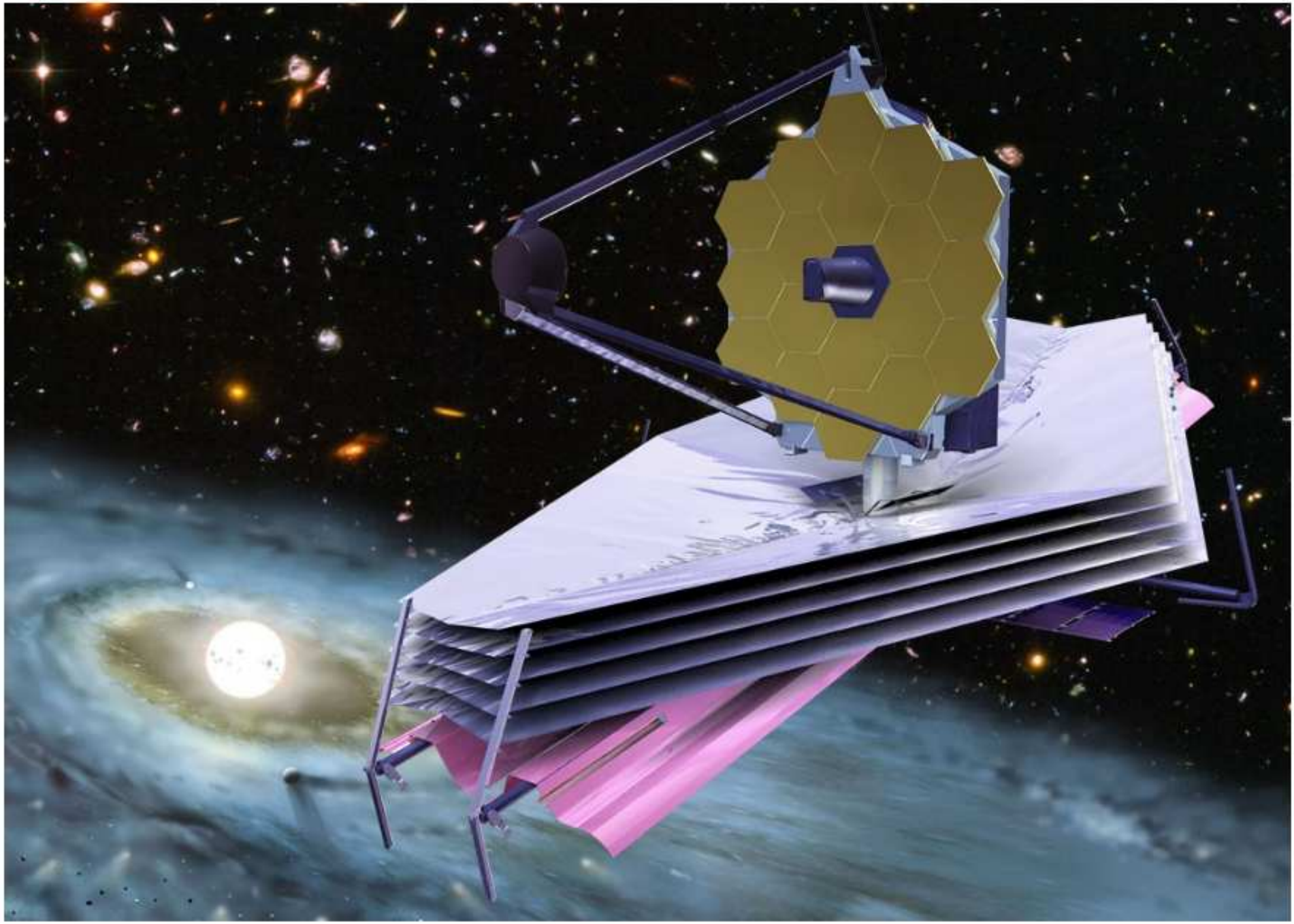

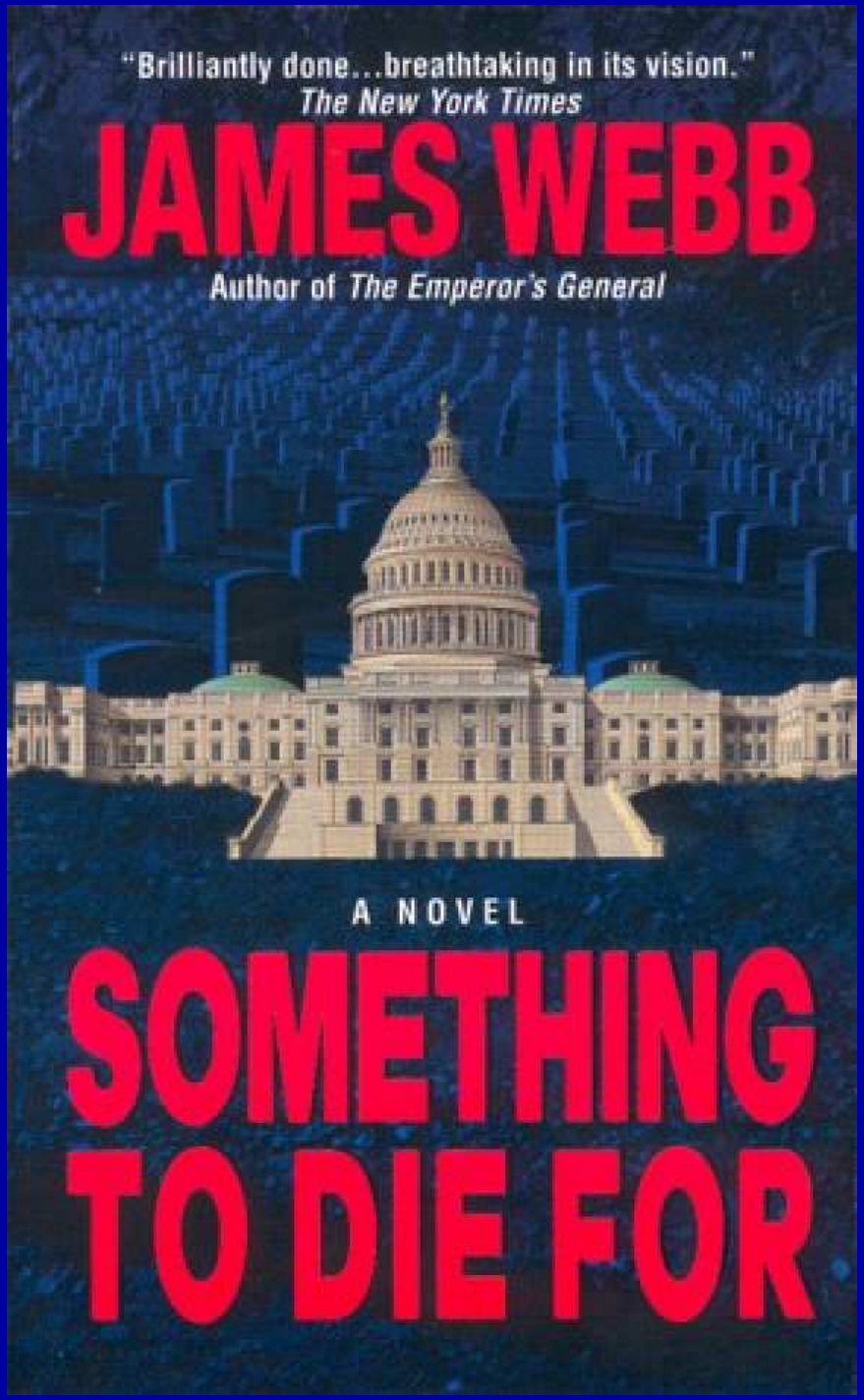

Need hard-working grad students & postdocs in $\gtrsim$2013 ... It'll be worth it!

- (1) What is the James Webb Space Telescope (JWST)?

- A fully deployable 6.5 meter (25 m^2) segmented IR telescope for imaging and spectroscopy from 0.6 to 28 μm, to be launched by NASA $\gtrsim$2013. It has a nested array of sun-shields to keep its ambient temperature at 35-45 K, allowing faint imaging (AB$\lesssim$31.5) and spectroscopy (AB$\lesssim$29 mag).

Life size model of JWST: on display at the Jan. 2007 AAS mtg in Seattle.

Life-sized model of JWST, used to test the deployment of its sun-shield.

Life-sized model of JWST, at NASA/GSFC Friday afternoon after 5 pm ...

- (1) How will JWST travel to its L2 orbit?

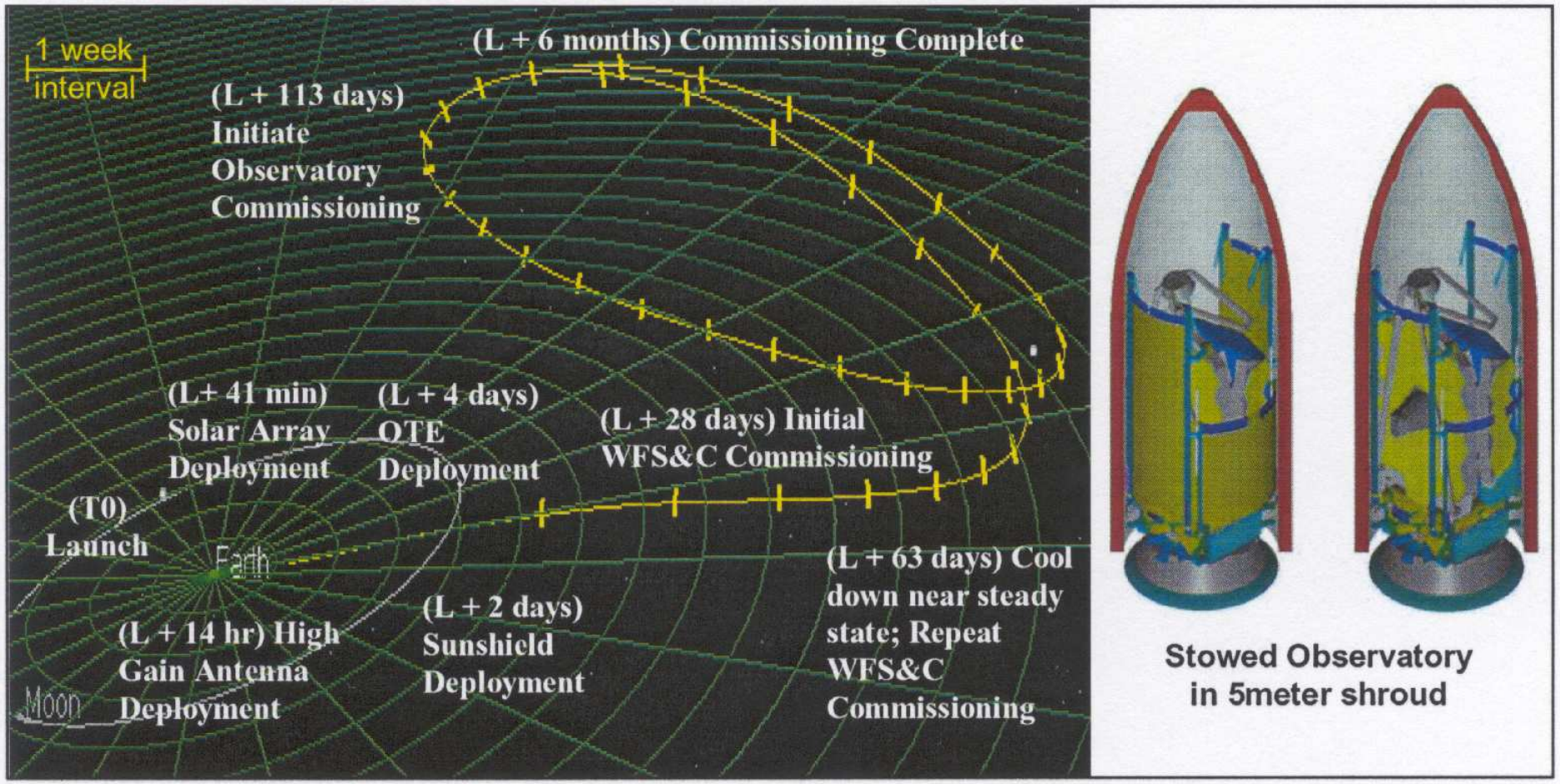

Figure 52. JWST orbit and trajectory to L2, and stowed view in 5 meter shroud.

After launch in $\gtrsim$2013 with an Ariane V vehicle, JWST will orbit around the the Earth–Sun Lagrange point L2. From there, JWST can cover the whole sky in segments that move along in RA with the Earth, have an observing efficiency $\gtrsim$70%, and send data back to Earth every day.

- (1) How will the JWST be automatically deployed?

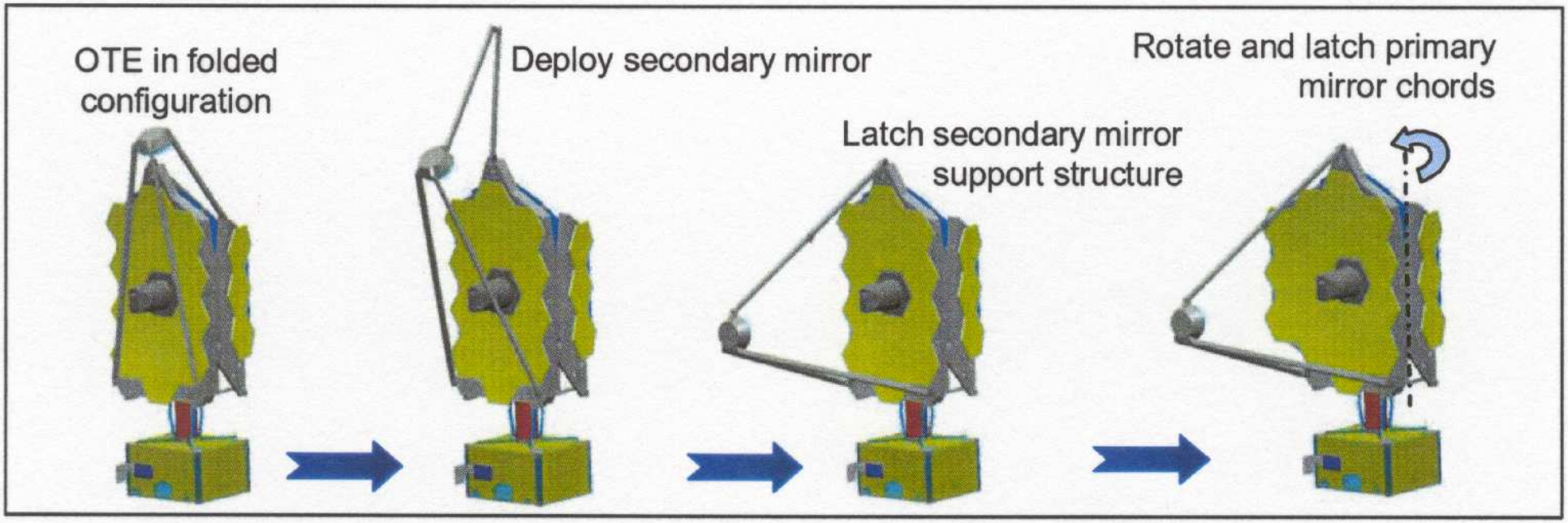

Figure 53. Telescope Deployment Sequence (Deployment steps 4 and 5)

During its several month journey to L2 (shown on a previous page), JWST will be automatically deployed in phases (as shown here), its instruments will be tested, and it will then be inserted into an L2 halo orbit.

From an orbit around the the Earth–Sun Lagrange point L2, JWST can cover the whole sky in segments, have an observing efficiency $\gtrsim$70%, and send data back to Earth every day.

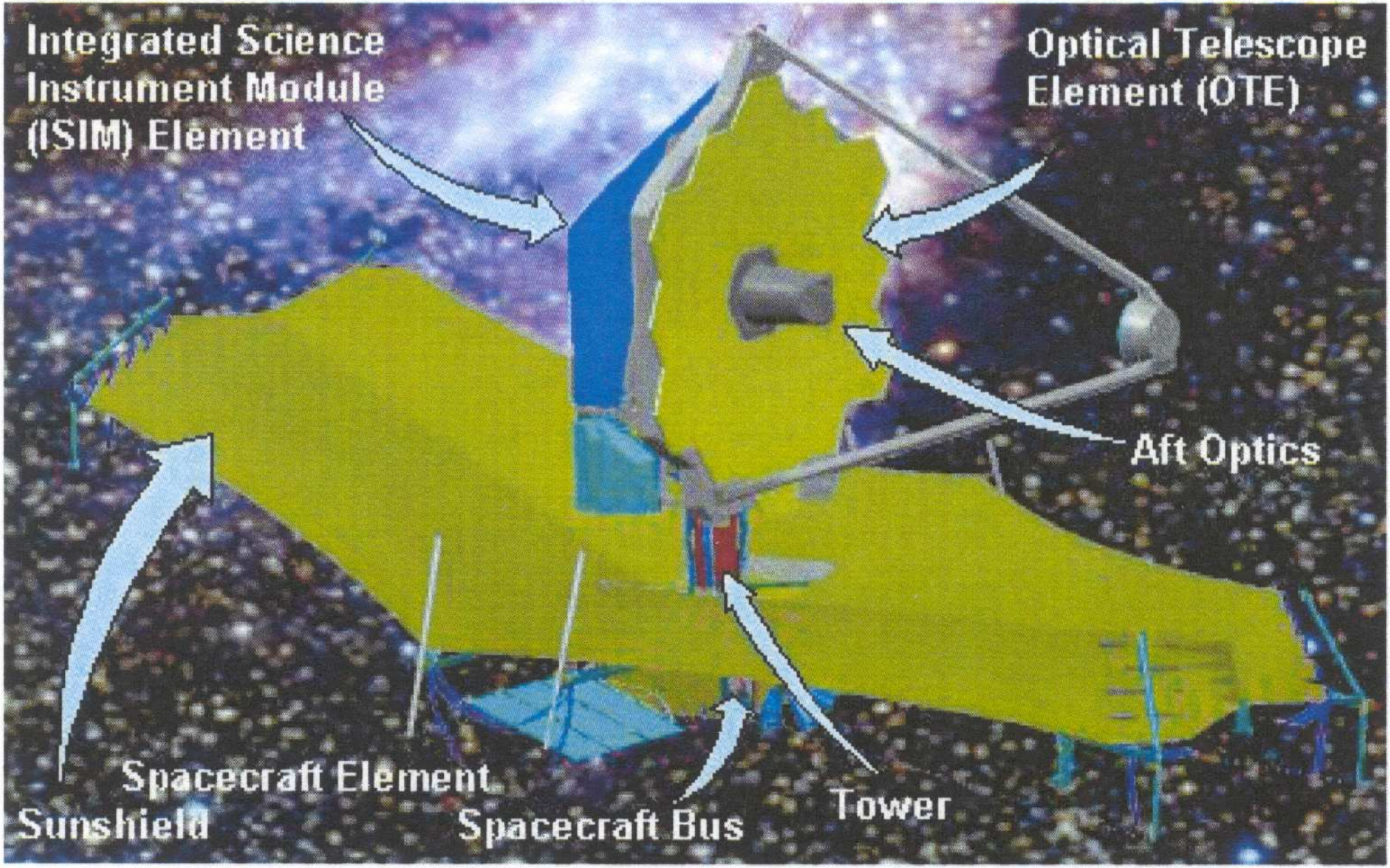

JWST mission reviewed in Gardner, J. P., et al. 2006, Space Science Reviews, p. 1–80, in press; astro-ph/0606175)

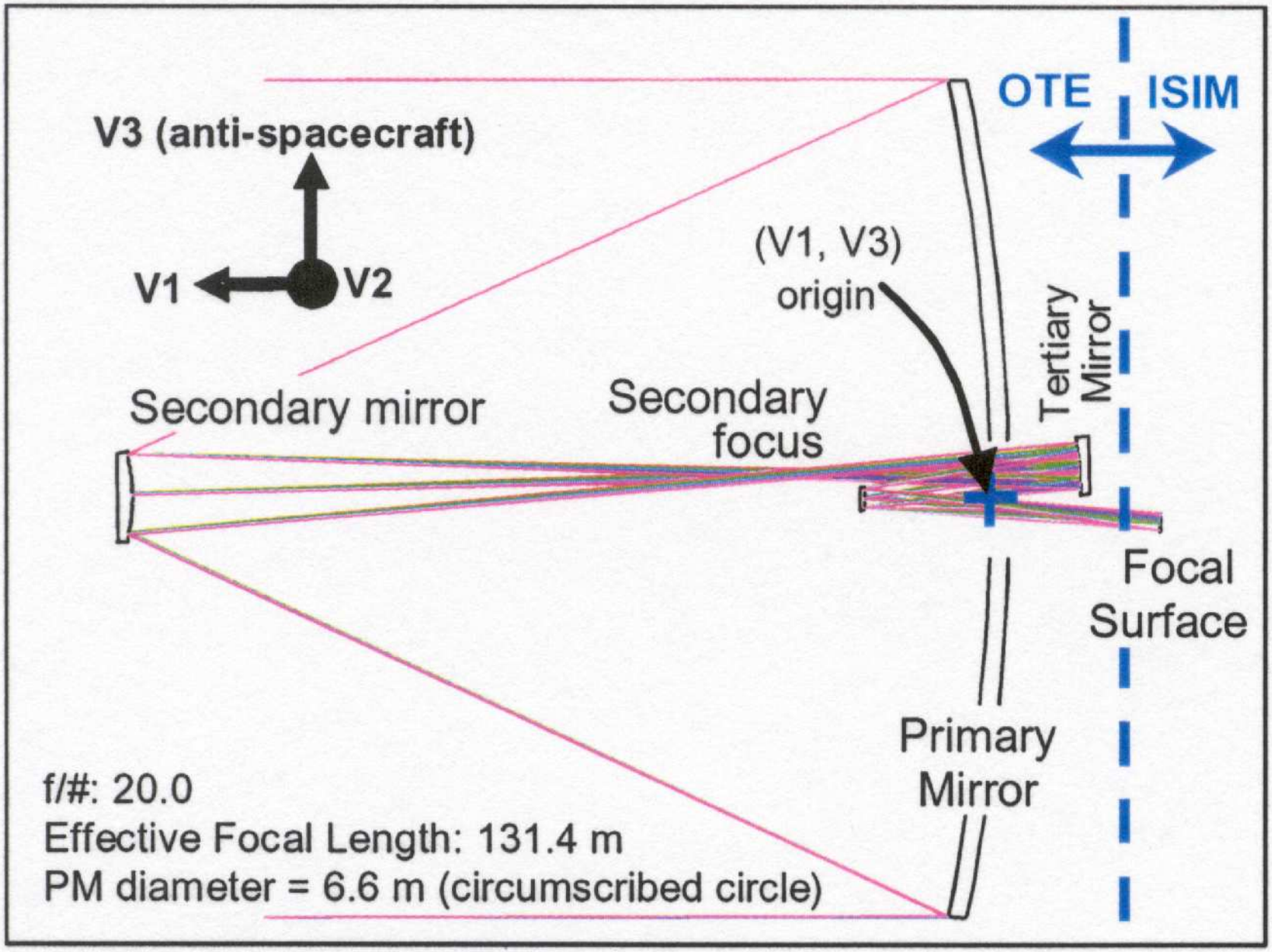

Figure 33. OTE optical layout

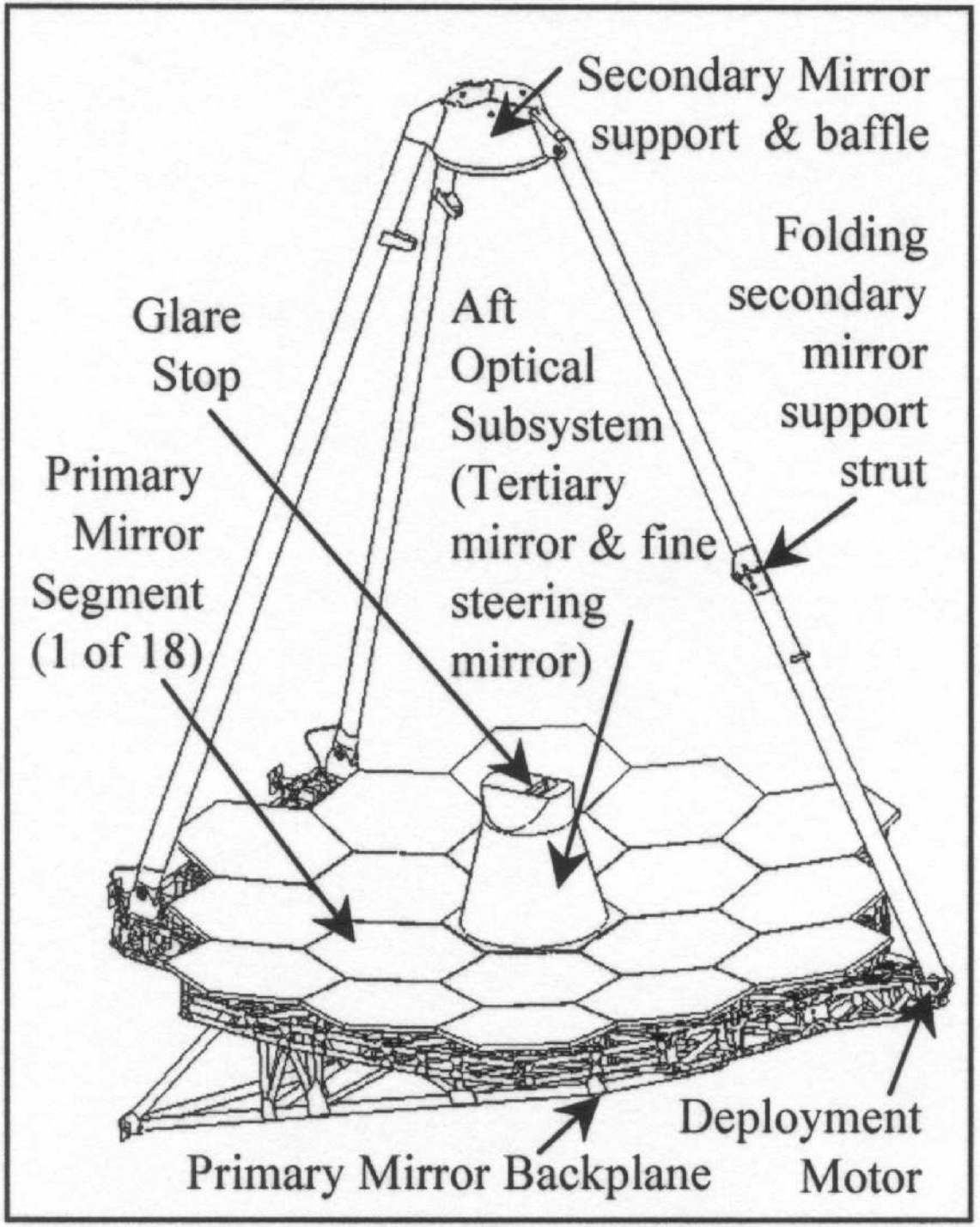
Secondary Mirror
support & baffle
Folding
secondary
mirror
support
strut
Glare
Stop
Aft
Optical
Subsystem
(Tertiary
mirror & fine
steering
mirror)
Primary
Mirror
Segment
(1 of 18)
Deployment
Motor
Primary Mirror Backplane

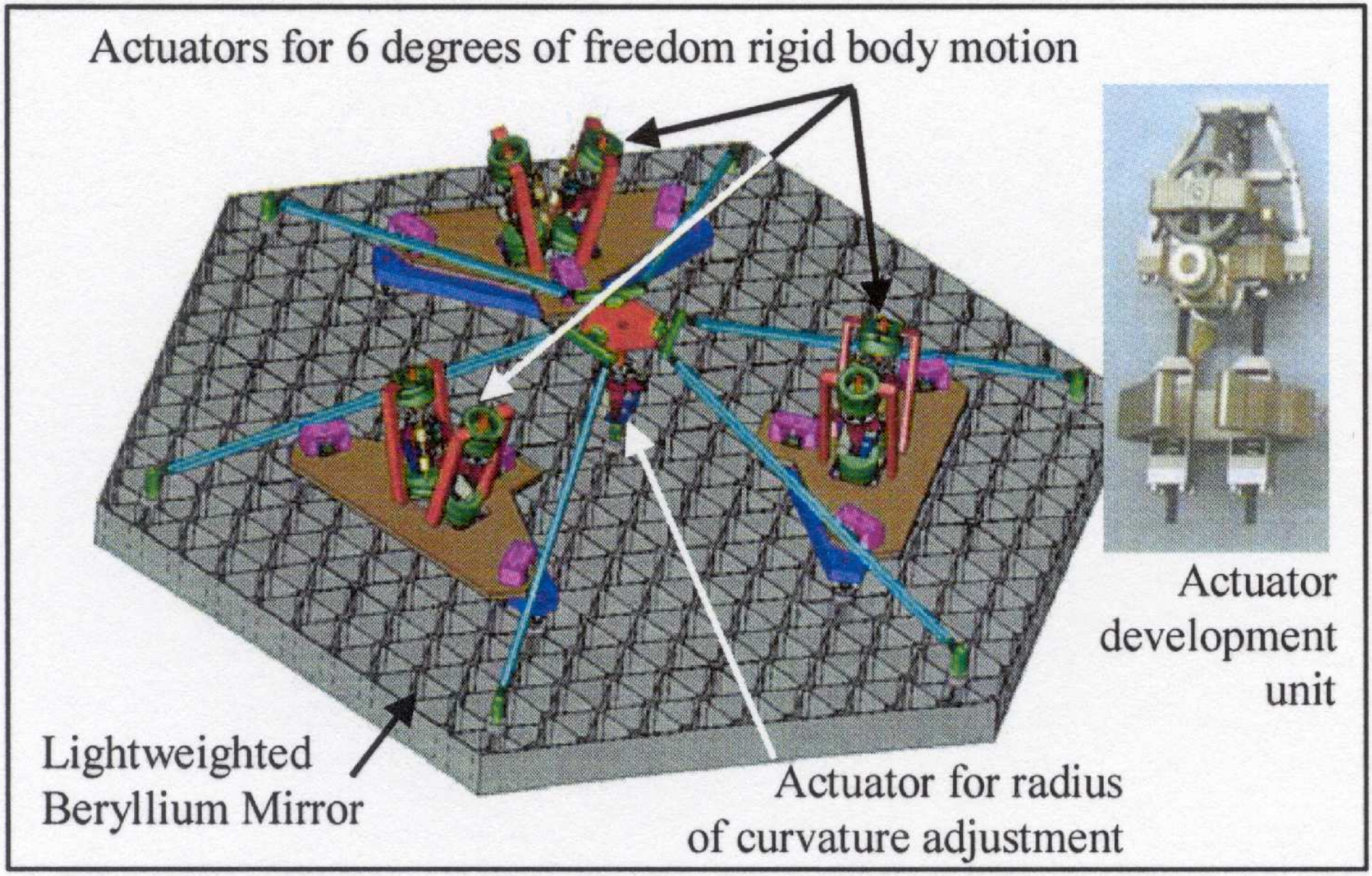

Figure 36. Rear view of a primary mirror segment.

Active mirror segment support through hexapods, like Keck whiffle-trees.

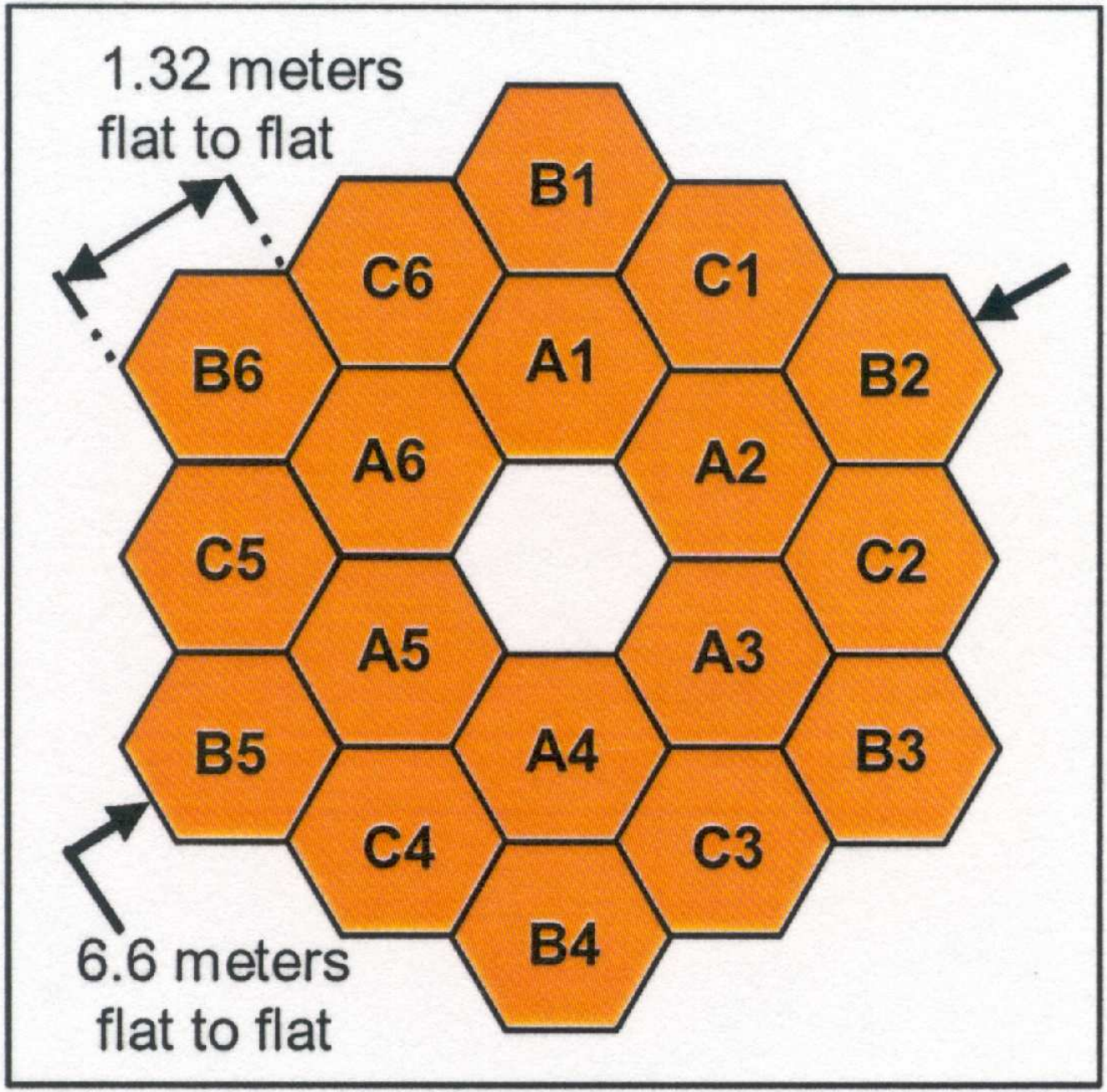

Edge-to-edge diameter is 6.60 m, but effective circular diameter is 5.85 m.

Cannot cleanly descope aperture without doing major harm to PSF.

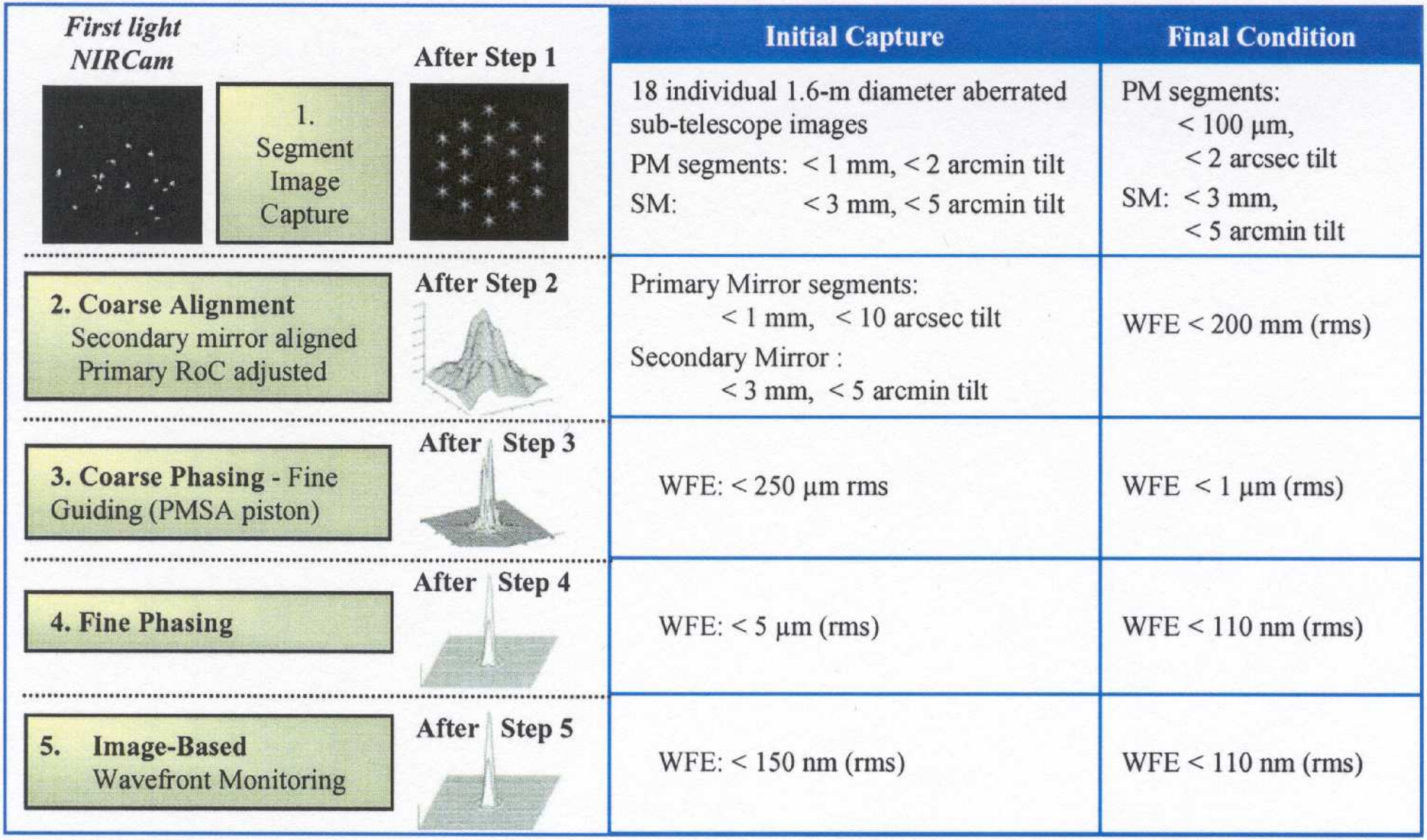

Initial Capture	Final Condition
18 individual 1.6-m diameter aberrated sub-telescope images PM segments: < 1 mm, < 2 arcmin tilt SM: < 3 mm, < 5 arcmin tilt	PM segments: < 100 μm, < 2 arcsec tilt SM: < 3 mm, < 5 arcmin tilt
Primary Mirror segments: < 1 mm, < 10 arcsec tilt Secondary Mirror : < 3 mm, < 5 arcmin tilt	WFE < 200 mm (rms)
WFE: < 250 μm rms	WFE < 1 μm (rms)
WFE: < 5 μm (rms)	WFE < 110 nm (rms)
WFE: < 150 nm (rms)	WFE < 110 nm (rms)

Figure 38. WFS&C commissioning and maintenance.

JWST's Wave Front Sensing and Control is similar to that at Keck and HET.

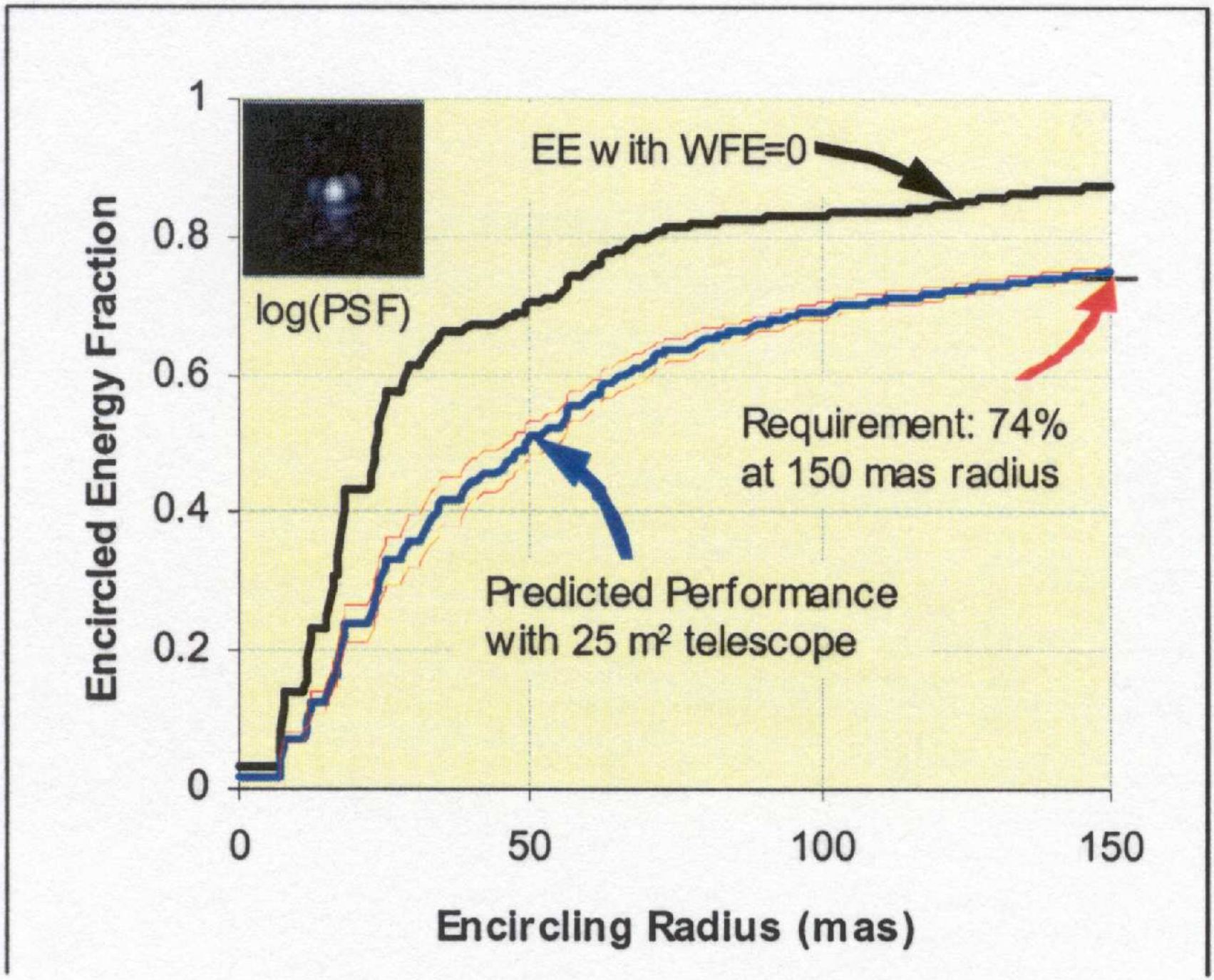
Encircled Energy Fraction
1
0.8
0.6
0.4
0.2
0
log(PSF)
EE with WFE=0
Requirement: 74%
at 150 mas radius
Predicted Performance
with 25 m² telescope
0
50
100
150
Encircling Radius (mas)

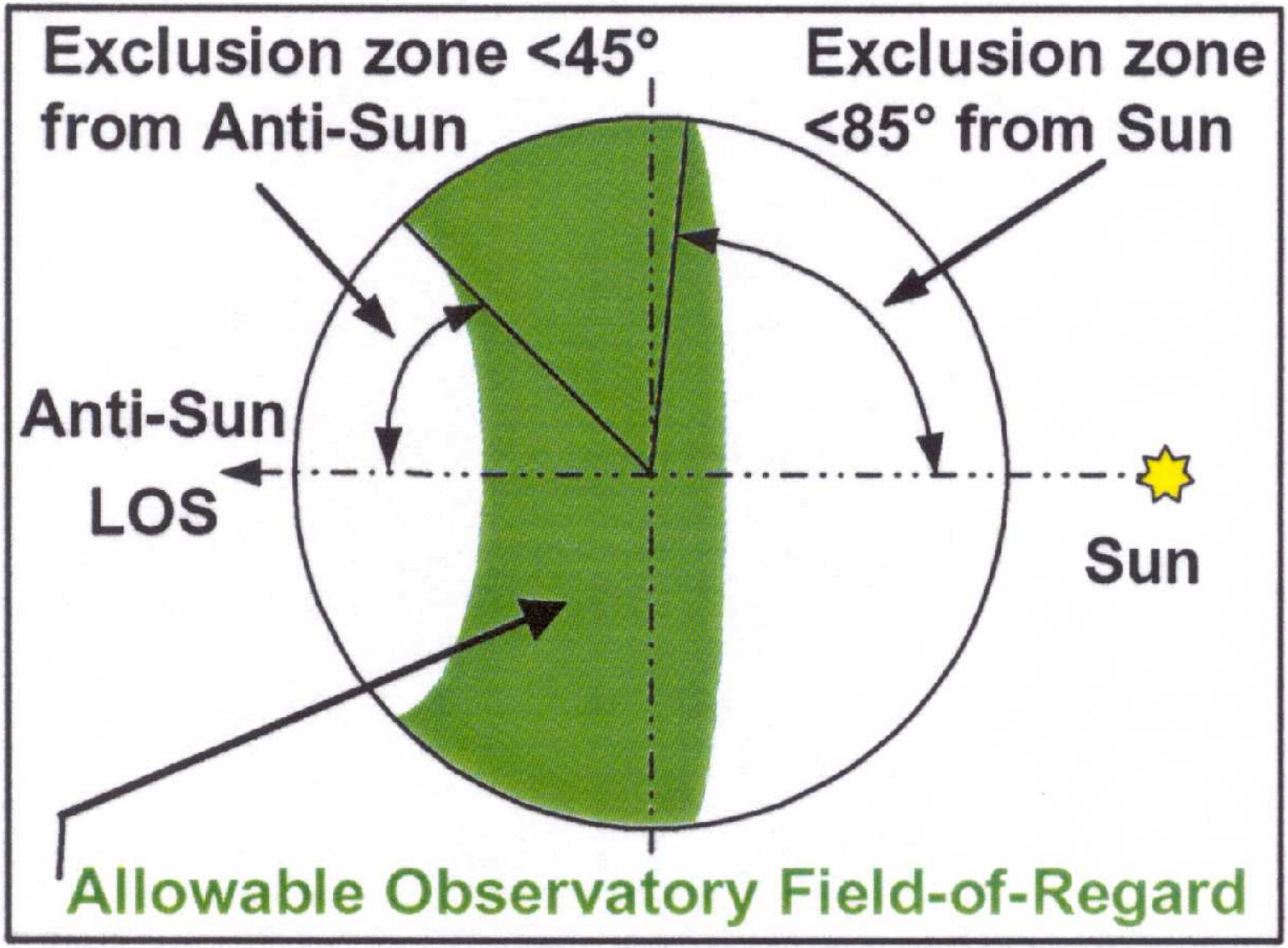

Figure 30. Observatory field of regard (FOR).

JWST can observe segments of sky that move around as it orbits the Sun.

- (2) What instruments will JWST have?

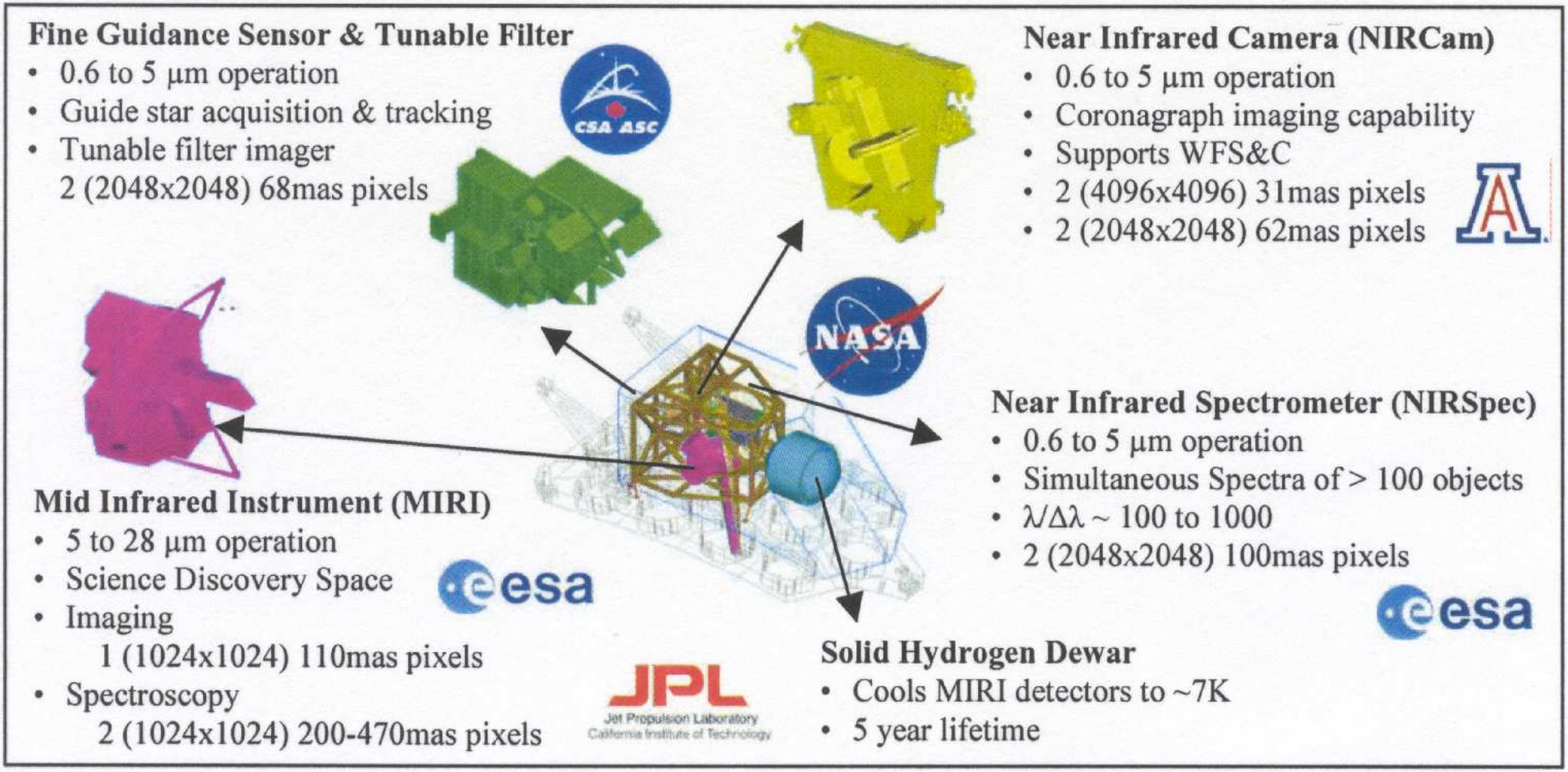

Figure 37. ISIM element and its science instrumentation.

The JWST instrument complement: US (UofA), ESA, and CSA.

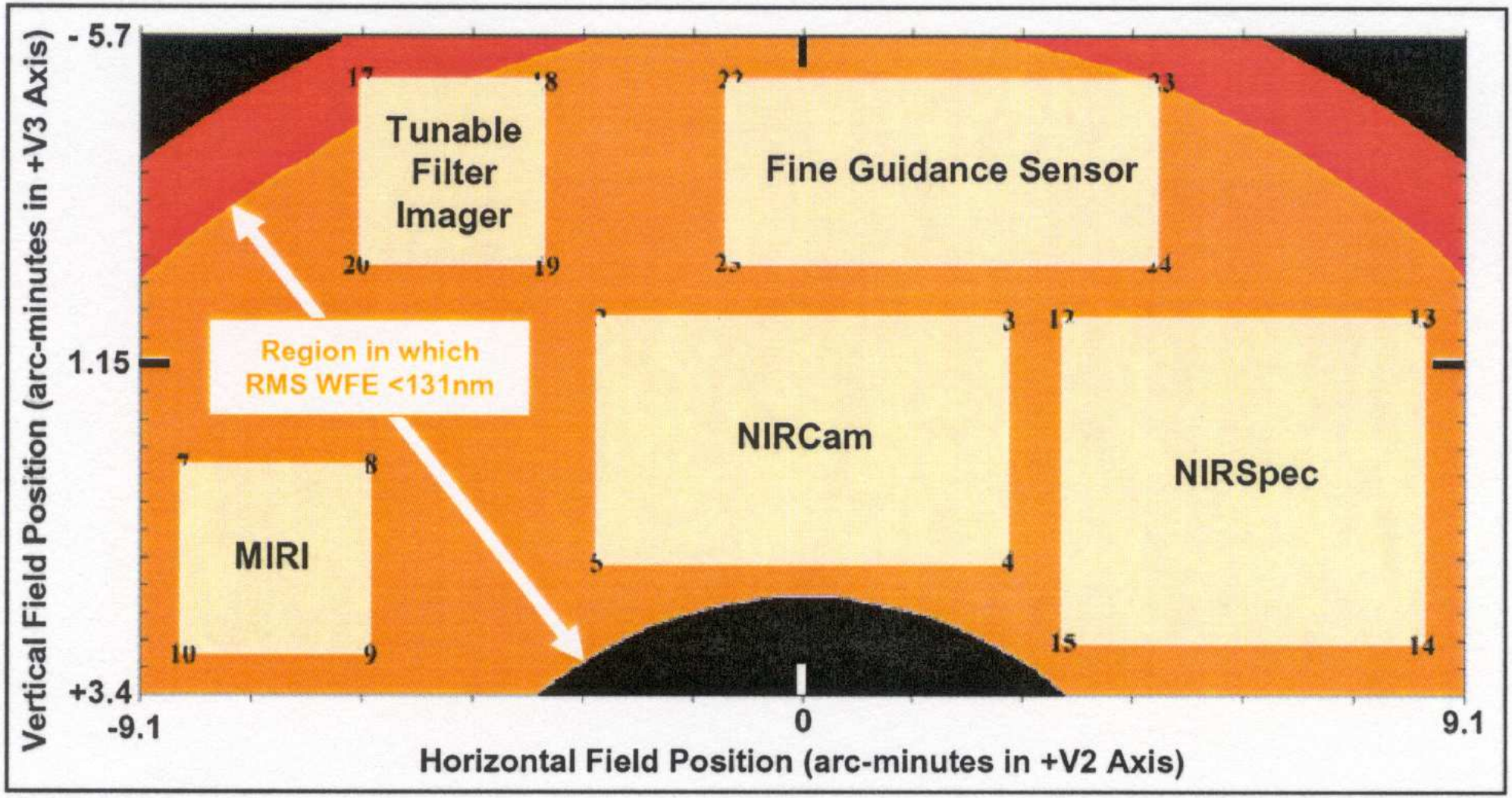

Figure 34. Placement of the ISIM instrument FPAs in the OTE field of view.

JWST instruments can in principle be used in parallel (not yet implemented).

Table 10. Predicted Performance of the JWST Observatory

Parameter	Capability
Wavelength	0.6 to 29 μm. Reflective gold coatings
Sensitivity	SNR=10, integration time = τ_i, R=$\lambda/\Delta\lambda$ and Zodiacal of 1.2 times that at north ecliptic pole
NIRCam	12 nJy (1.1μm, τ_i=10,000s, and $\lambda/\Delta\lambda = 4$)
NIRCam	10.4 nJy (2.0μm, τ_i=10,000s, and $\lambda/\Delta\lambda = 4$)
TFI	368 nJy (3.5μm, τ_i=10,000s, and $\lambda/\Delta\lambda = 100$)
NIRSpec	120 nJy (3.0μm, τ_i=10,000s, and $\lambda/\Delta\lambda = 100$)
NIRSpec	560 nJy (10μm, τ_i=10,000s, and $\lambda/\Delta\lambda = 5$)
MIRI	5000 nJy (21μm, τ_i=10,000s, and $\lambda/\Delta\lambda = 4.2$)
NIRSpec Med	5.2×10^{-22} Wm^{-2} (2 μm, τ_i=100,000s, R= 1000)
MIRI Spec	3.4×10^{-21} Wm^{-2} (9.2 μm, τ_i=10,000s, R= 2400)
MIRI Spec	3.1×10^{-20} Wm^{-2} (22.5 μm, τ_i=10,000s, R= 1200)
Spatial Resolution & Stability	Encircled Energy of 75% at 1 μm for 150mas radius Strehl ratio of ~ 0.86 at 2 μm. PSF stability better than 1%

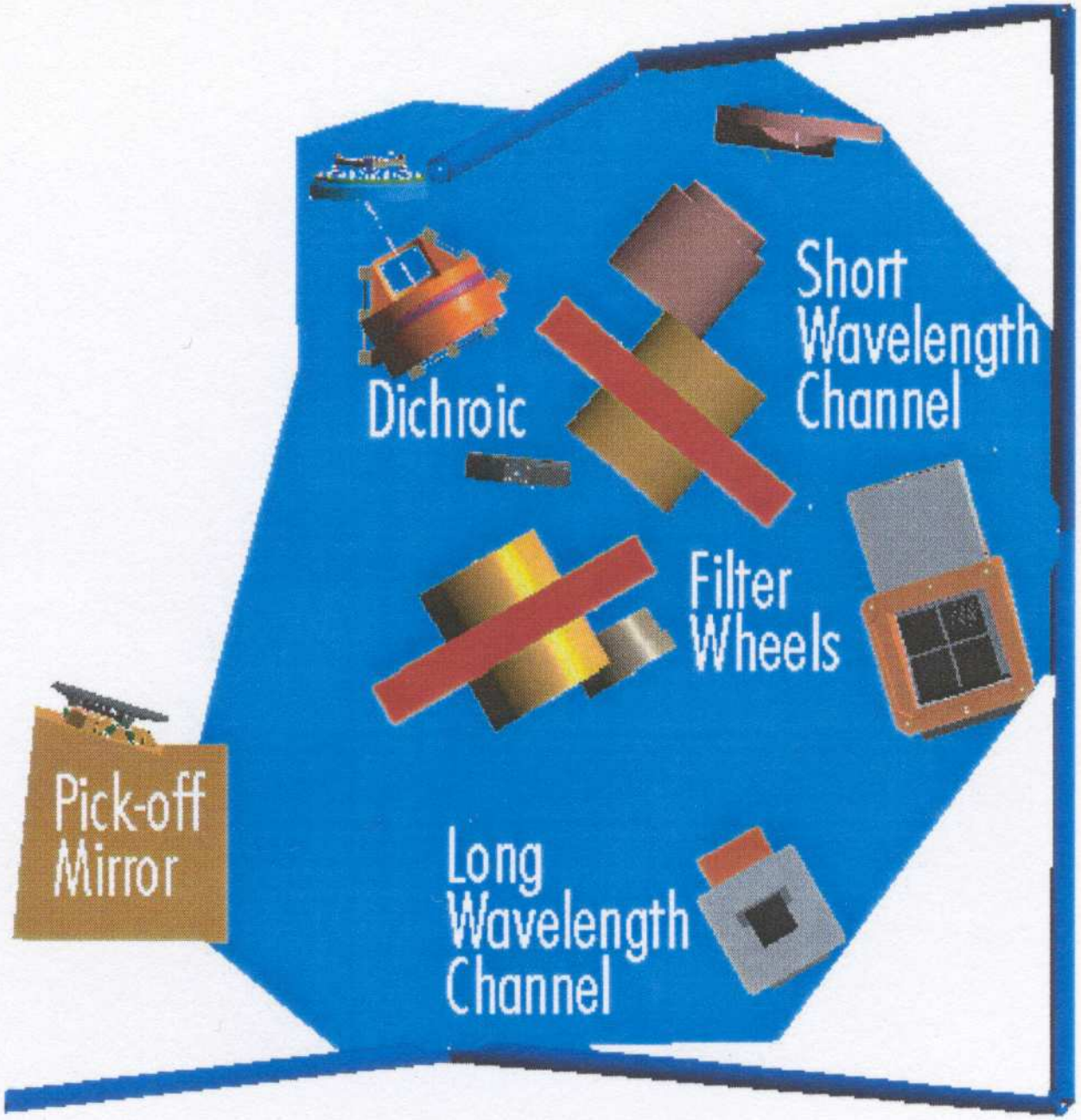

Figure 43. Optical layout of one of two NIRCam imaging modules.

- (2) What instruments will JWST have?

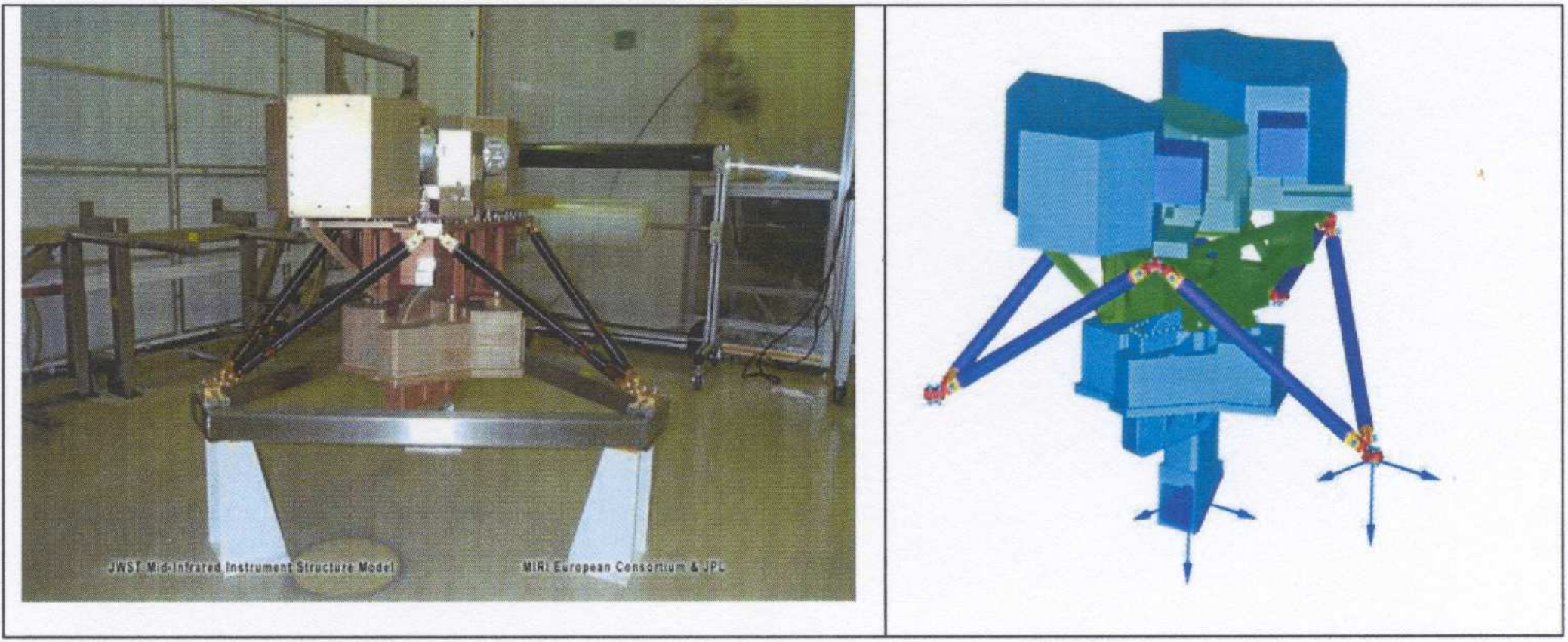

Figure 47. The MIRI structural and thermal model (left) compared to a computer design of the instrument (right).

The Mid-Infra-Red Instrument MIRI made by an UofA + JPL + ESA consortium will do imaging and spectroscopy from 5–28 μm. MIRI is actively cooled by a cryocooler, so that its lifetime is not limited by consumables.

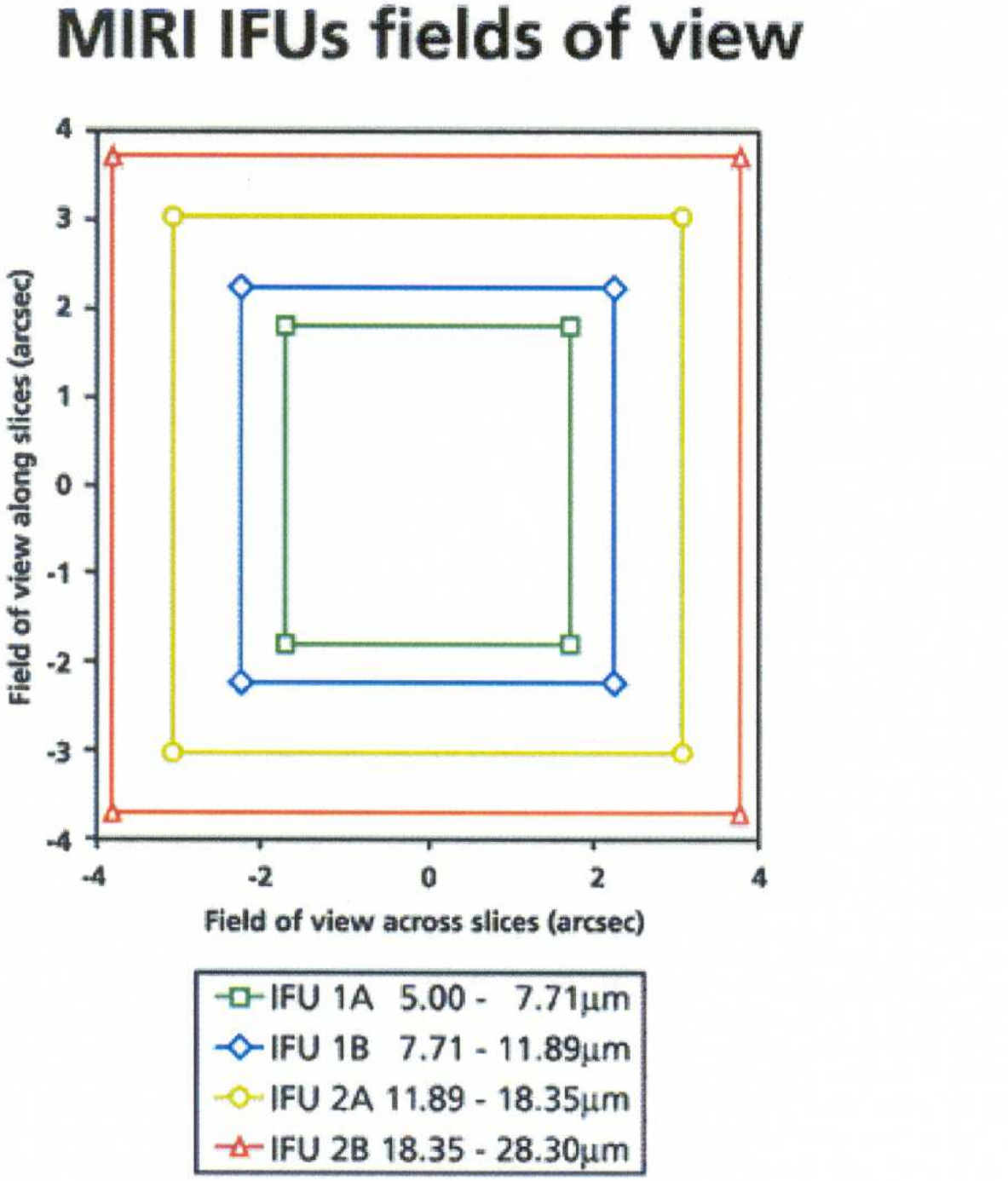

Figure 49. Fields of view of the MIRI IFU spectrograph.

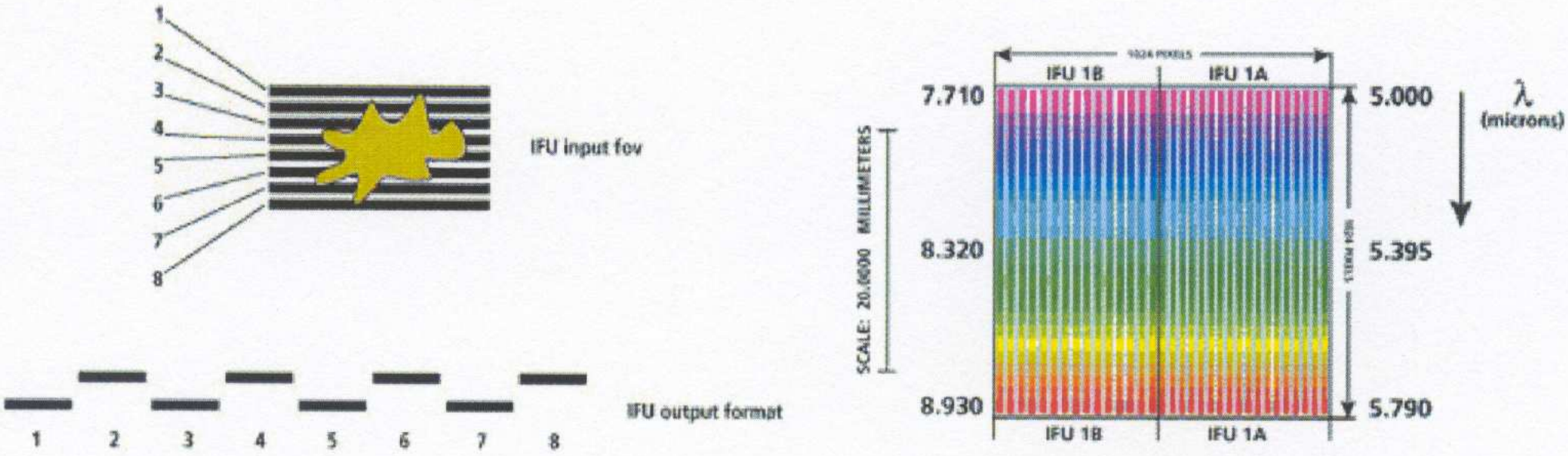

Figure 50. Schematic illustration of the MIRI IFU image slicer format (left) and dispersed spectra on detector (right)

The MIRI Integral Field Unit (IFU) has an image slicer that makes spatially resolved spectra at 5 μm $\lesssim \lambda \lesssim$ 9 μm.

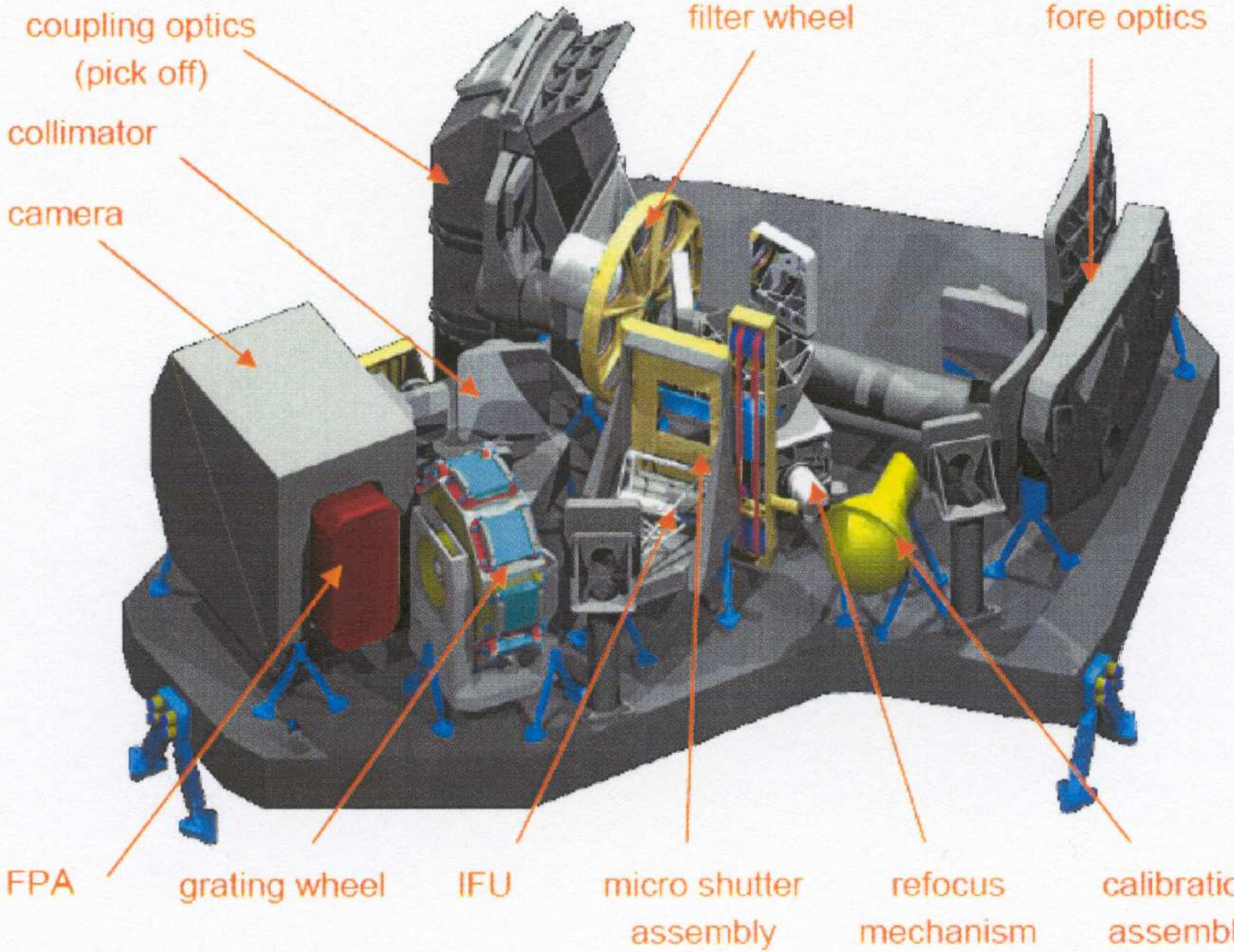

Figure 45. The NIRSpec instrument.

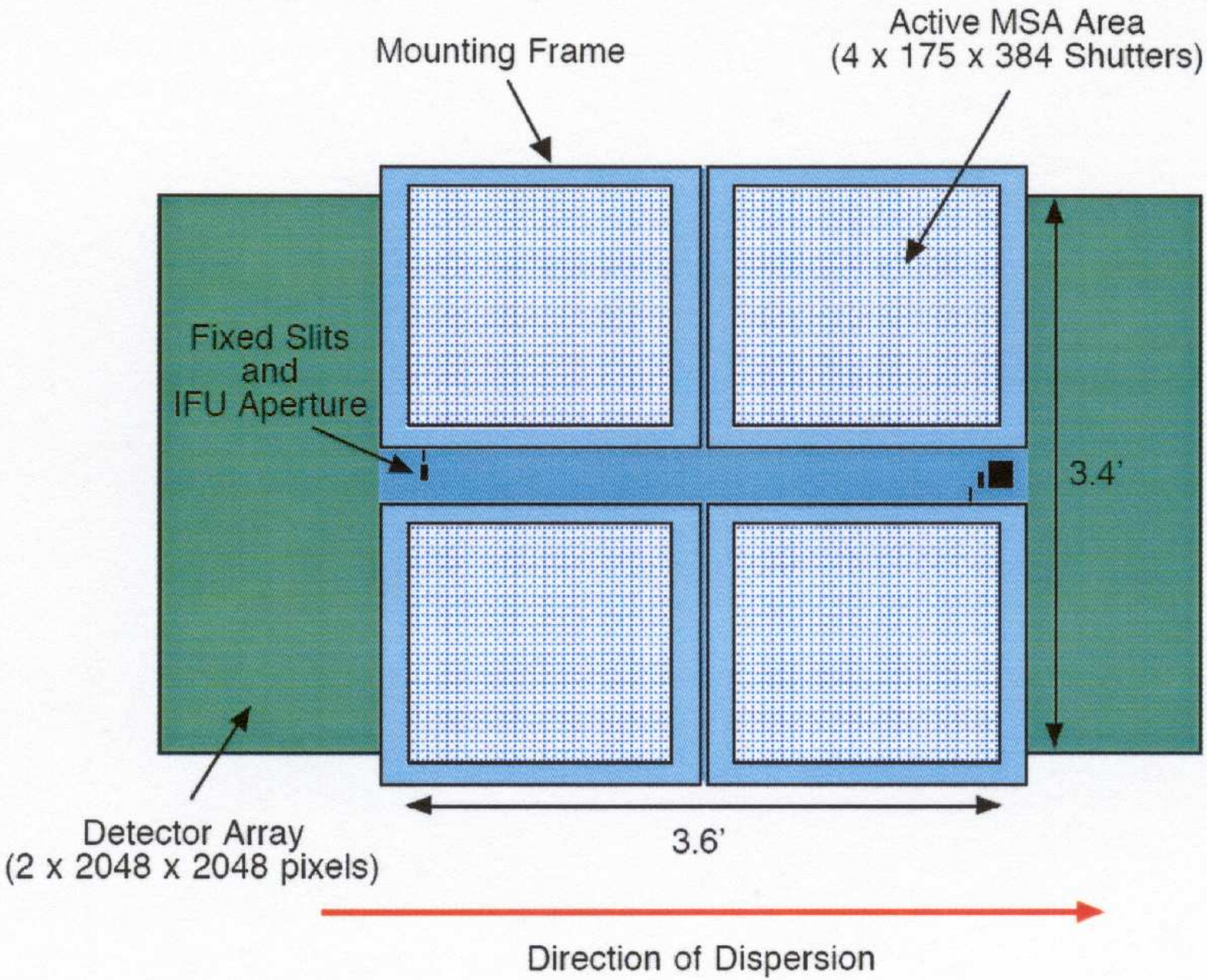

Figure 46. Schematic layout of the NIRSpec slit mask overlaid the detector array projected to the same angular scale.

• (2) What sensitivity will JWST have?

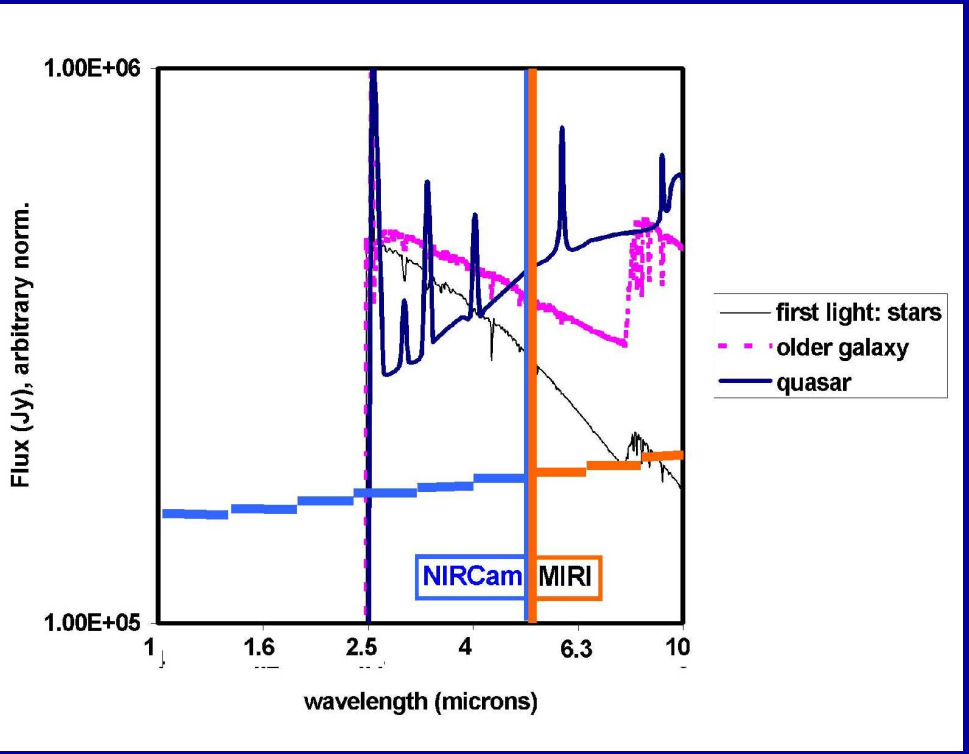

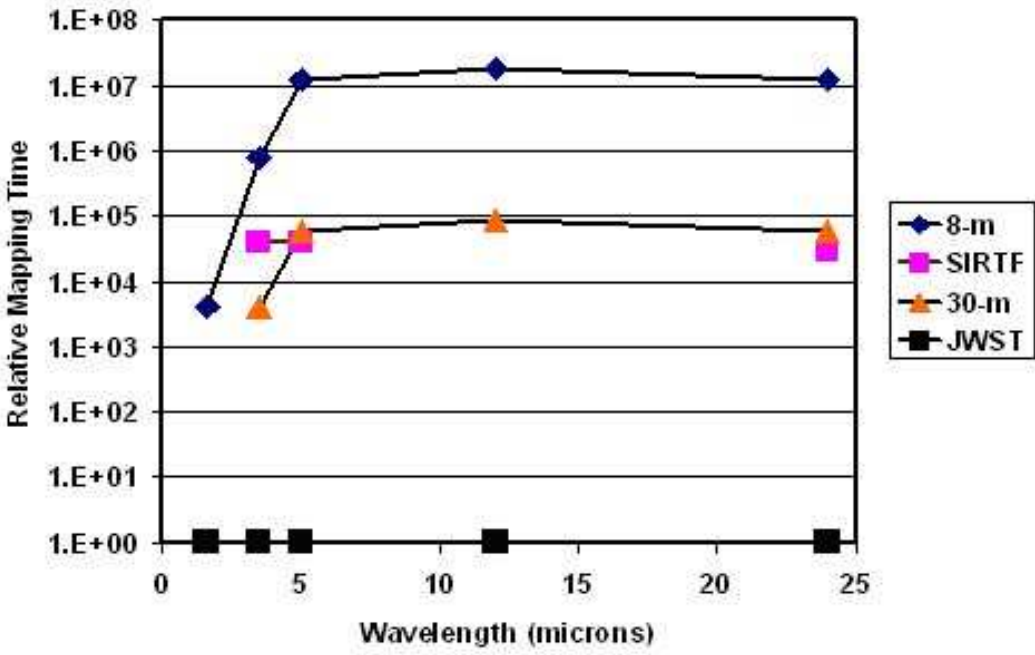

The NIRCam and MIRI sensitivity complement each other straddling 5 μm in wavelength, and together allow objects to be found to redshifts z=15–20 in $\sim 10^5$ sec (28 hrs) integration times.

The left panel shows the NIRCam and MIRI broadband sensitivity to a Quasar, a "First Light" galaxy dominated by massive stars, and a 50 Myr "old" galaxy, all at z=20. The right panel shows the relative survey time versus wavelength that Spitzer, a ground-based IR-optimized 8-m (Gemini) and a 30-m telescope would need to match JWST.

240 hrs HST/ACS in Vi'z' in the Hubble UltraDeep Field (HUDF)

6.5m JWST PSF's models (Ball Aerospace and GSFC):

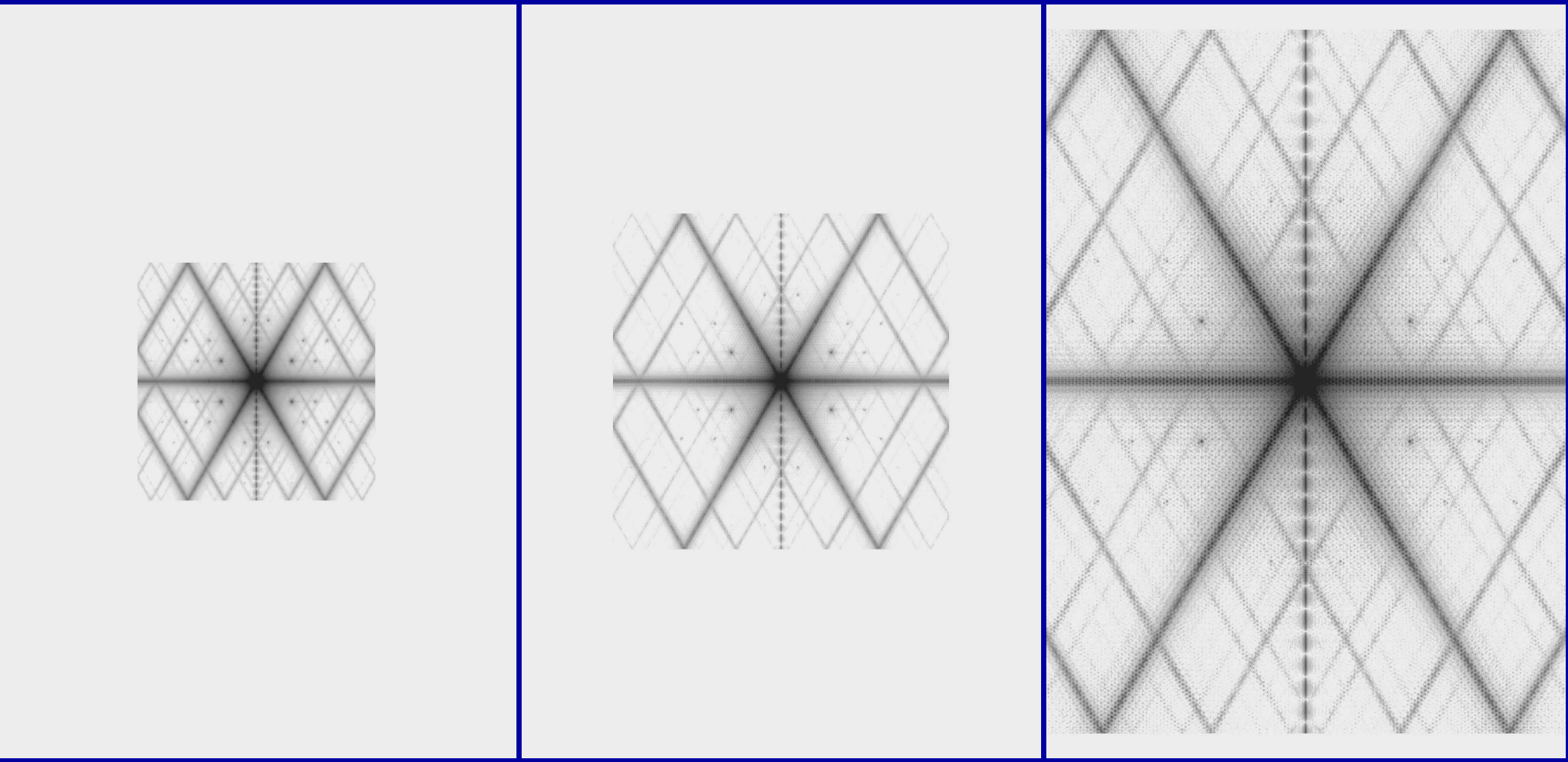

NIRCam 0.7 μm 1.0 μm ($<$150 nm WFE) 2.0 μm (diffr. limit)

PSF's are shown at logarithmic stretch — they have $\gtrsim$74% EE at r$\lesssim$0$''$.15

$\lesssim$20 hrs JWST NIRCam at 0.7, 0.9, 2.0 μm in the HUDF

Truth≡240 hrs HUDF Vi'z' $\lesssim$20 hrs JWST 0.7, 0.9, 2.0 μm

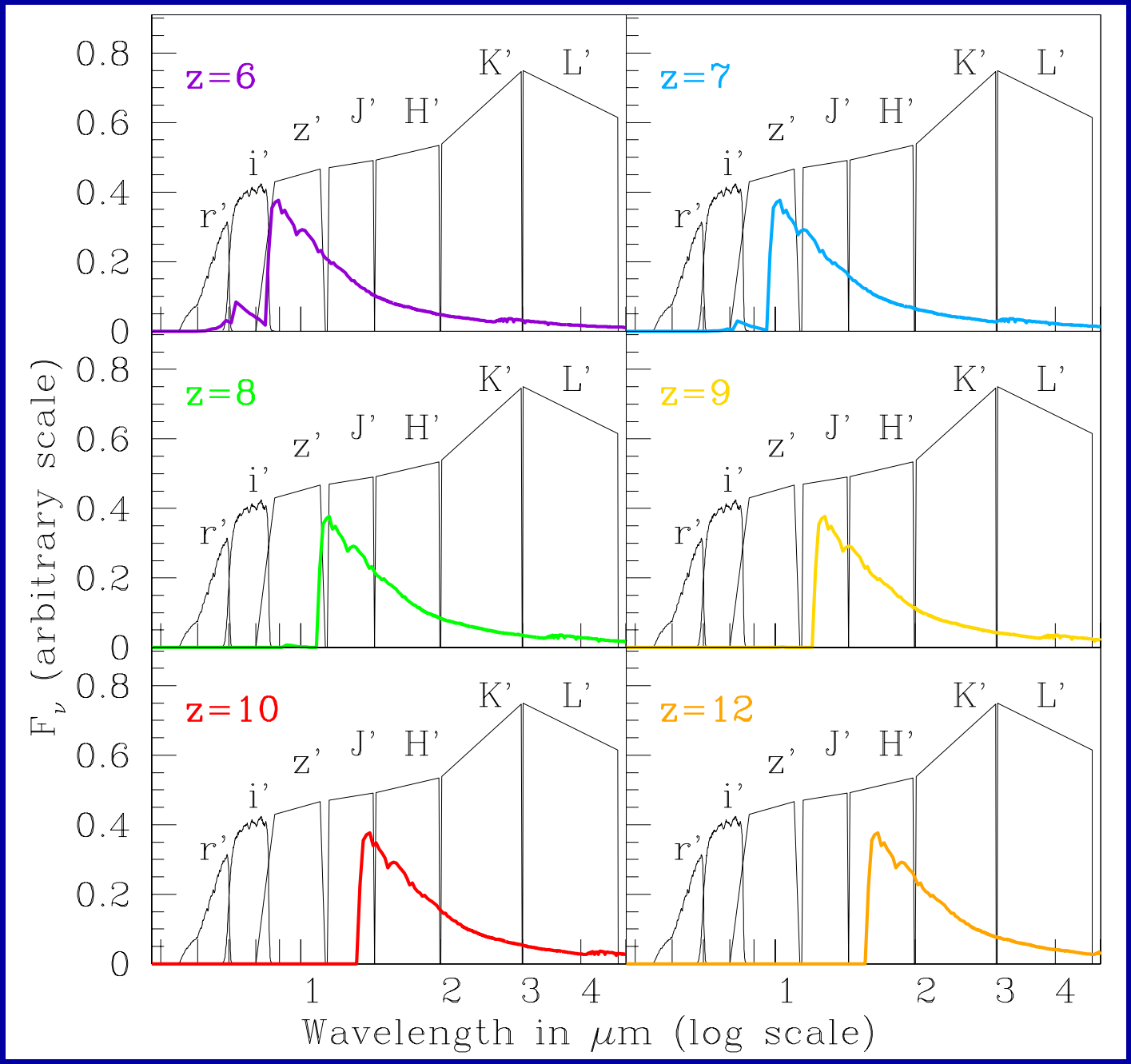

- Can't beat redshift: to see First Light, must observe near–mid IR.

$\Rightarrow$ This is why JWST needs NIRCam at 0.8–5 μm and MIRI at 5–28 μm.

(3a) What is First Light, Reionization, and Galaxy Assembly?

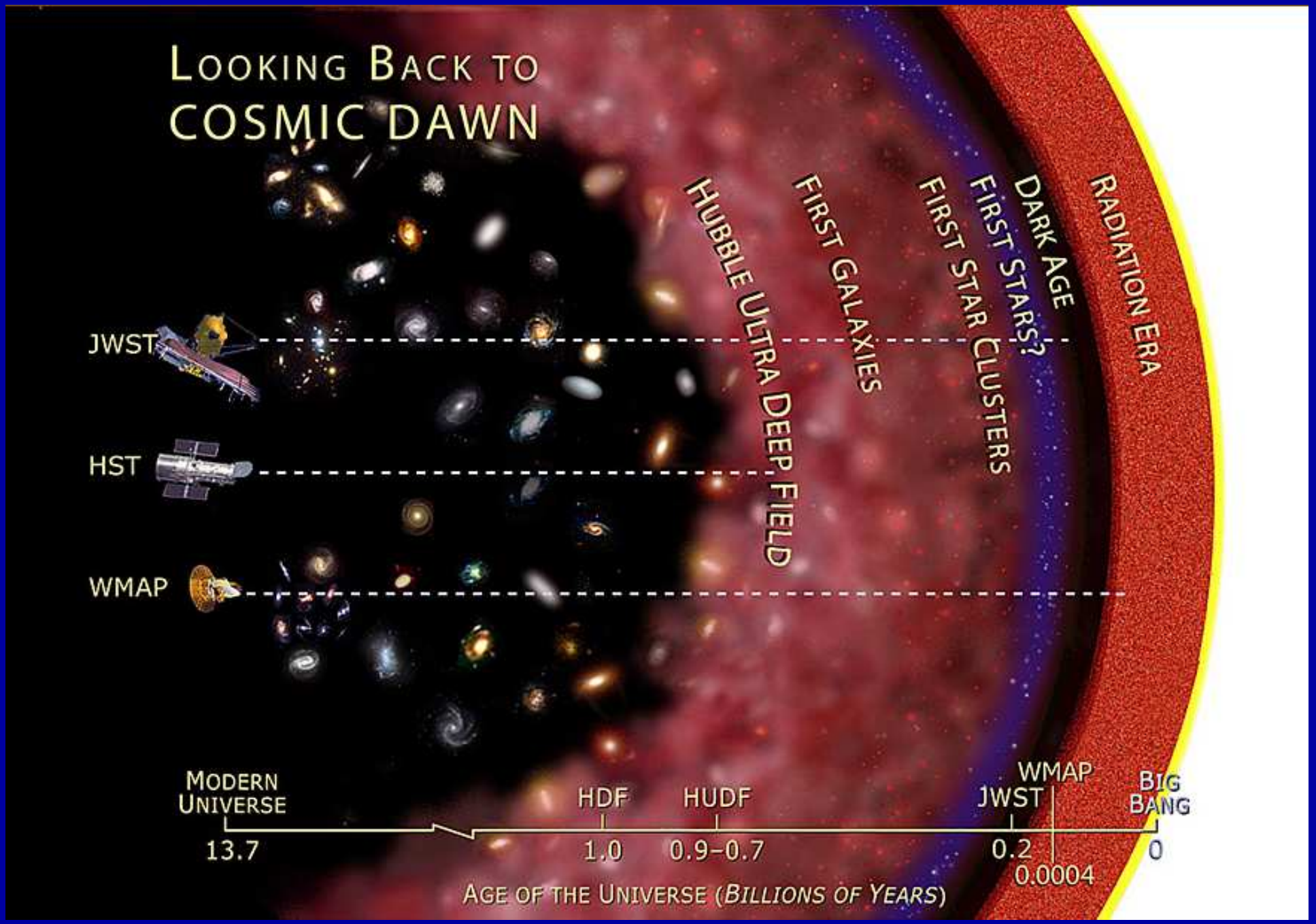

NASA telescopes penetrating Cosmic Dawn, First Light, & Recombination

- (3a) What is First Light and Reionization?

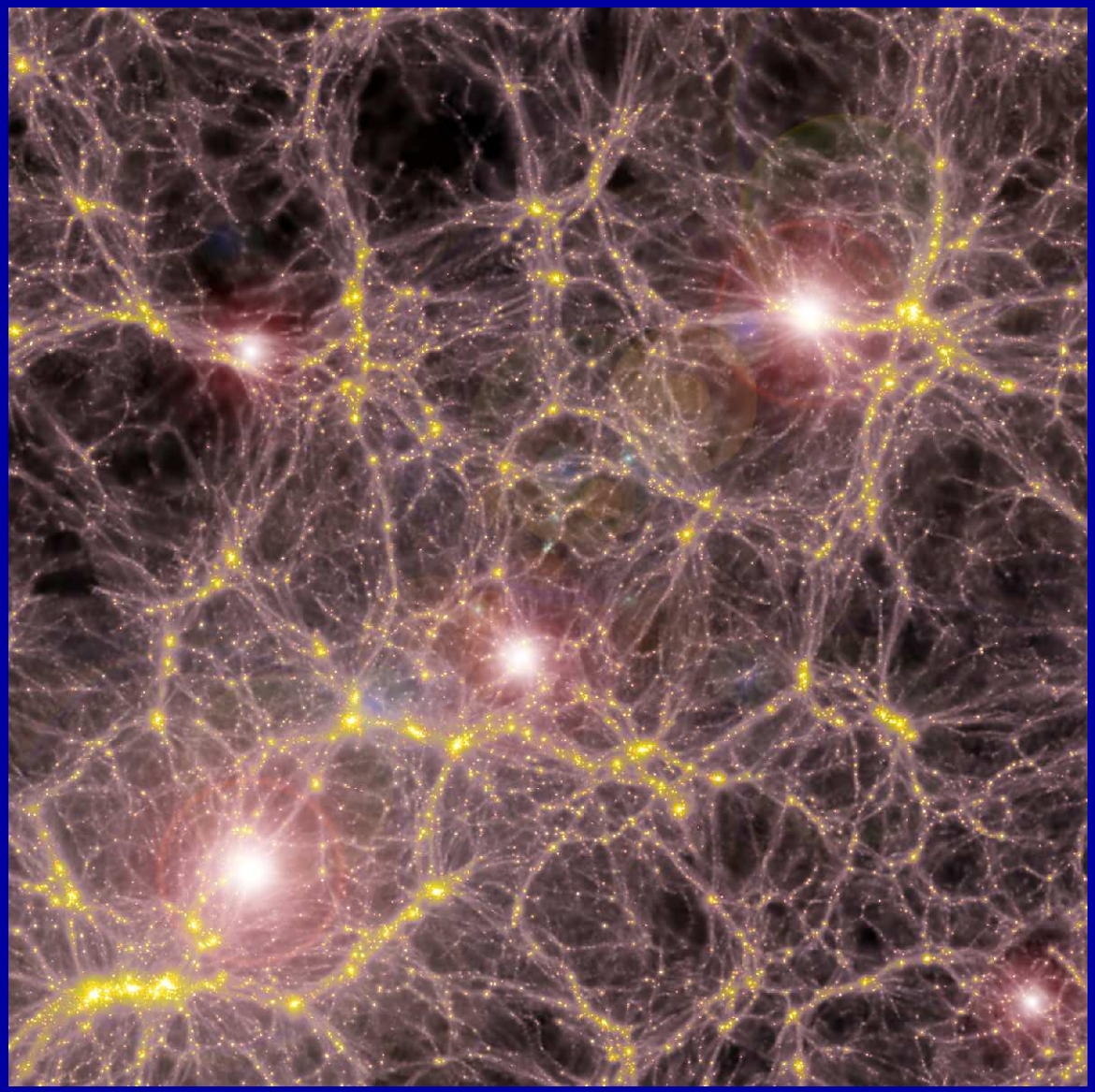

- Detailed Hydrodynamical models (V. Bromm) show that formation of Pop III stars reionized universe for the first time at $z \lesssim 10$–30 (First Light).
- A this should be visible to JWST as the first Pop III star clusters, and perhaps their extremely luminous supernovae at $z \simeq 10 \longrightarrow 30$.

- (3a) What is First Light and Reionization?

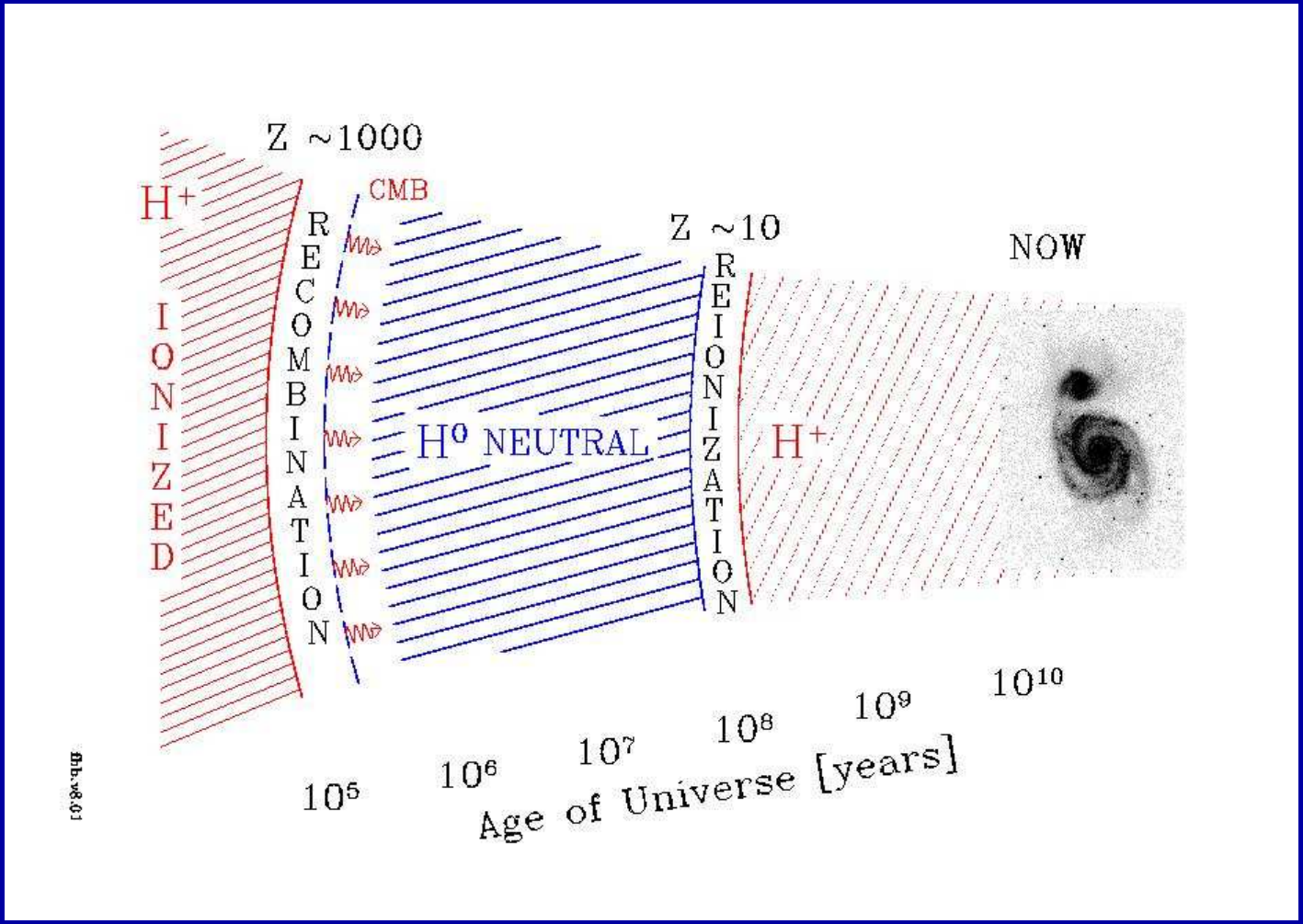

WMAP: First light may have happened in two epochs (Cen 2003):

- (1) Population III stars with $\gtrsim$200 $M_\odot$ at z$\simeq$11–20 (First Light).
- (2) First Population II stars (halo stars) form in dwarf galaxies of mass=10^6 to 10^9 $M_\odot$ at z$\simeq$6–9, which complete reionization (*cf.* F. Briggs 2002).

$\Rightarrow$ JWST needs NIRCam at 0.8–5 μm and MIRI at 5–28 μm.

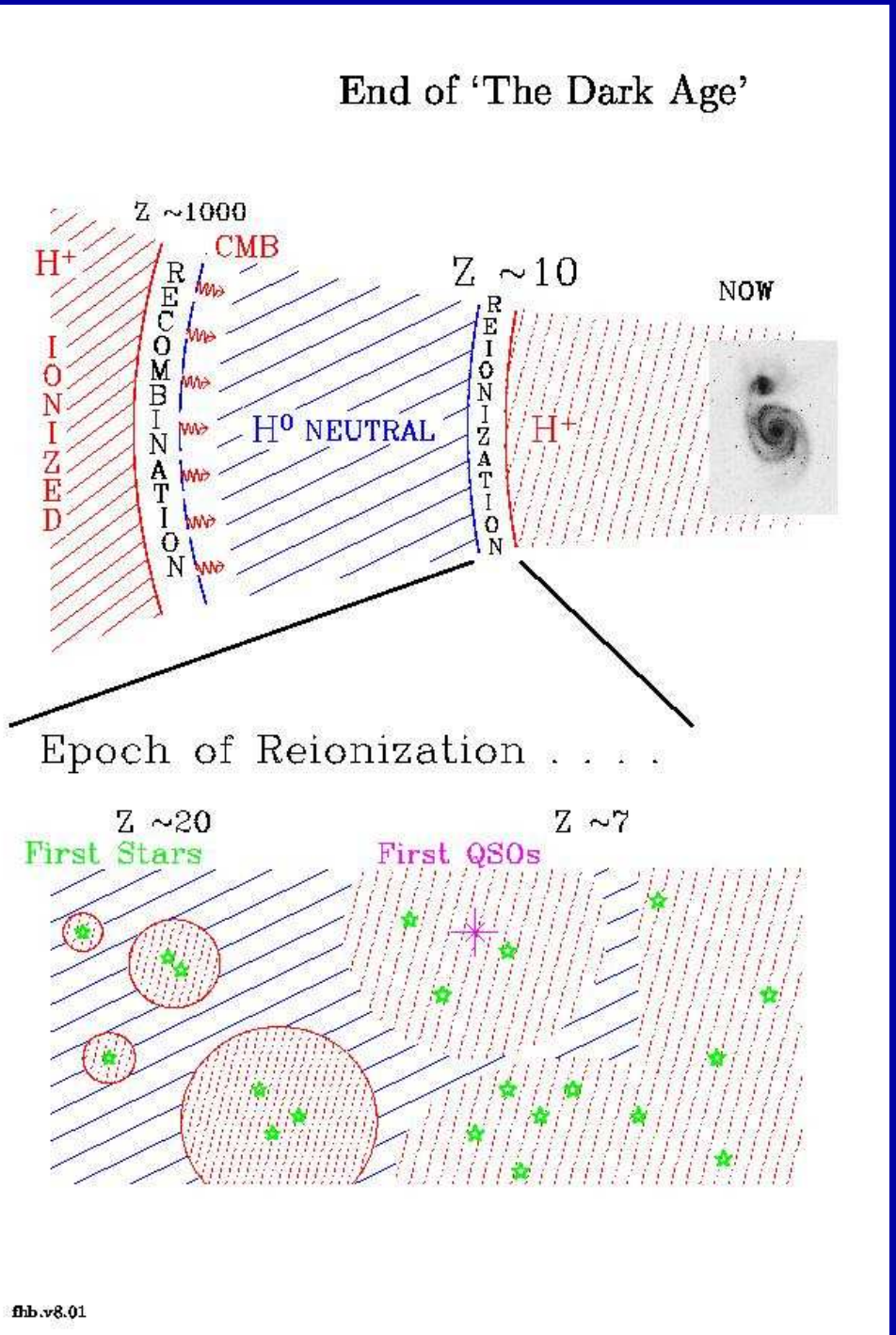

WMAP: First Light may have happened as following:

- (0) First Dark Ages since recombination (z=1089) until first light objects started shining (z=11–20)
- (1) First Light when Population III stars start shining with mass $\gtrsim$200 $M_\odot$ at z$\simeq$11–20.
- (2) Second Dark Ages since Pop III supernovae heated gas which could not cool and form normal Pop II halo stars until z$\simeq$9–11.
- (3) This is followed by Pop II stars forming in dwarf galaxies (mass$\simeq 10^7$–10^9 $M_\odot$) at z$\simeq$6–9, ending the epoch of reionization.

(Fig. courtesy of Dr. F. Briggs)

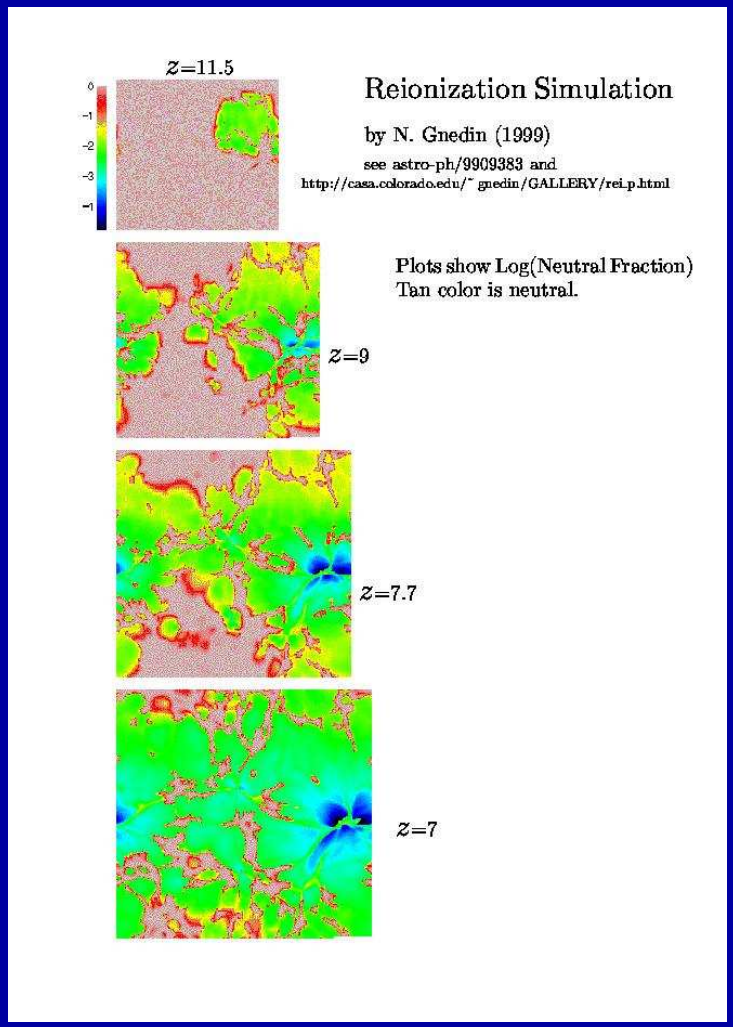

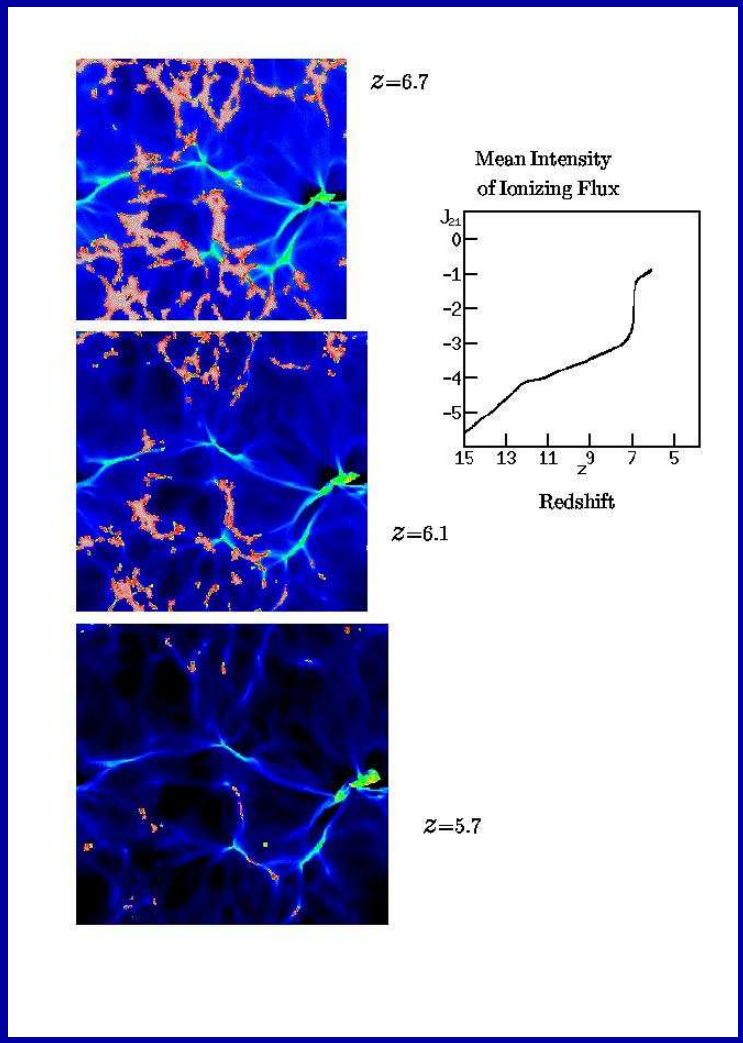

• Hydrodynamical models (Gnedin 2000) show that percolation of H-II regions due to Pop II stars started at z≃9 and ended in fully overlapping H-II regions at z≃6 (reionization completed, now seen in z≃6 QSO spectra).

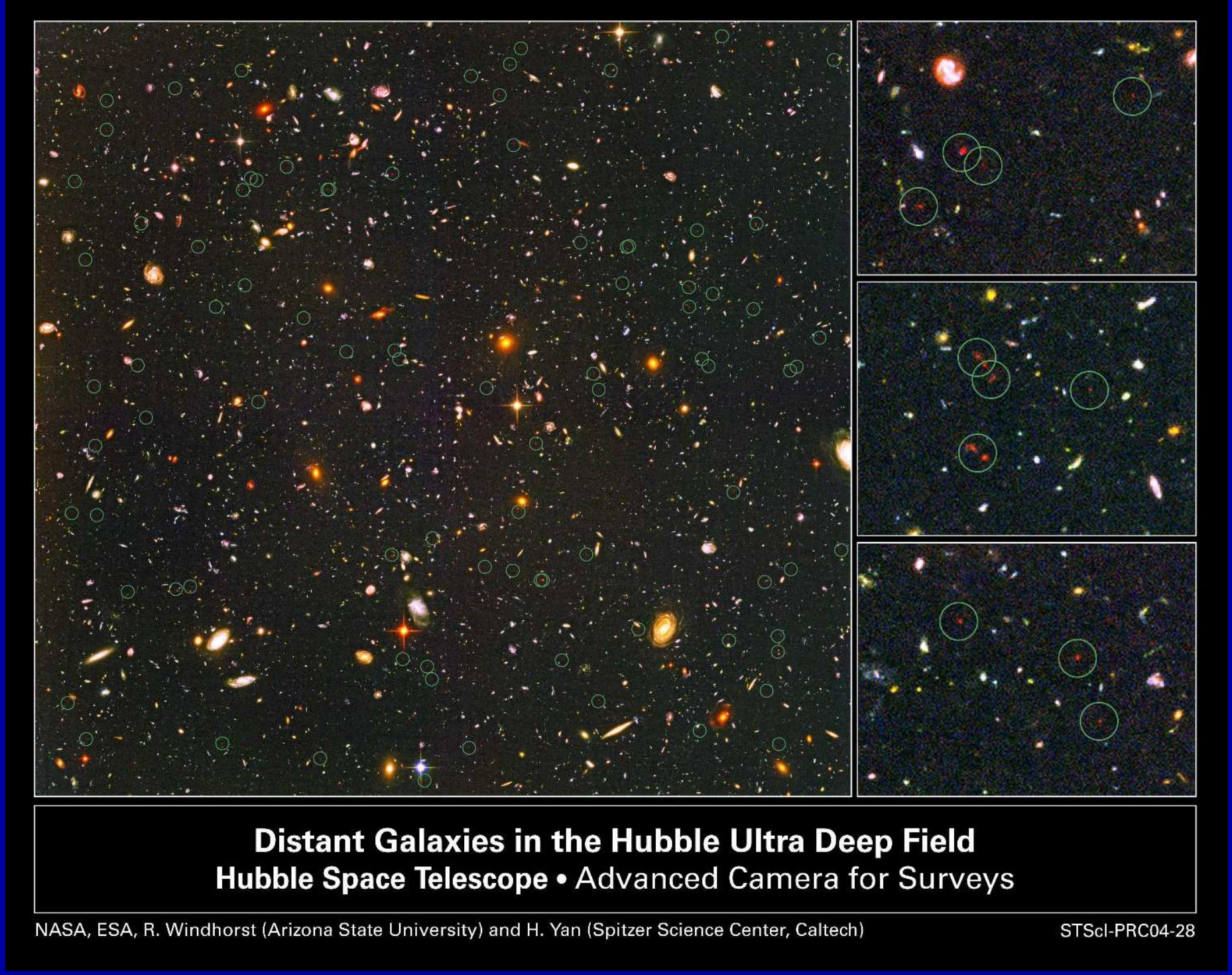

i-band drops in the HUDF: Most confirmed at z≃6 (Malhotra et al. 2005)

- (3b) How JWST can measure First Light and Reionization

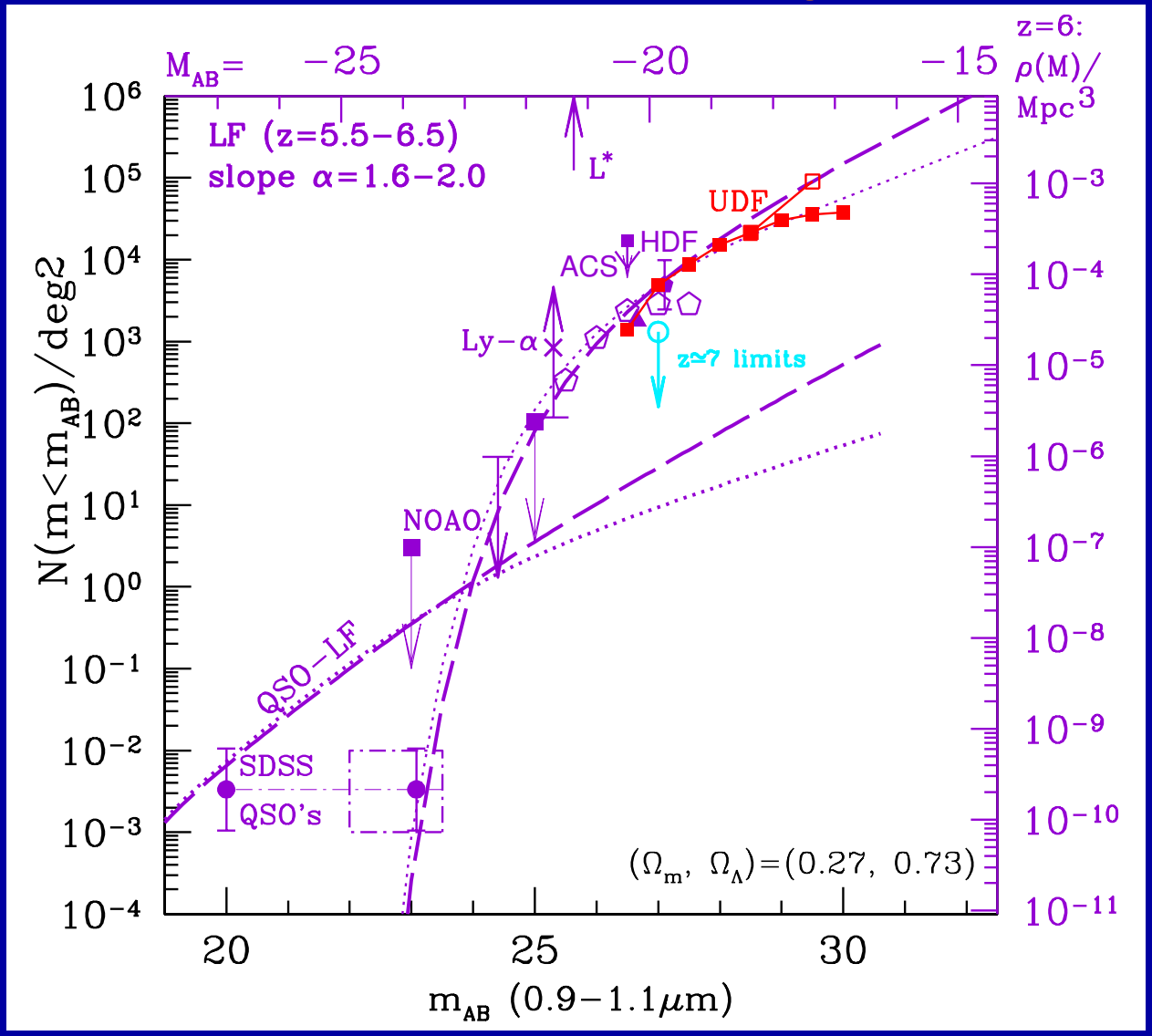

HUDF shows that luminosity function of z≃6 objects (Yan & Windhorst 2004a, b) may be very steep: faint-end Schechter slope $|\alpha| \simeq 1.6$–2.0.

$\Rightarrow$ Dwarf galaxies and not quasars likely completed the reionization epoch at z≃6. This is what JWST will observe in detail to z$\gtrsim$20.

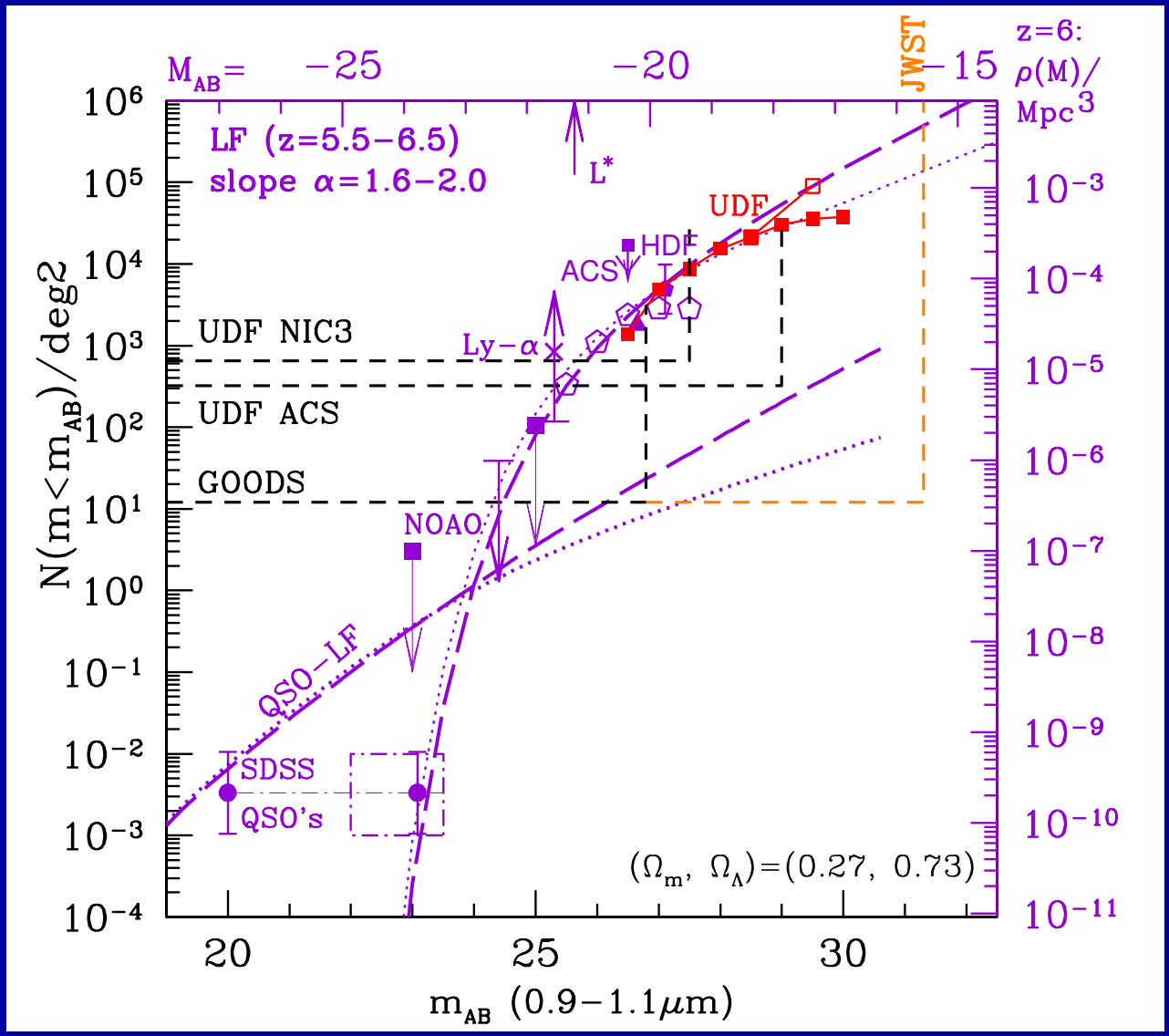

• HST/ACS has made significant progress at z$\simeq$6, surveying very large areas (GOODS, GEMS, COSMOS), or using very long integrations (HUDF). ACS can detect objects at z$\lesssim$6.5, but its discovery space A.Ω.Δlog(λ) cannot map the entire reionization epoch. NICMOS similarly is limited to z$\lesssim$8–10. JWST will be able to trace the entire reionization epoch.

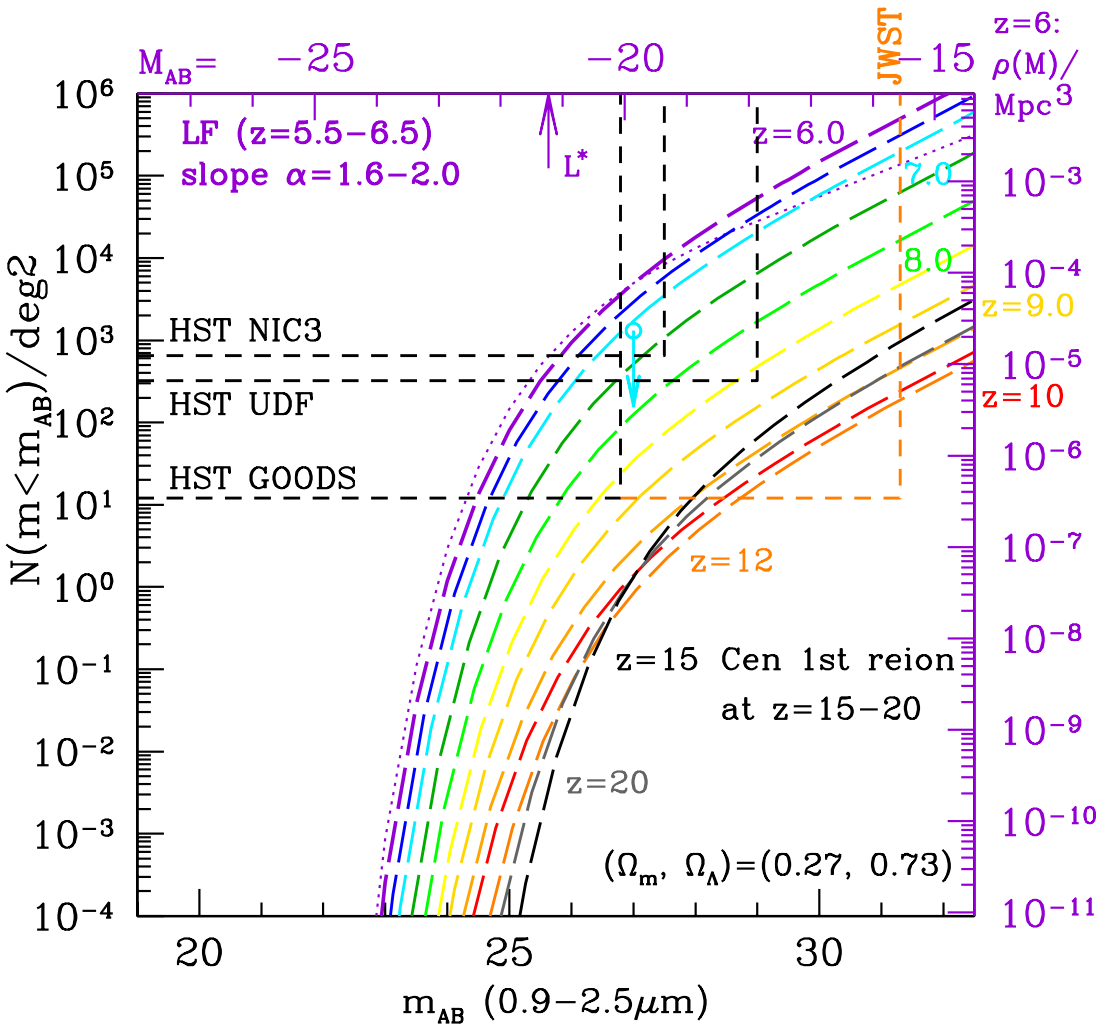

- With proper survey strategy (area AND depth), JWST can trace the entire reionization epoch and detect the first star-forming objects.
- Objects at $z \gtrsim 9$ are rare, since volume element is small and JWST samples brighter part of LF. JWST needs the quoted sensitivity/aperture (A), field-of-view (FOV$=\Omega$), and wavelength range (0.7-28 μm).

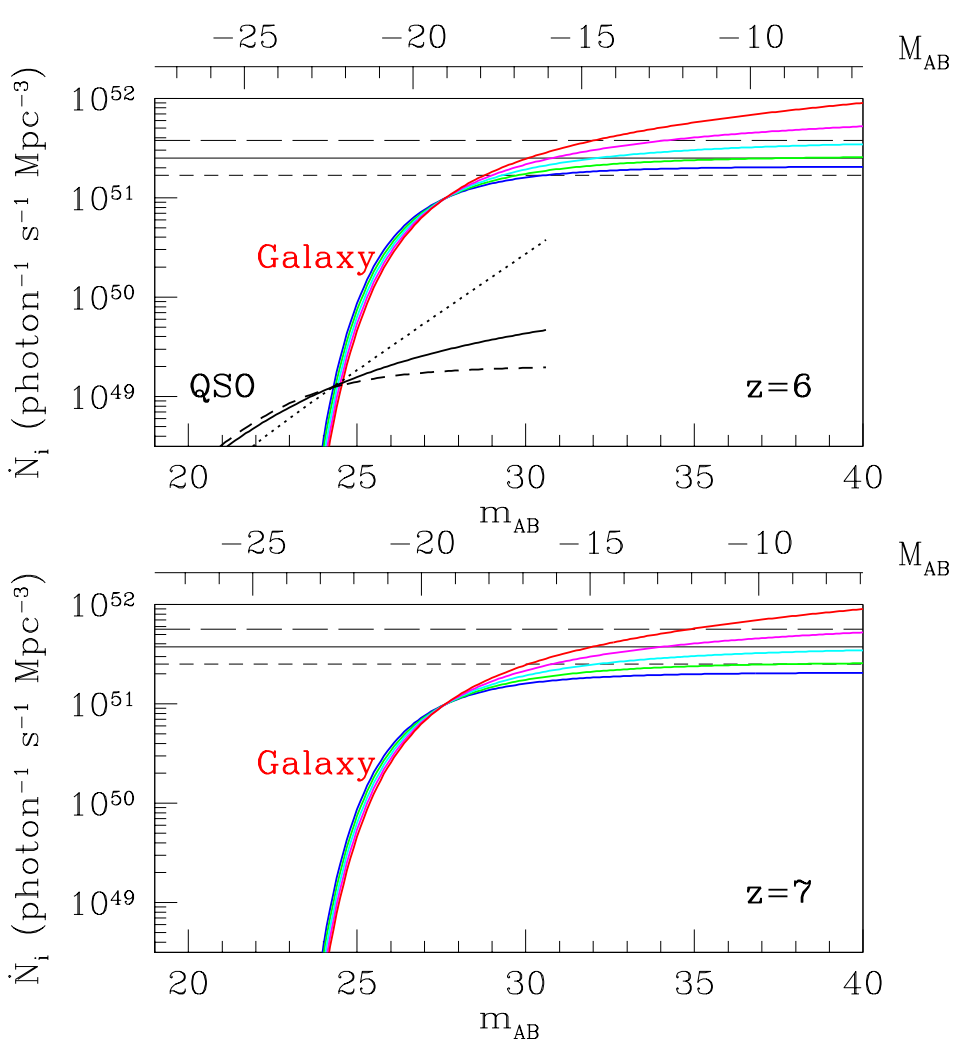

- A steep LF of z≃6 objects (Yan & Windhorst 2004a, ApJL, 600, L1) could provide enough UV-photons to complete the reionization epoch at z≃6.
- Pop II dwarf galaxies may not have started shining *pervasively* much before z≃7–8, or no H-I would be seen in the foreground of z≳6 quasars.
- JWST will measure this numerous population of dwarf galaxies from the end of the reionization epoch at z≃6 into the epoch of First Light (Pop III stars) at z≳10.

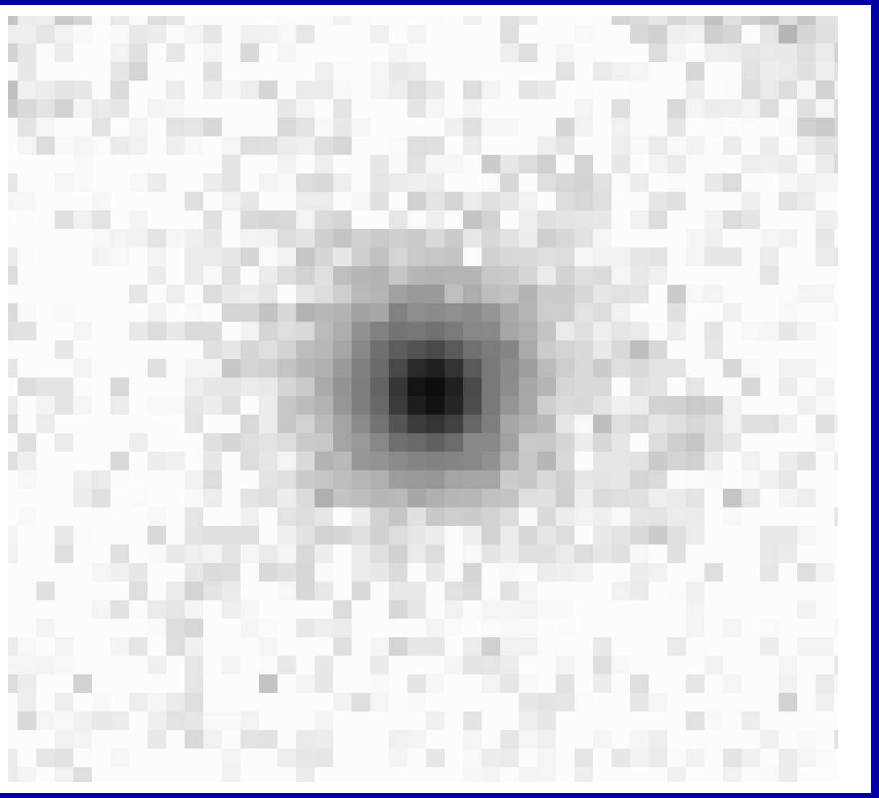

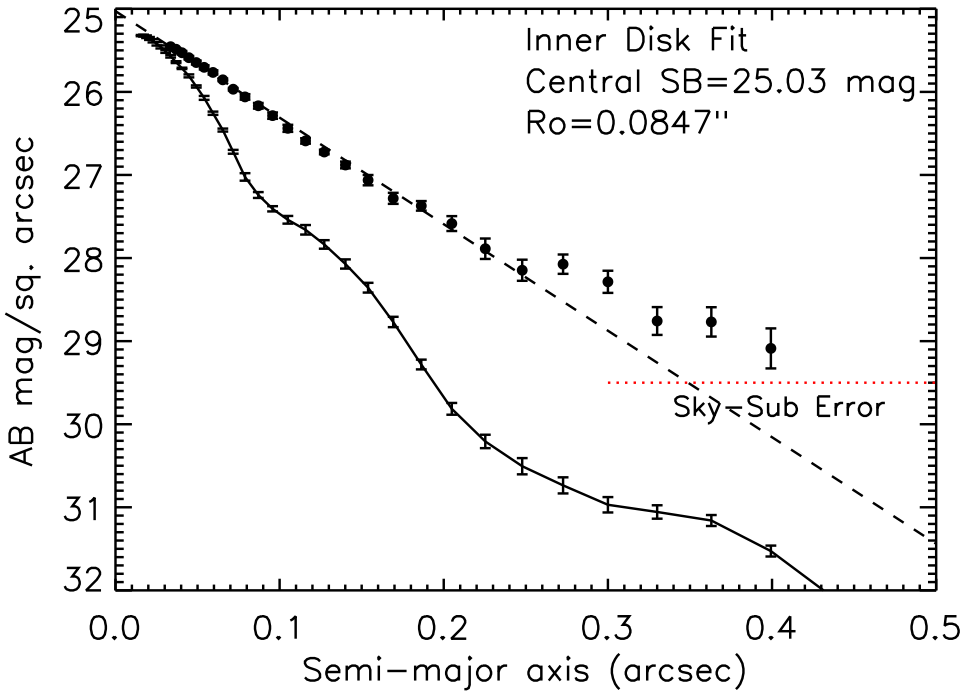

Sum of 49 isolated i-drops:
$=$5000 hrs HUDF z-band.
[$\simeq$ 330 hrs JWST 1 μm]

ACS light-profile, PSF and sky-error:
Deviates from exp. disk at $r_e \gtrsim 0''.25$
$\Rightarrow$ Dyn. age (z$\simeq$6) $\simeq$ 100-200 Myr
($cf.$ N. Hathi et al. 2006)

HST/ACS cannot accurately measure individual light-profiles at z$\simeq$6.

JWST can do this well for z$\gtrsim$6 in very long integrations.

Dynamical timescale $\simeq$ SED timescale $\Rightarrow$ Bulk of SF at $z_{form} \simeq 7.0 \pm 0.5$??

• (4) How JWST can measure Galaxy Assembly

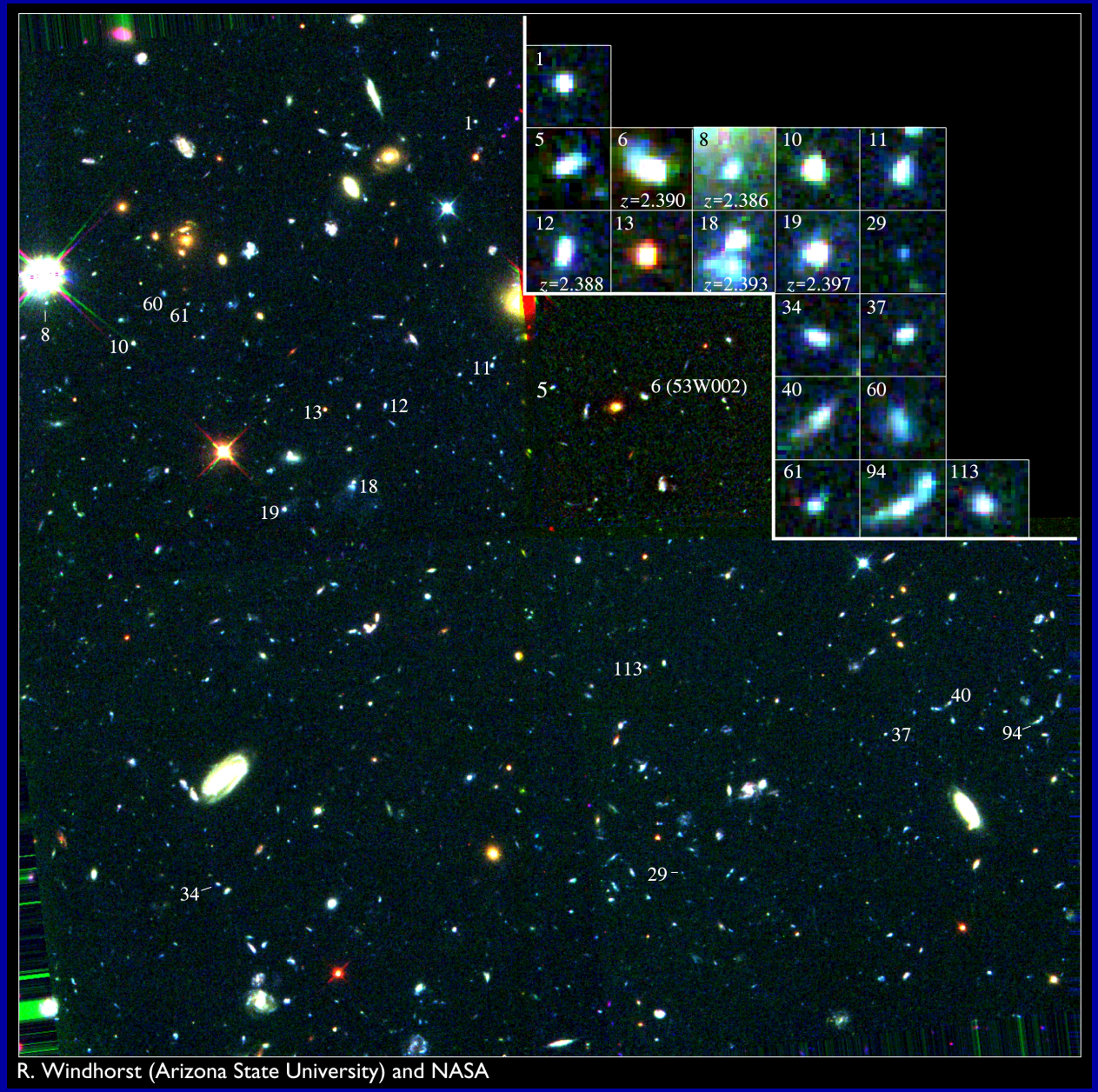

R. Windhorst (Arizona State University) and NASA

One of the remarkable discoveries of HST was how numerous and small faint galaxies are — the building blocks of the giant galaxies seen today.

THE HUBBLE DEEP FIELD CORE SAMPLE ($I < 26.0$)

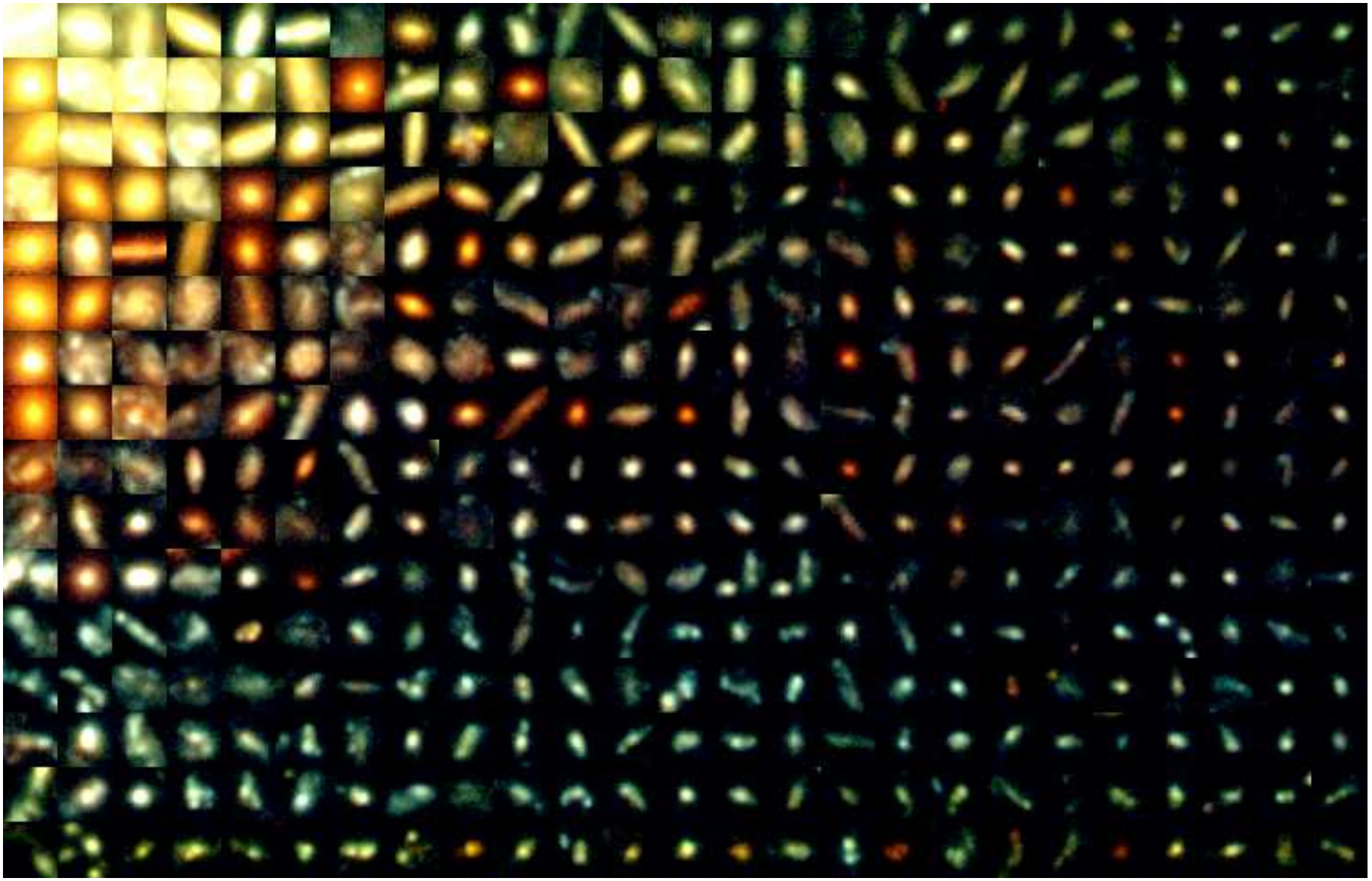

• (4) How JWST can measure Galaxy Assembly

• Galaxies of Hubble types formed over a wide range of cosmic time, but with a notable phase transition around $z \simeq 0.5$–1.0:

(1) Subgalactic units rapidly merge from $z \simeq 7 \longrightarrow 1$ to grow bigger units.

(2) Merger products start to settle as galaxies with giant bulges or large disks around $z \simeq 1$. These evolved mostly passively since then, resulting in the giant galaxies that we see today.

• JWST can measure how galaxies of all types formed over a wide range of cosmic time, by accurately measuring their distribution over rest-frame structure and type as a function of redshift or cosmic epoch.

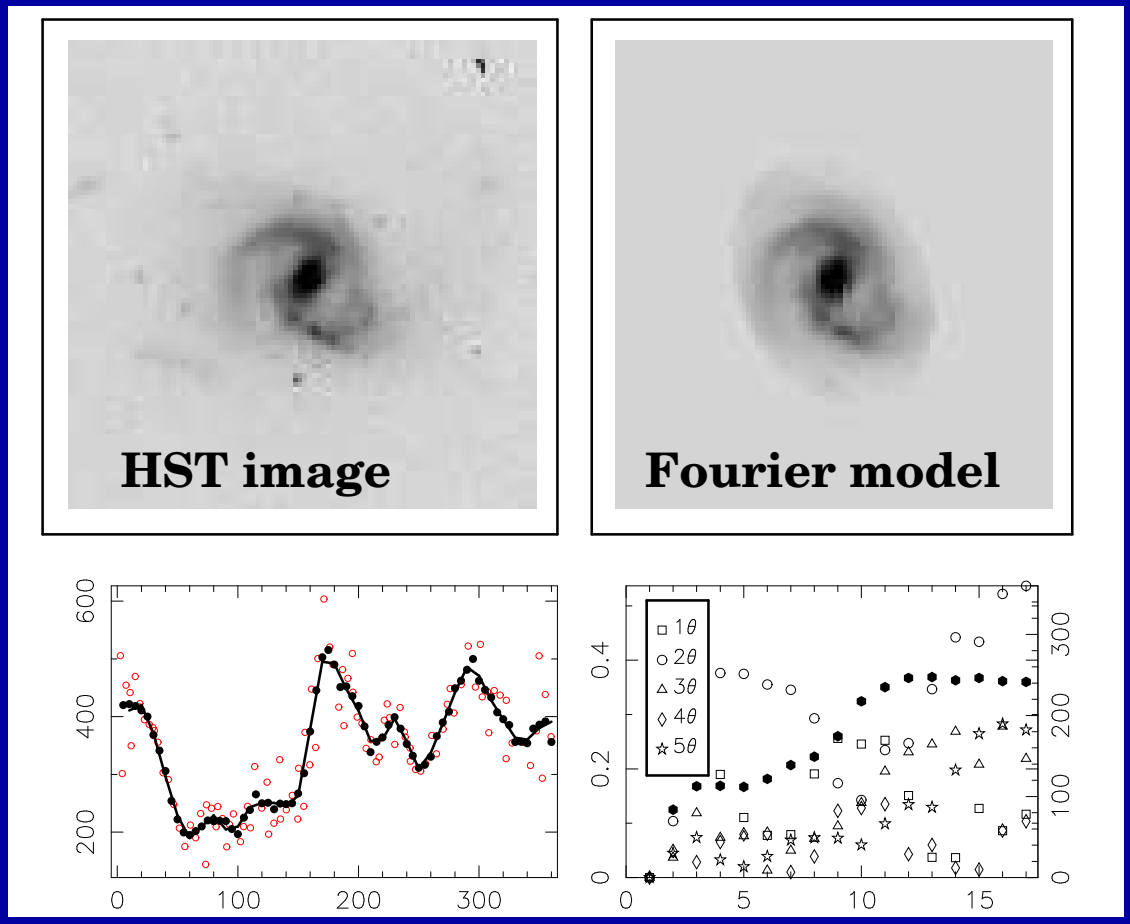

Fourier Decomposition is a robust way to measure galaxy morphology and structure in a quantitative way (Odewahn et al. 2002):

- (1) Fourier series are made in successive concentric annuli.
- (2) Even Fourier components indicate symmetric parts (arms, rings)
- (3) Odd Fourier components indicate asymmetric parts (bars etc).
- (4) JWST can measure the evolution of each feature directly.

Massive Star Formation: Near and Far

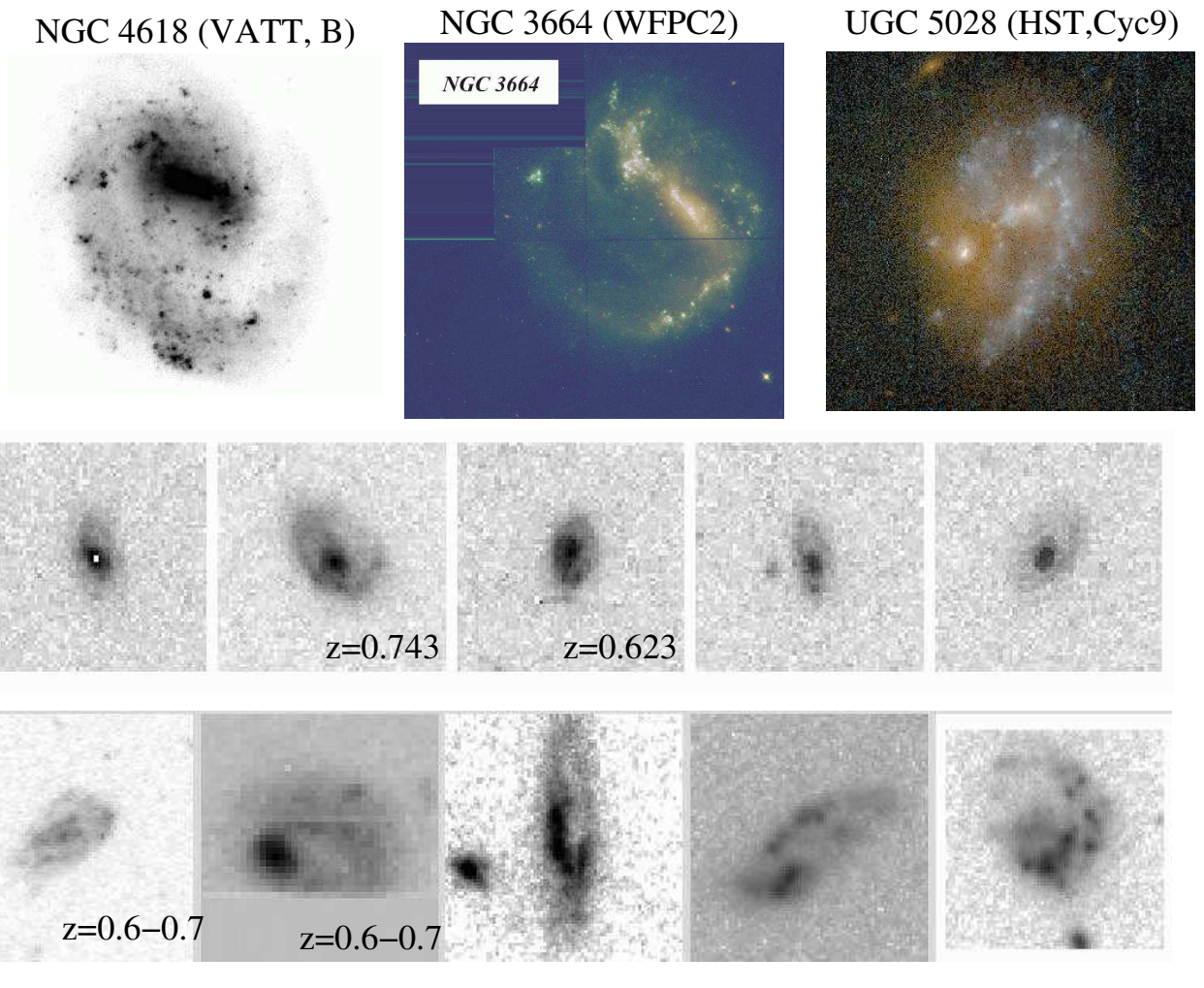

Fourier Decomposition of nearby and distant galaxies in JWST images will directly trace the evolution of bars, rings, spiral arms, and other structural features. This measures the detailed history of galaxy assembly in the epoch $z \simeq 1$–3 when most of today's giant galaxies were made.

Total Ell/S0 Sabc Irr/Mergers

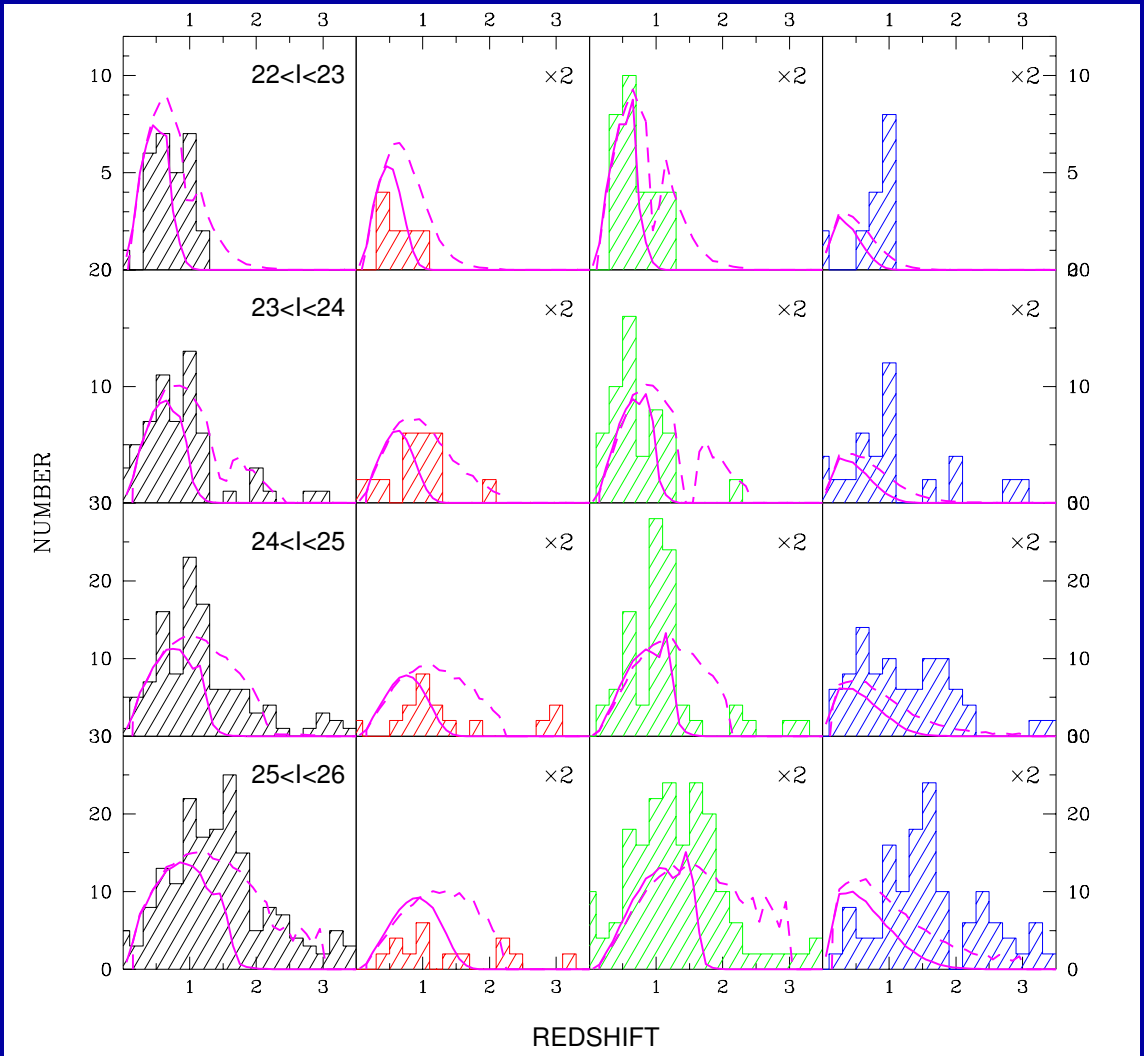

- JWST can measure how galaxies of all Hubble types formed over a wide range of cosmic time, by measuring their redshift distribution as a function of rest-frame type.
- For this, the types must be well imaged for large samples from deep, uniform and high quality multi-wavelength images, which JWST can do.

Driver et al. 1998, Astrophys. J. Letters, 496, L93

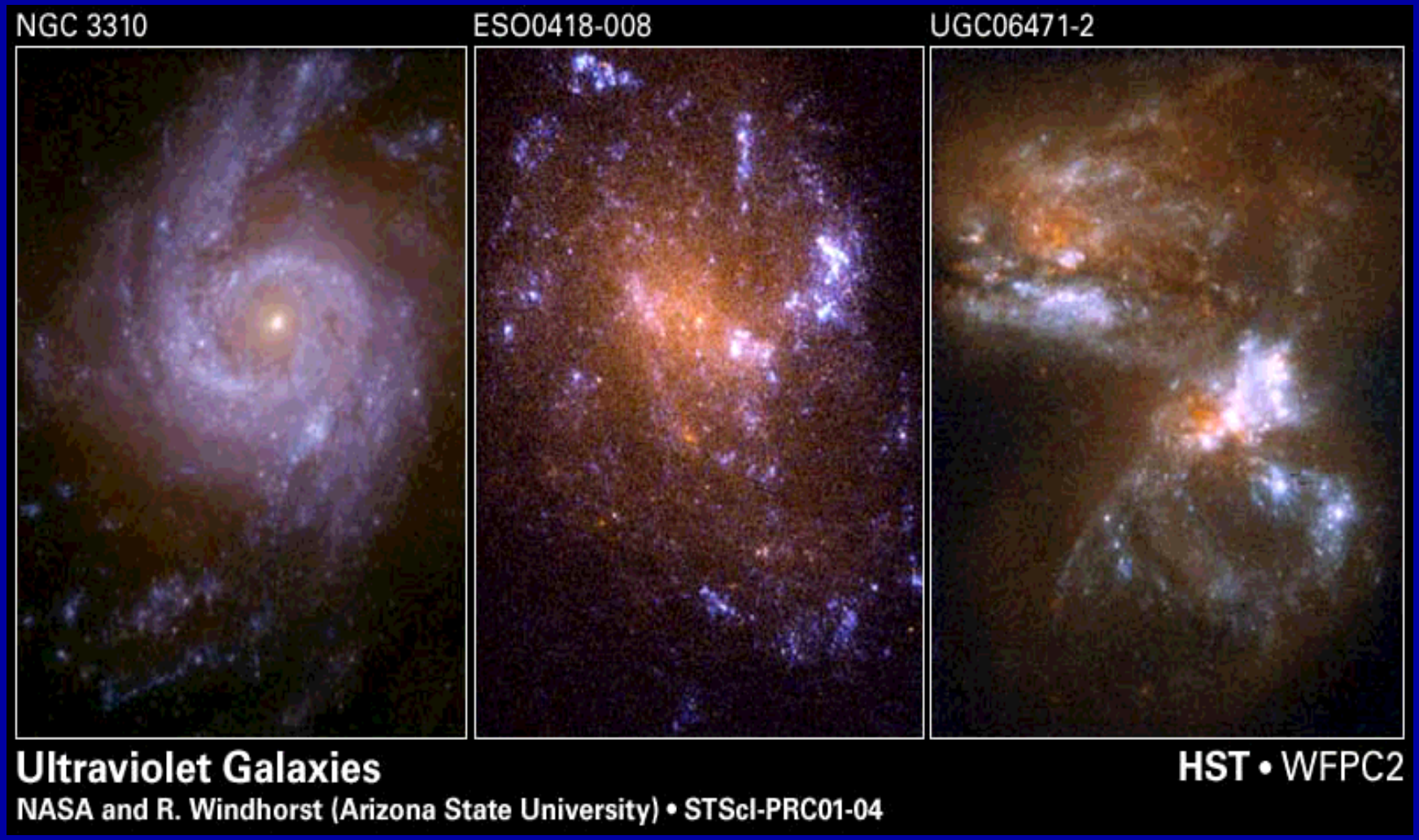

• The uncertain rest-frame UV-morphology of galaxies is dominated by young and hot stars, with often copious amounts of dust superimposed.

• This makes comparison with very high redshift galaxies seen by JWST complicated, although with good images a quantitative analysis of the restframe-wavelength dependent morphology and structure can be made.

Hubble UV image of galaxy NGC 6782: spectacular star-forming rings

(5) Predicted Galaxy Appearance for JWST at z≃1–15

HST z=0 JWST z=2 z=5 z=9 z=15

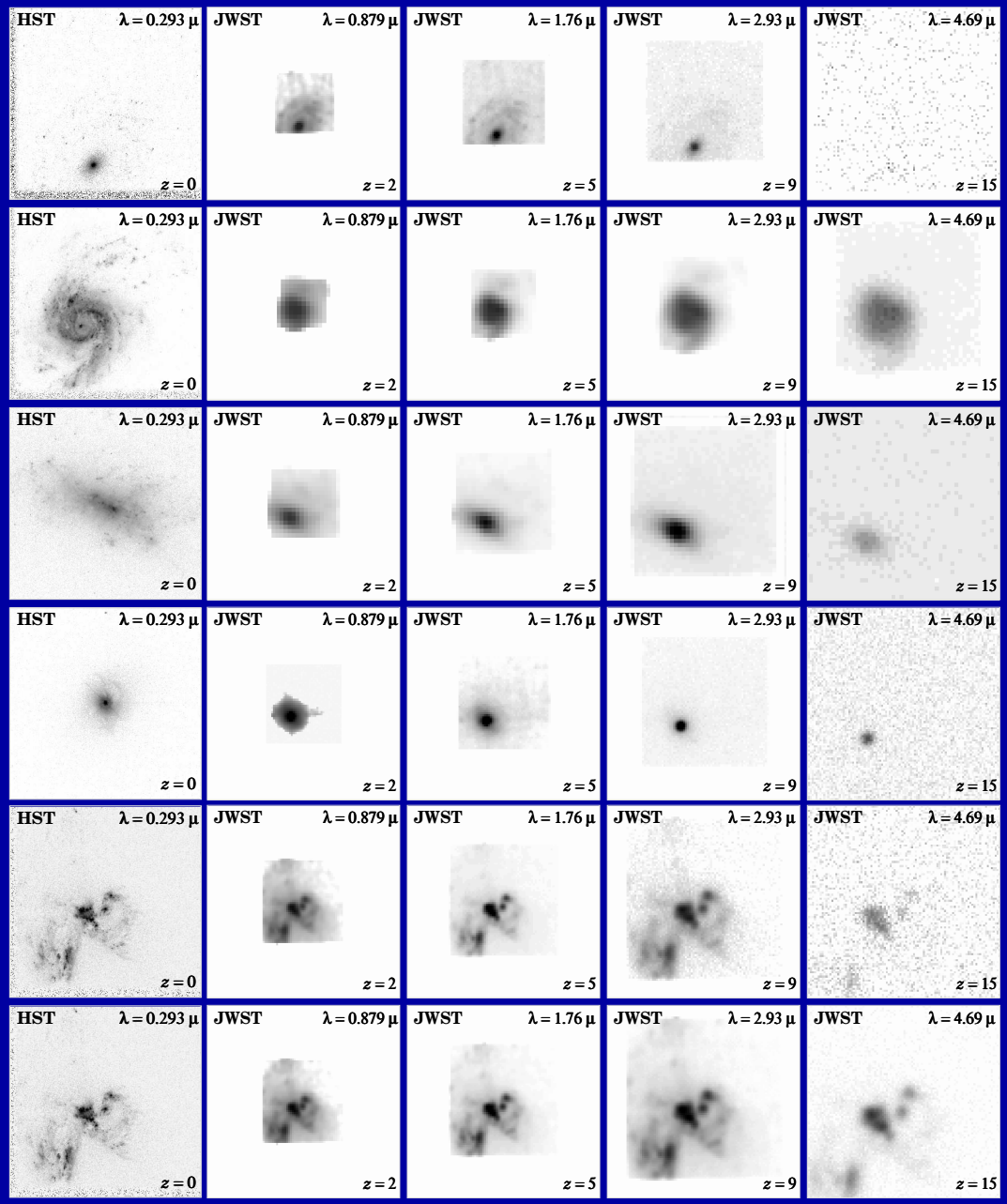

With proper restframe-UV training, JWST can quantitatively measure the evolution of galaxy morphology and structure over a wide range of cosmic time:

- (1) Most disks will SB-dim away at high z, but most formed at $z \lesssim z_{form} \simeq$1–2.
- (2) High SB structures are visible to very high z.
- (3) Point sources (AGN) are visible to very high z.
- (4) High SB-parts of mergers/train-wrecks are visible to very high z.

(6) Conclusions

(1) JWST Project is technologically front-loaded and well on track:

- Most items at Technical Readiness Level 6 (TRL-6) by Jan. 2007 ($i.e.$, demonstration in a relevant environment — ground or space).
- Technical Non-Advocate Review (T-NAR) in 2007 and Mission Preliminary Design Review (PDR) in March 2008.

(2) JWST will map the epochs of First Light, Reionization, and Galaxy Assembly in detail. It will determine:

- The formation and evolution of the first (reionizing) Pop III star-clusters.
- The origin of the Hubble sequence in hierarchical formation scenarios.

(3) JWST and SKA will (just) avoid the natural confusion limit.

- Courtesy of Hierarchical galaxy formation and $\mathbf{\Lambda}$. But corollary of this:
- Having $\lesssim 0\farcs1$ FWHM resolution is essential, since galaxy sizes$\simeq 0\farcs1$–$0\farcs2$.

SPARE CHARTS

- References and other sources of material shown:

http://www.jwst.nasa.gov/

http://www.stsci.edu/jwst/

http://www.jwst.nasa.gov/ISIM/index.html

http://ircamera.as.arizona.edu/nircam/

http://ircamera.as.arizona.edu/MIRI/

http://www.stsci.edu/jwst/instruments/nirspec/

http://www.stsci.edu/jwst/instruments/nirspec/mems.html

http://www.stsci.edu/jwst/instruments/guider/

Gardner, J. P., Mather, J. C., Clampin, M., Doyon, R., Greenhouse, M. A., Hammel, H. B., Hutchings, J. B., Jakobsen, P., Lilly,S. J., Long, K. S., Lunine, J. I., McCaughrean, M. J., Mountain, M., Nella, J., Rieke, G. H., Rieke, M. J., Rix, H.-W., Smith, E. P., Sonneborn, G., Stiavelli, M., Stockman, H. S., Windhorst, R. A., & Wright, G. S. 2006, Space Science Reviews, p. 1–80, in press (astro-ph/0606175)

Mather, J., Stockman, H. 2000, Proc. SPIE Vol. 4013, p. 2-16, in "UV, Optical, and IR Space Telescopes and Instruments", Eds. J. B. Breckinridge & P. Jakobsen (Berlin: Springer)

(7) Appendix: will JWST & SKA reach the Natural Confusion Limit?

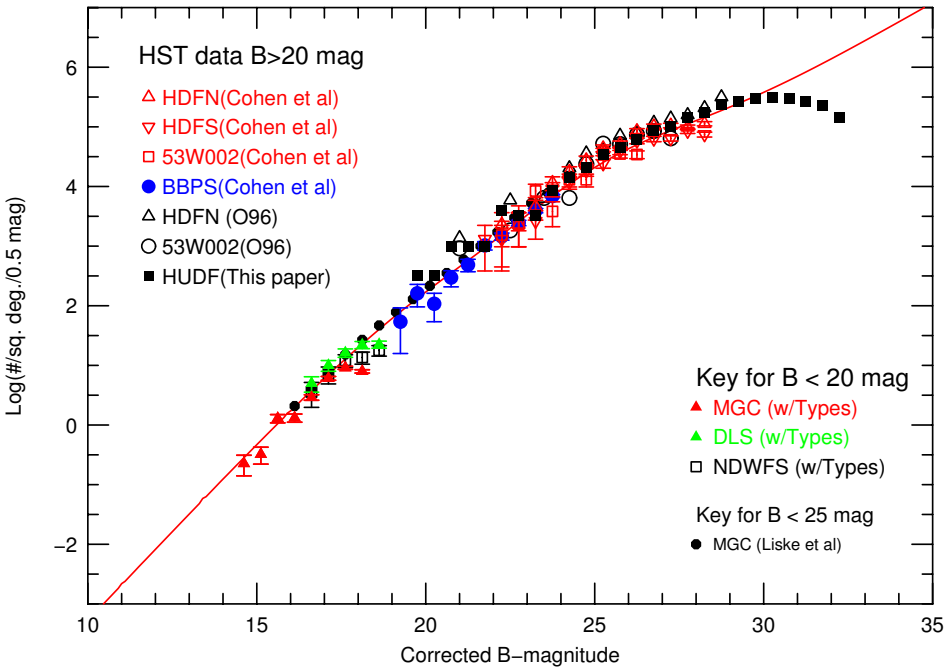

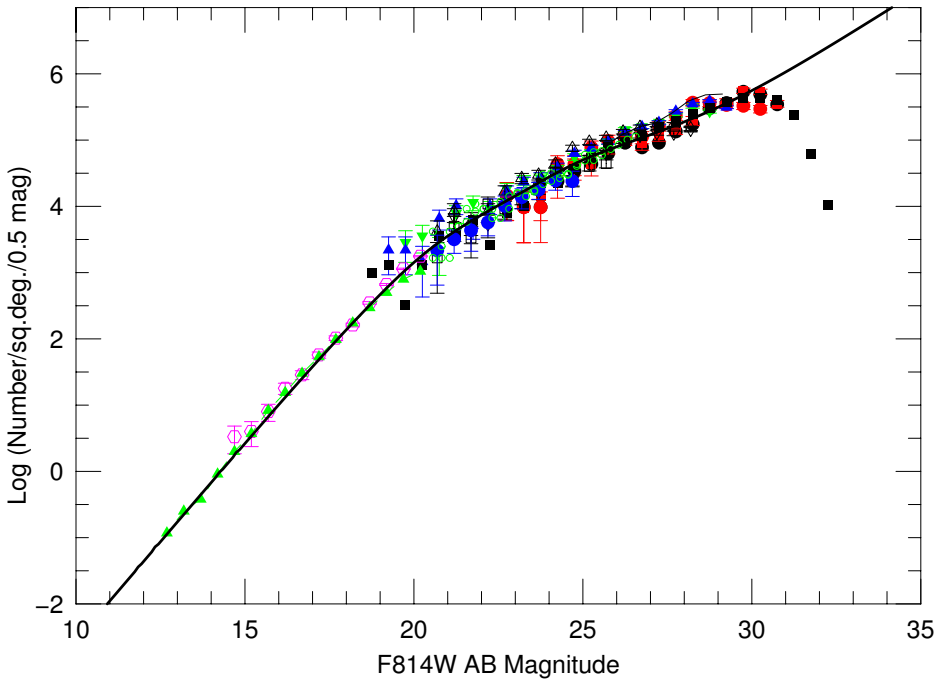

- HUDF galaxy counts (Cohen et al. 2006): expect an integral of $\gtrsim 2\times10^6$ galaxies/deg^2 to AB=31.5 mag ($\simeq$ 1 nJy at optical wavelengths). JWST and SKA will see similar surface densities to $\simeq$1 and 10 nJy, resp.
- $\Rightarrow$ Must carry out JWST and SKA nJy-surveys with sufficient spatial resolution to avoid object confusion (from HST: this means FWHM$\lesssim 0\farcs08$).
- $\Rightarrow$ Always obtain SKA HI line channels, so can disentangle overlapping continuum sources in redshifts space, and find all the enclosed HI.

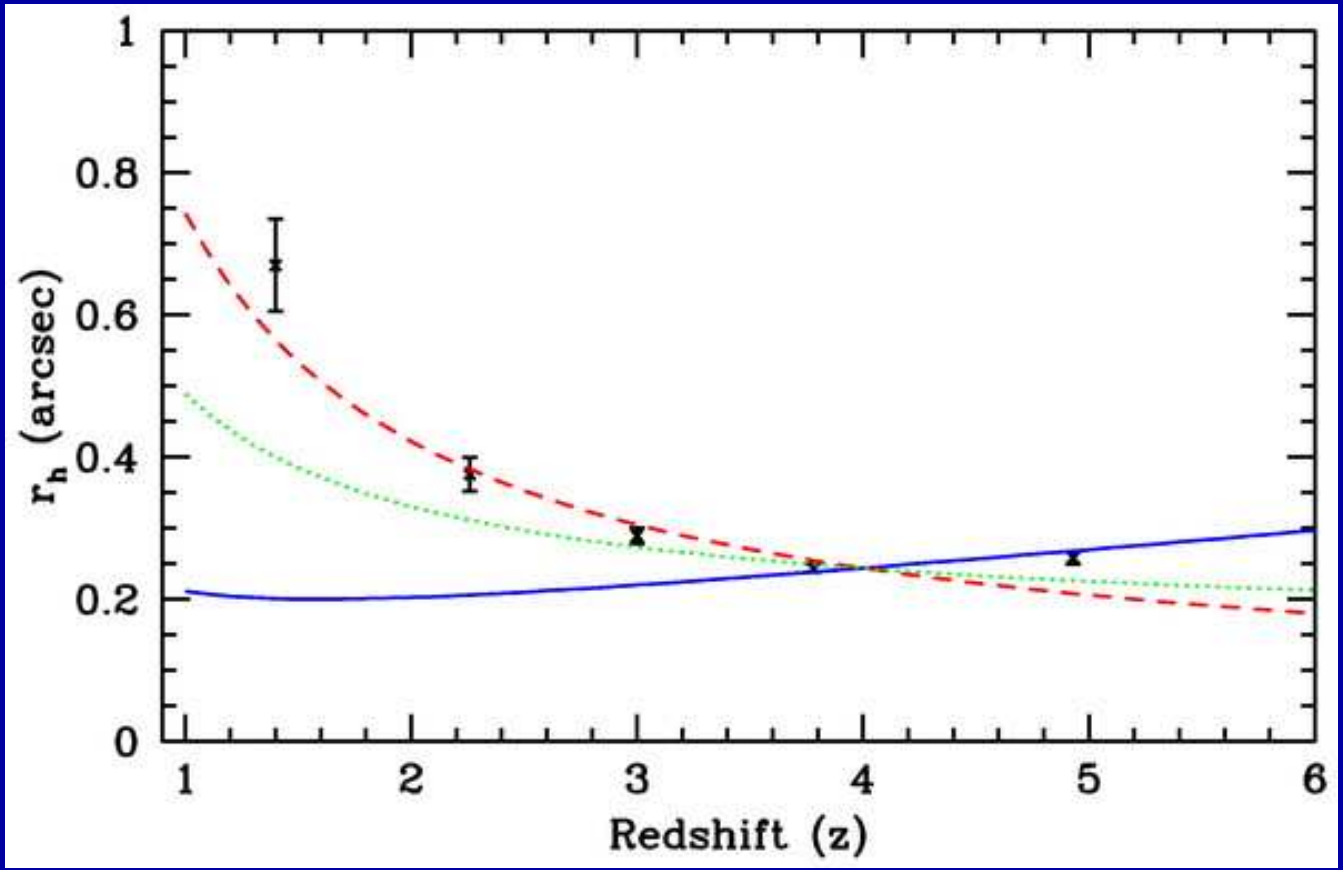

HST GOODS measured galaxy size evolution (Ferguson et al. 2004 ApJL):

- Median galaxy sizes decline steadily at higher redshifts, despite the cosmological Θ–z relation that minimizes at z$\simeq$1.6 for Λ-cosmology.
- Evidence of intrinsic size evolution: $r_{hl}(z) \propto r_{hl}(0)\ .\ (1+z)^{-s}$, $s \simeq 1$.
- Caused by hierarchical formation of galaxies, leading to intrinsically smaller galaxies at higher redshifts, where fewer mergers have occurred.
- SKA must anticipate the small $\lesssim 0\farcs15$ radio sizes of faint galaxies.

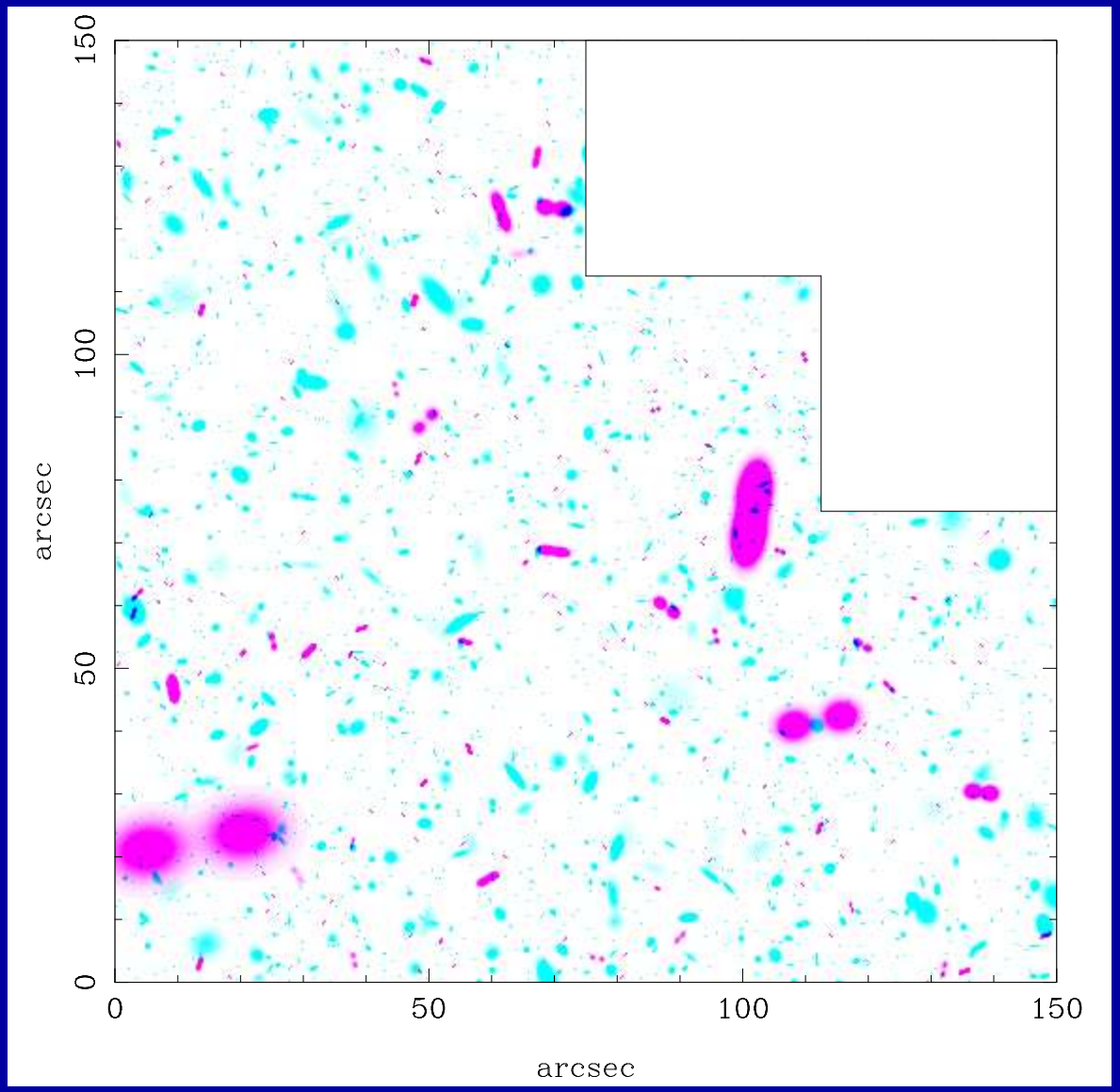

Simulated 12-hr SKA 1.4 GHz image: FWHM$\simeq$0$''$.1 and flux limit $\mathbf{0.1}$ μJy (5-σ). Of the 1 deg^2 FOV, only an HST/HDF area is shown (2$'$.5$\times$2$'$.5).

Red extended radio sources are AGN in early-type galaxies. Blue mostly point-like or disk-shaped sources reside in star-forming galaxies, which dominate the counts below 1 mJy. Normal spiral will dominate below 100 nJy.

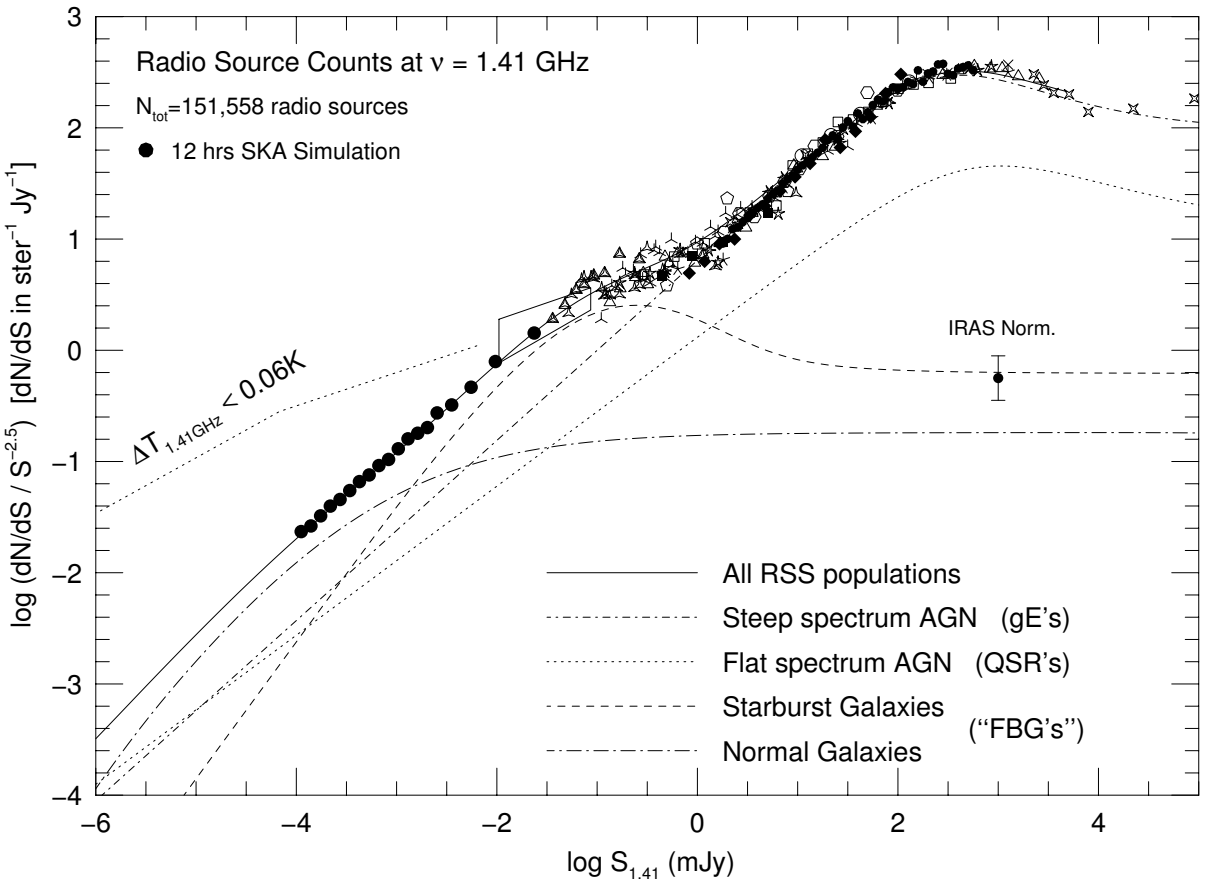

Normalized differential 1.41 GHz source counts (Windhorst et al. 1993, 2003; Hopkins et al. 2000) from 100 Jy down to 100 nJy. Filled circles below 10μJy show the 12-hr SKA simulation of Hopkins et al. (2006).

Models: giant ellipticals (dot-dash) and quasars dominate the counts to 1 mJy, starbursts (dashed) below 1 mJy. Normal spirals at cosmological distances (dot-long dash) will dominate the SKA counts below 100 nJy.

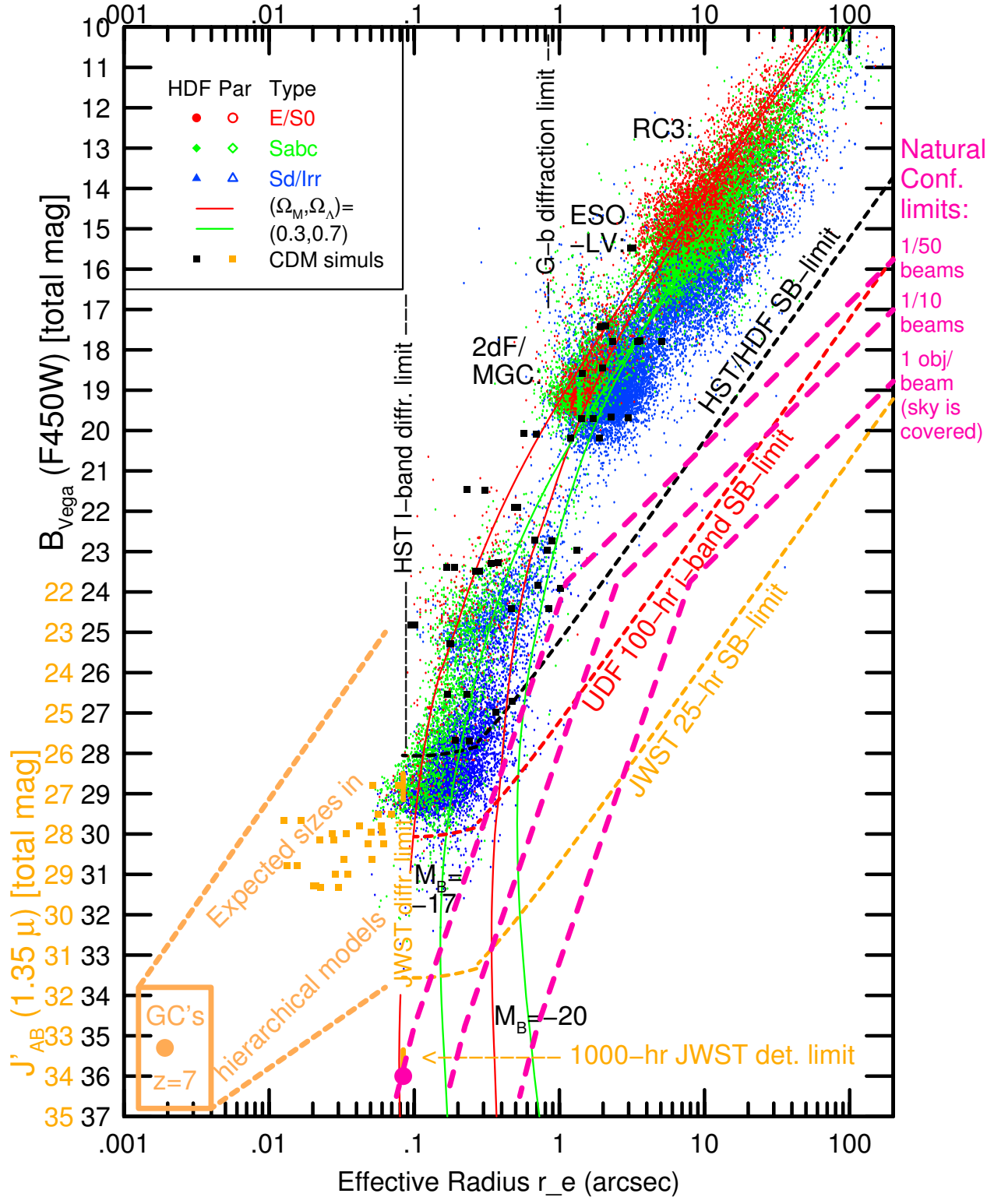
HDF Par Type
E/S0
Sabc
Sd/Irr
(ΩM,ΩΛ)=
(0.3,0.7)
CDM simuls
RC3:
ESO
–LV:
2dF/
MGC:
G–b diffraction limit
HST I–band diffr. limit
HST/HDF SB–limit
UDF 100–hr I–band SB–limit
JWST 25–hr SB–limit
JWST diffr. limit
Expected sizes in
hierarchical models
GC's
z=7
MB=
–17
MB=–20
1000–hr JWST det. limit
Natural
Conf.
limits:
1/50
beams
1/10
beams
1 obj/
beam
(sky is
covered)
BVega (F450W) [total mag]
J'AB (1.35 μ) [total mag]
Effective Radius r_e (arcsec)
.001
.01
.1
1
10
100

Combination of ground-based and space-based HST surveys show:

- (1) Apparent galaxy sizes decline from the RC3 to the HUDF limits:
- (2) At the HDF/HUDF limits, this is not due SB-selection effects (cosmological $(1+z)^4$-dimming), but instead due to:
- (2a) hierarchical formation causes size evolution: $r_{hl}(z) \propto r_{hl}(0)\,(1+z)^{-1}$
- (2b) increasing inability of object detection algorithms to deblend galaxies at faint mags ("natural" confusion $\neq$ "instrumental" confusion).
- (3) At AB$\gtrsim$30 mag, JWST and at $\gtrsim$10 nJy, SKA will see more than 2×10^6 galaxies/deg^2. Most of these will be unresolved ($r_{hl} \lesssim 0\farcs1$ FWHM. Since $z_{med}\gtrsim$1.5, this will significantly mitigate the $(1+z)^4$-dimming.

SKA needs to strike the right balance between having a resolution that is:

- High enough to disentangle the expected faint small HI and continuum sources from their neighbors, and
- Not so high that small HI and continuum sources at very redshifts are highly resolved, so as to mitigate the SB-dimming as much as possible.

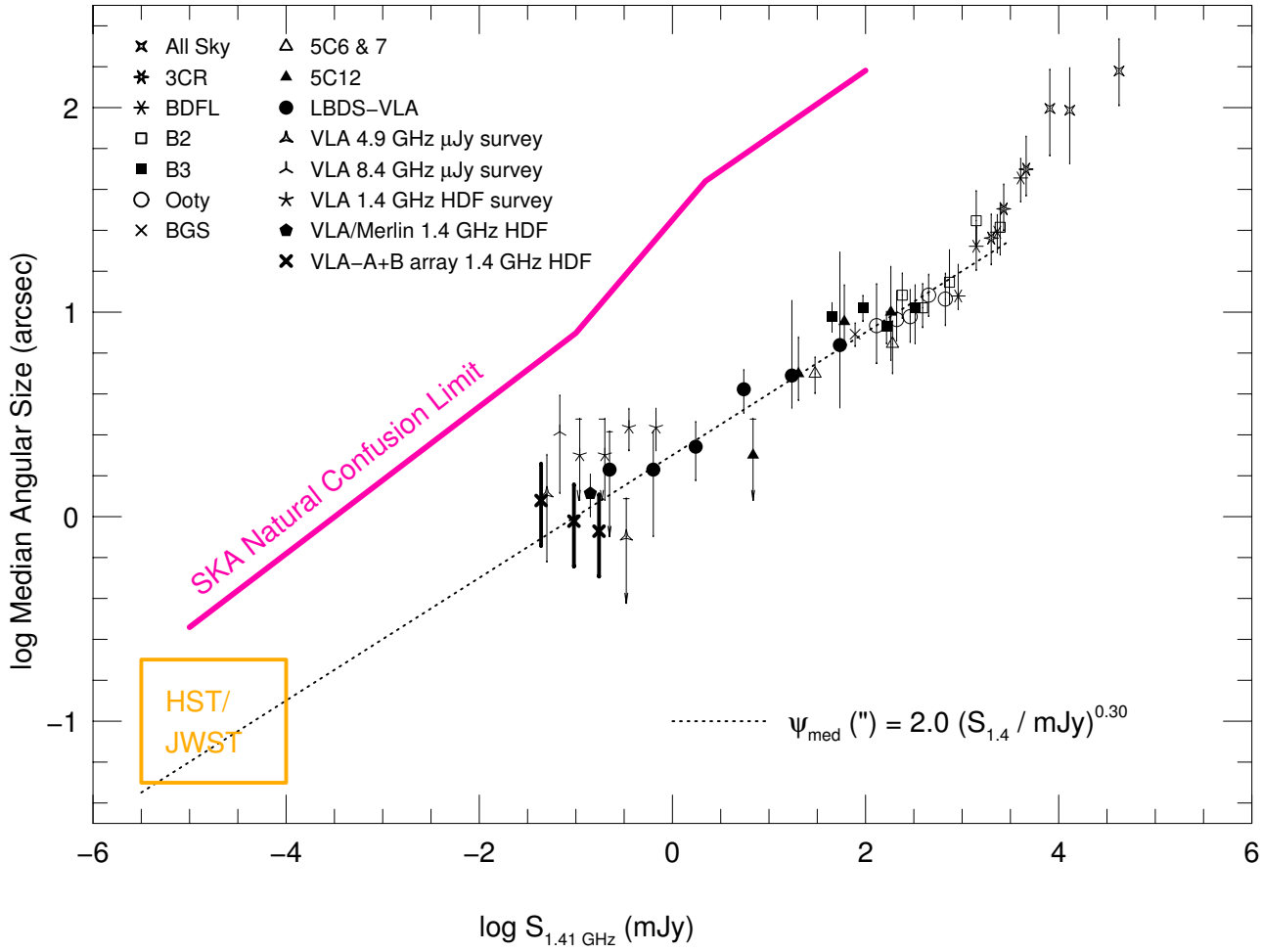

Median angular size vs. 1.41 GHz flux from 100 Jy down to 30 μJy (Windhorst et al. 2003). SKA sizes at 10–100 nJy are estimated from the HST N(r_{hl}) to AB=30 mag (3 nJy), where both detect $\gtrsim 10^6$ objects/deg^2.

Purple line is the natural confusion limit due to the intrinsic source sizes, above which sources unavoidably overlap. SKA needs $\sim$0$''$.10 FWHM resolution to best match the expected HI and radio continuum sizes.

MORE SPARE CHARTS

- (2) What instruments will JWST have?

The Near-Infrared Camera NIRCam made by an UofA + Lockheed + CSA consortium will do imaging from 0.6–5.3 μm using a suite of broad-, medium-, and narrow-band filters. NIRCam uses two identical and independently operated imaging modules, with two wavelengths observable simultaneously via a dichroic that splits the beam around 2.35 μm. Each of these two channels has an independently operated $2\farcm2 \times 4\farcm6$ FOV. Both channels are Nyquist-sampled: the short-wavelength channel at 2 μm with $0\farcs0317$/pixel, and the and long-wavelength at 4 μm with $0\farcs0648$/pixel. NIRCam's 10 2k×2k HgCdTe arrays will be passively cooled.

The Near-Infrared Spectrograph NIRSpec made by an ESA + GSFC consortium will do spectroscopy with resolving powers of R$\sim$100 in prism mode, of R$\sim$1000 in multi-object mode using a micro-electromechanical array system (MEMS) of micro-shutters that can open slitlets on previously imaged known objects, and of R$\sim$3000 using long-slit spectroscopy. All NIRSpec spectroscopic modes have a $\sim 3.4 \times 3.4'$ FOV.

- (2) What instruments will JWST have?

The Mid-Infra-Red Instrument MIRI made by an UofA + JPL + ESA consortium will do imaging and spectroscopy from 5–28 μm. MIRI is actively cooled by a cryocooler, which will cool it without using consumable gas.

The Fine Guidance Sensor (FGS) is made by CSA and provide stable pointing at the milli-arcsecond level. The FGS will have sufficient sensitivity and a large enough FOV to find guide stars with $\gtrsim$95% probability at any point in the sky. The FGS will have three simultaneously imaged fields of view of $2.3 \times 2.3'$, one of which feeds a pure guider channel, one feeding a guider channel plus a long-wavelength R$\sim$100 tunable filter channel with light split by a dichroic, and another feeding the short wavelength tunable filter R$\sim$100 channel.

JWST has fully redundant imaging and spectroscopic modes. It will not be serviced at L2, and therefore will undergo an extensive series of ground-testing and thermal vacuum testing in 2008–2009, after its main construction in 2004–2008. The main NASA contractor is Northrop Grumman Space Technology ("NGST") in Redondo Beach (CA).

Table 11. Science Instrument Characteristics

Instrument	Wavelength (μm)	Optical Elements	FPA	Plate Scale (milliarcsec/ pixel)	Field of View
NIRCam (Short Wavelength)	0.6 - 2.3	fixed filters (R~4, R~10, R~100), coronagraphic spots	Two 2×2 mosaics of 2048x2048 arrays	32	2.2×4.4 arcmin
NIRCam (Long Wavelength)[1]	2.4 - 5.0	fixed filters (R~4, R~10, R~100), coronagraphic spots	Two 2048×2048 arrays	65	2.2×4.4 arcmin
NIRSpec (prism, R=100)	0.6 - 5.0	Transmissive slit mask: four 384×175 micro-shutter array, 250 (spectral) by 500 (spatial) milliarcsec; fixed slits 200 or 300 mas wide by 4 arcsec long	Two 2048×2048 arrays	100	3.4×3.1 arcmin
NIRSpec (grating, R=1000)	1.0-5.0				
NIRSpec (IFU, R=3000)	1.0-5.0	Integral field unit			3.0×3.0 arcmin
MIRI (imaging)	5 - 27	Broad-band filters, coronagraphic spots & phase masks	1024×1024	110	1.4×1.9 arcmin (26×26 arcsec coronographic)
MIRI (prism spectroscopy)	5 - 10	R ~ 100			
MIRI (spectroscopy)	5 - 27	Integral field spectrograph (R~3000) in 4 bands	Two 1024×1024 arrays	200 to 470	3.6×3.6 arcmin to 7.5×7.5 arcmin
TFI (Short-wavelength)	1.2 - 2.4	Order-blocking filters+etalon (R~100)	2048×2048	68	2.3×2.3 arcmin
TFI (Long-wavelength)[2]	2.5 – 4.8	Order-blocking filters+etalon (R~100)	2048×2048	68	2.3×2.3 arcmin

NOTE: [1]Use of a dichroic renders the NIRCam long-wavelength field of view co-spatial with the short wavelength channel, and the two channels acquire data simultaneously.

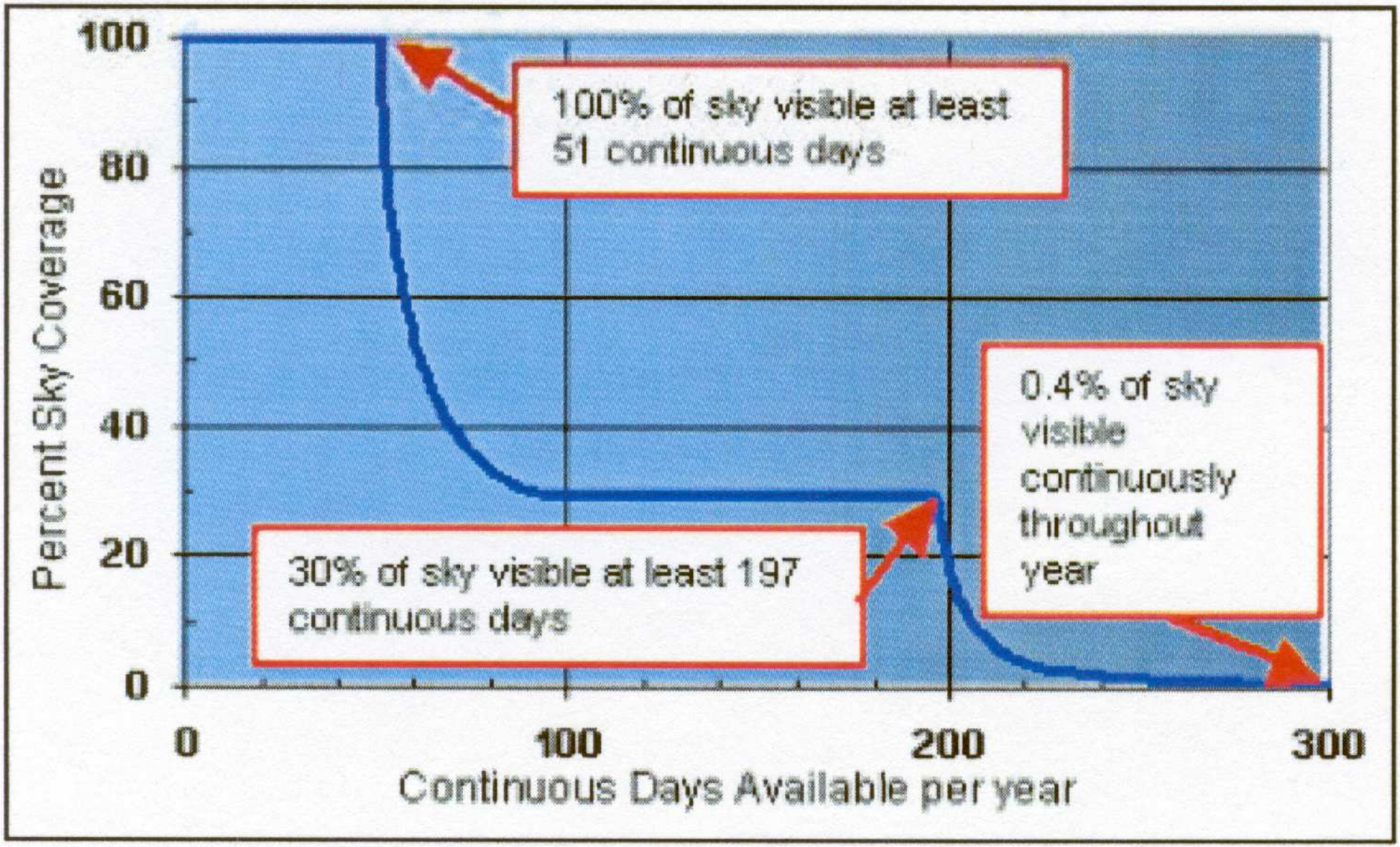

Figure 29. Sky coverage and continuous visibility.

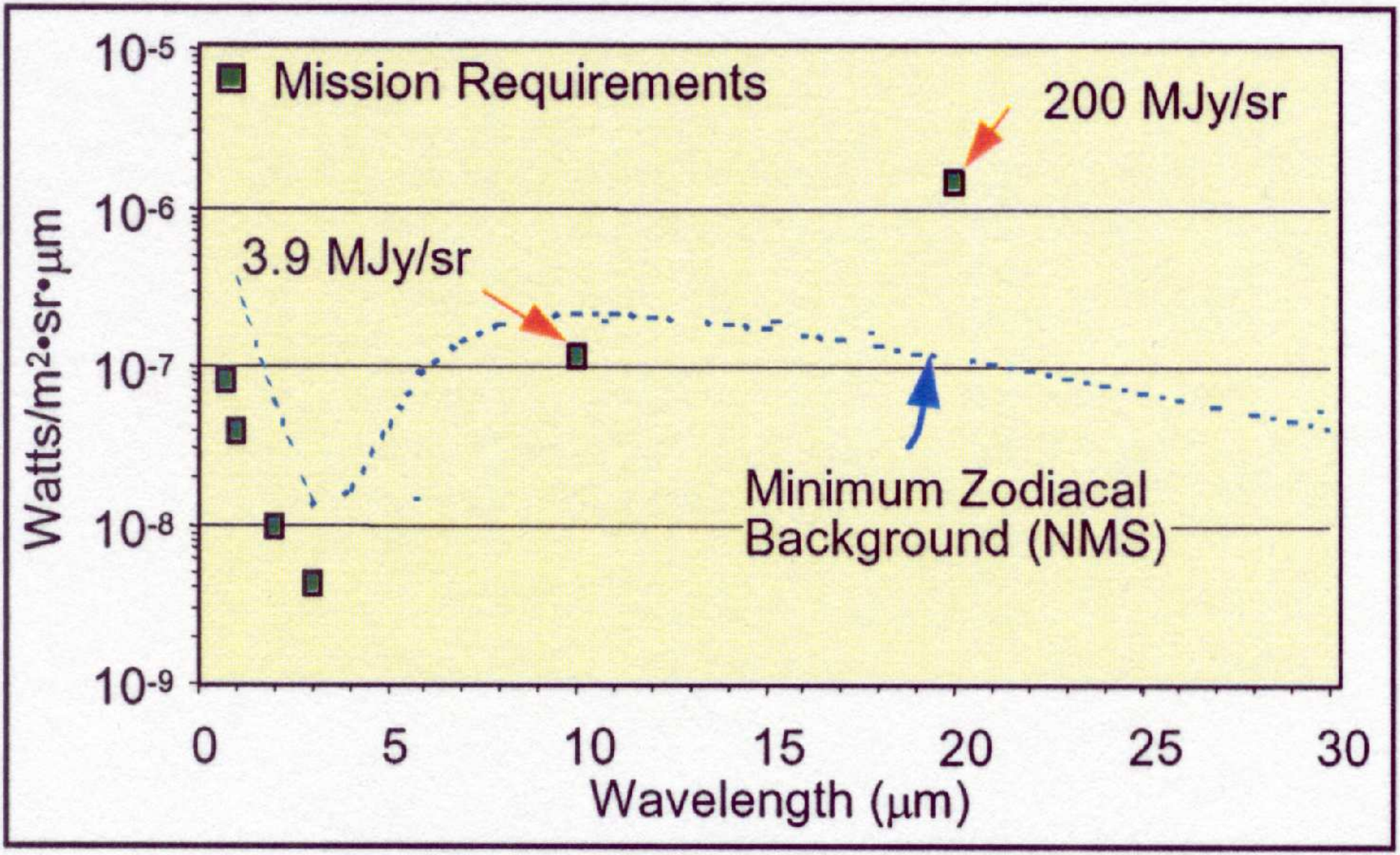

JWST L2 sky minimizes $\lambda \simeq 3$ μm: $\gtrsim 10^4\times$ fainter than ground-based sky!

Telescope FOV	~ 166 square arcminutes FOV. ISIM instruments share FOV with common aperture
Orbit	Lissajous orbit about L2
Celestial Sphere Coverage	100% annually 39.7% at any given time 100% of sphere has at least 51 contiguous days visibility 30% for > 197 days Continuous within 5 degrees of ecliptic poles
Overall Observing Efficiency	Observatory ~ 80.7%
Mission Life	5-year minimum lifetime 11 years for fuel Commissioning in less than 6 months
Schedule	August 2011 launch

Table 6. Required Sensitivity Values

Wave-length (μm)	Instrument / Mode	Sensitivity	Equivalents
1.1	NIRCam	1.21×10^{-34} $Wm^{-2}Hz^{-1}$ SN=10 in 10,000 s or less and R=4 bandwidth	12.1 nJy, AB=28.7
2	NIRCam	1.04×10^{-34} $Wm^{-2}Hz^{-1}$ SN=10 in 10,000 s or less and R=4 bandwidth	10.4 nJy, AB=28.9
3.5	TFI	3.68×10^{-33} $Wm^{-2}Hz^{-1}$ SN=10 in 10,000 s or less and R=100 bandwidth	368 nJy, AB=25.0
3.0	NIRSpec/ Low Res	1.2×10^{-33} $Wm^{-2}Hz^{-1}$ SN=10 in 10,000 s or less and R=100 bandwidth	120 nJy, AB=26.2
2.0	NIRspec/ Med Res	5.2×10^{-22} Wm^{-2} SN=10 in 100,000 s or less and R=1000 bandwidth	5.2×10^{-19} erg s^{-1} cm^{-2}
10	MIRI/ Broad-Band	7.0×10^{-33} $Wm^{-2}Hz^{-1}$ SN=10 in 10,000 s or less and R=5 bandwidth	700 nJy, AB=24.3
21	MIRI/ Broad-Band	7.3×10^{-32} $Wm^{-2}Hz^{-1}$ SN=10 in 10,000 s or less and R=4.2 bandwidth	7.3 μJy, AB=21.7
9.2	MIRI/ Spect.	1.0×10^{-20} Wm^{-2} SN=10 in 10,000 s or less and R=2400 bandwidth	1.0×10^{-17} erg s^{-1} cm^{-2}
22.5	MIRI/ Spect.	5.6×10^{-20} Wm^{-2} SN=10 in 10,000 s or less and R=1200 bandwidth	5.6×10^{-17} erg s^{-1} cm^{-2}

Note: "Sensitivity" is defined to be the brightness of a point source detected with the signal-to-noise ratio and integration time specified. Targets at the North Ecliptic Pole are assumed.

Table 1. JWST Measurements for the End of the Dark Ages Theme

Observation	Primary Instrument	Magnitude or flux	Target Density
Ultra-deep survey, SNe	NIRCam	AB = 31 mag	1 arcmin^{-2}
In-depth study	NIRSpec MIRI	AB = 28 mag, R~100 AB = 28 mag	1 arcmin^{-2} 1 arcmin^{-2}
Ly α forest diagnostics	NIRSpec	2 x 10^{-19} erg cm^{-2} s^{-1}, R~1000	Individual
Transition in Ly α properties	TFI	2 x 10^{-19} erg cm^{-2} s^{-1}, R~1000	1 arcmin^{-2}
Transition in Ly α/Balmer	NIRSpec	2 x 10^{-19} erg cm^{-2} s^{-1}, R~1000	1 arcmin^{-2}
Measure ionizing continuum	NIRSpec	2 x 10^{-19} erg cm^{-2} s^{-1}, R~1000	1 arcmin^{-2}
Ionization source nature	NIRSpec MIRI		
LF of dwarf galaxies	NIRCam	AB = 31 mag	

Table 2. JWST Measurements for the Assembly of Galaxies Theme

Topic	Primary Instrument	Key Observation	Magnitude or Flux	Target Density
Faint galaxy identification and morphology	NIRCam	Detect the SMC at z = 5 in rest-frame V	L_{AB} = 30.3 mag	100 arcmin^{-2}
Metallicity determination	NIRSpec	Determine R_{23} from emission line ratios for galaxy with SFR = 3 $M_{\odot}$/yr at z = 5	5×10^{-19} erg s^{-1} cm^{-2}	100 arcmin^{-2}
Scaling relations	MIRI spectroscopy (short wavelength)	Measure stellar velocity dispersion for R_{AB}=24.5 Lyman Break galaxy at z = 3	AB (9μm) = 21.3 mag	1 arcmin^{-2}
Obscured galaxies	MIRI spectroscopy (long wavelength)	Measure [NeVI] in ULIRG with Arp220 L_{bol} assuming Circinus spectrum	1.4×10^{-19} Wm^{-2}	Individual

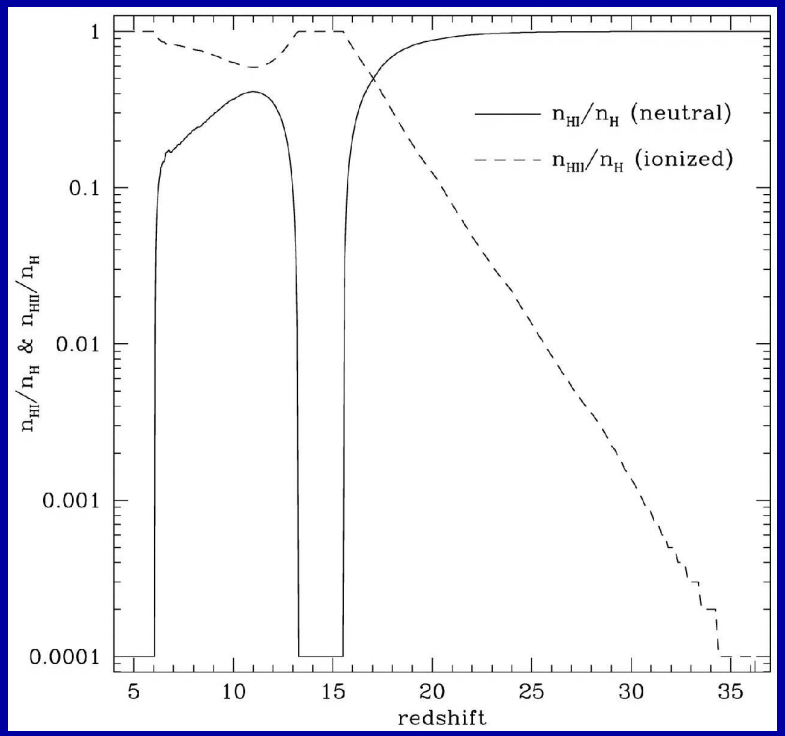

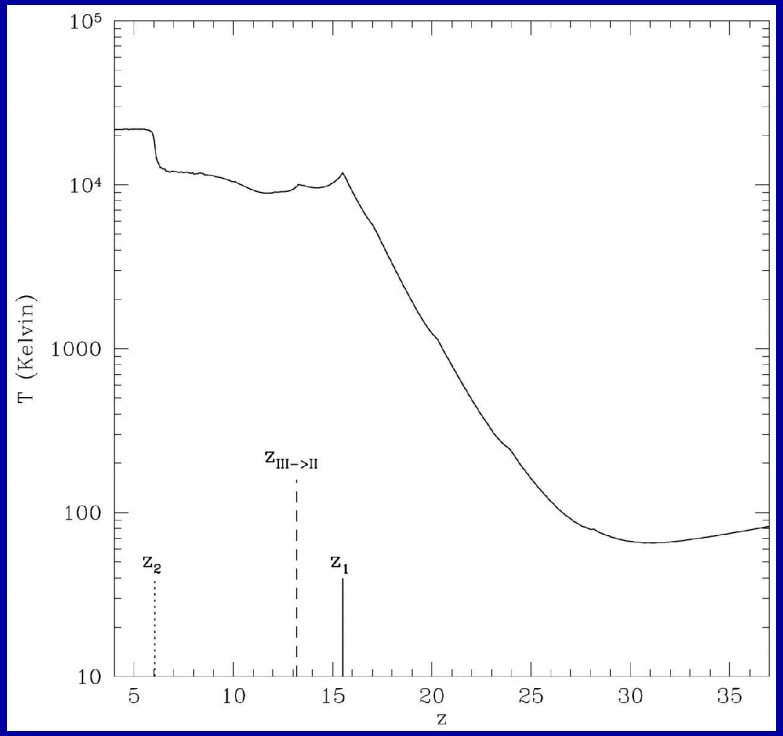

WMAP and detailed Hydrodynamical models (Cen 2003) suggest that:

- (1) Population III stars caused epoch of First Light at z≃11–20.
- (2) Pop III supernovae may have caused the Second Dark Ages at z=9–11, since they heated the IGM, which could not cool until:
- (3) The first Pop II stars started forming in dwarf galaxies with 10^7–10^9 $M_\odot$ at z≃6–9.

$\Rightarrow$ This will be visible to JWST in the luminosity function (LF) of the first star-forming objects at z≃20$\longrightarrow$6.

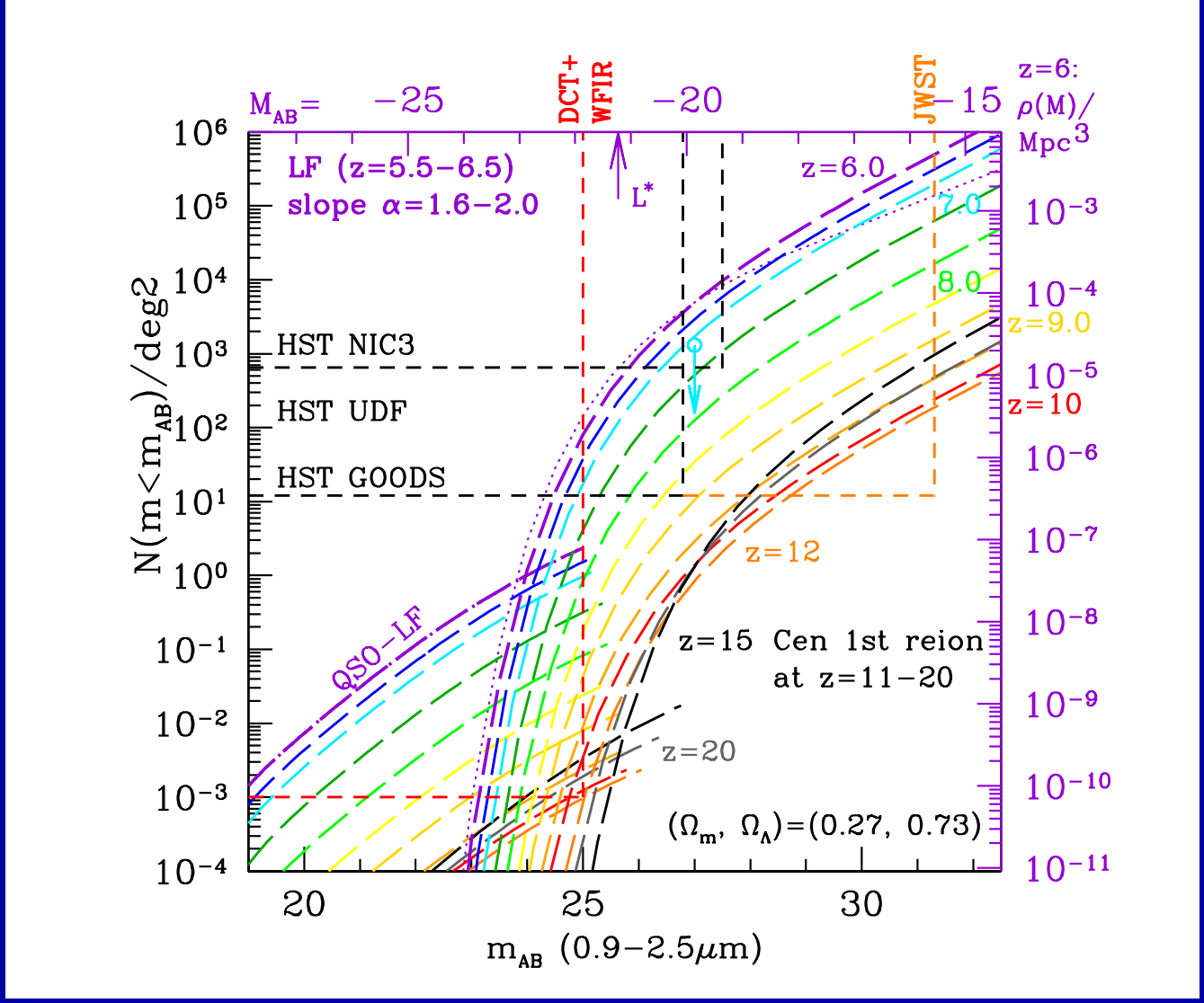

• Red boundaries indicate part of the galaxy and QSO LF that 4–10m class telescopes with WF IRCam can explore to z=10 and AB$\lesssim$25 mag.

• A ground-based wide-field near-IR survey to AB$\lesssim$25 mag z$\lesssim$10 is an essential complement to the JWST First Light studies:

Co-evolution of supermassive black-holes and proto-bulges for z$\lesssim$10.

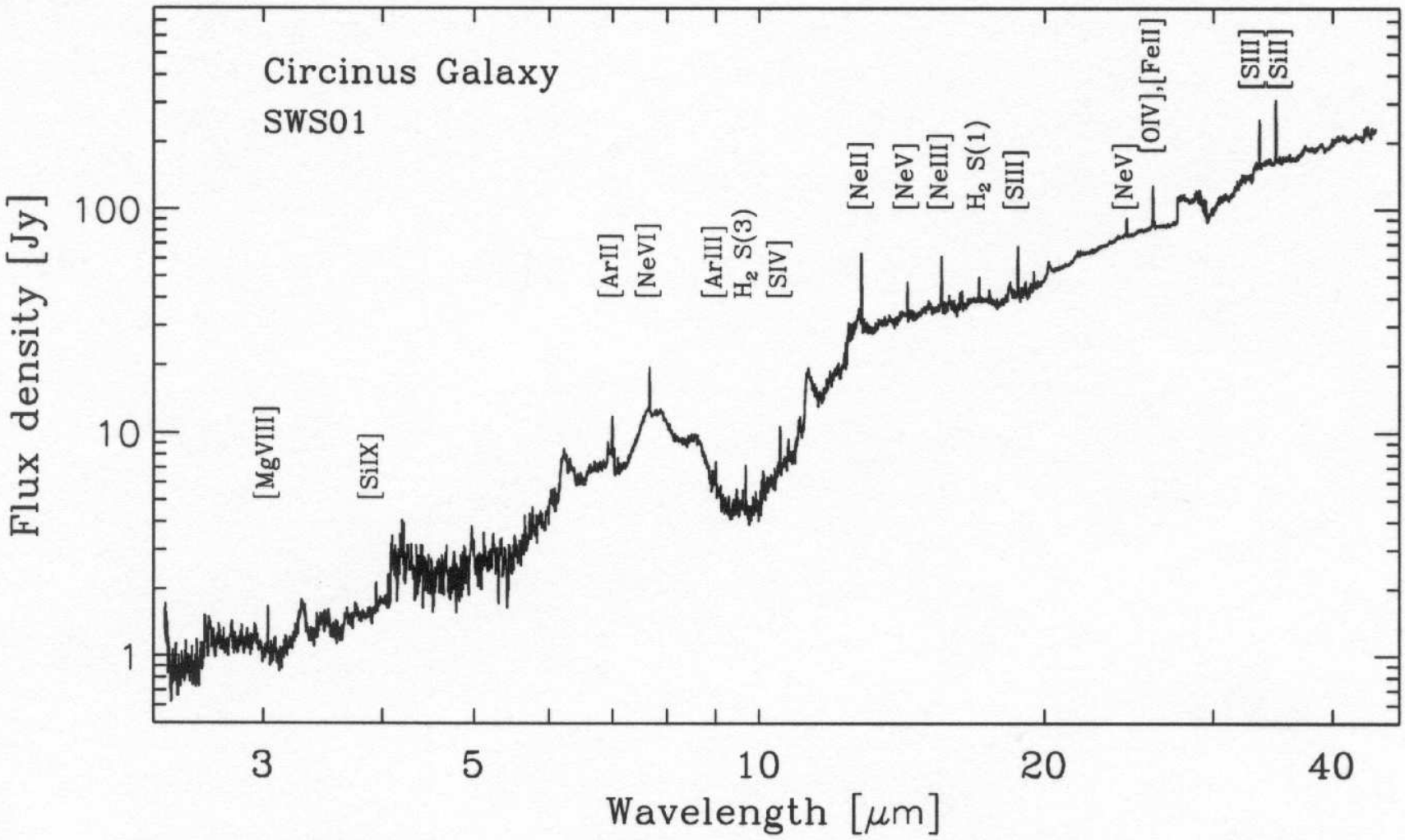

Figure 9. ISO Circinus Spectrum. Mid-infrared spectrum of the Circinus galaxy taken with ISO shows an abundance of emission lines useful for diagnosing the energy sources which power ULIRGs (From Moorwood et al. 1996).

Quantitative Morphology – We can numerically describe and identify m=1 galaxies!

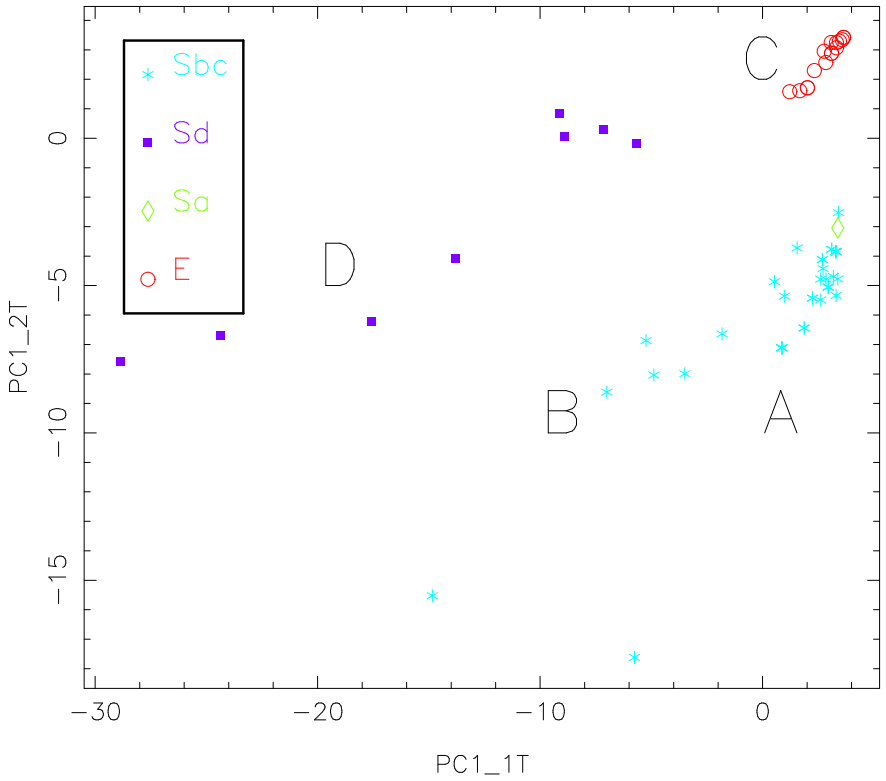

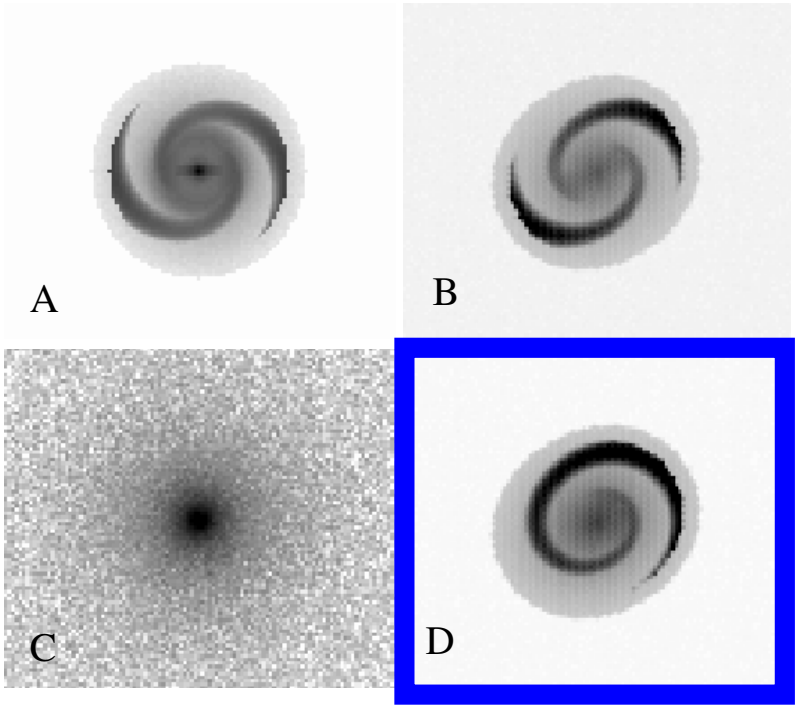

Odewahn et.al. 2002 ApJ, 568, 539

Fourier Decomposition is remarkably good in distinguishing and quantifying bars and (1-armed, 2-armed) spiral structure. JWST will be able to do this out to z=5 at least, hence enabling to quantitatively trace galaxy assembly.

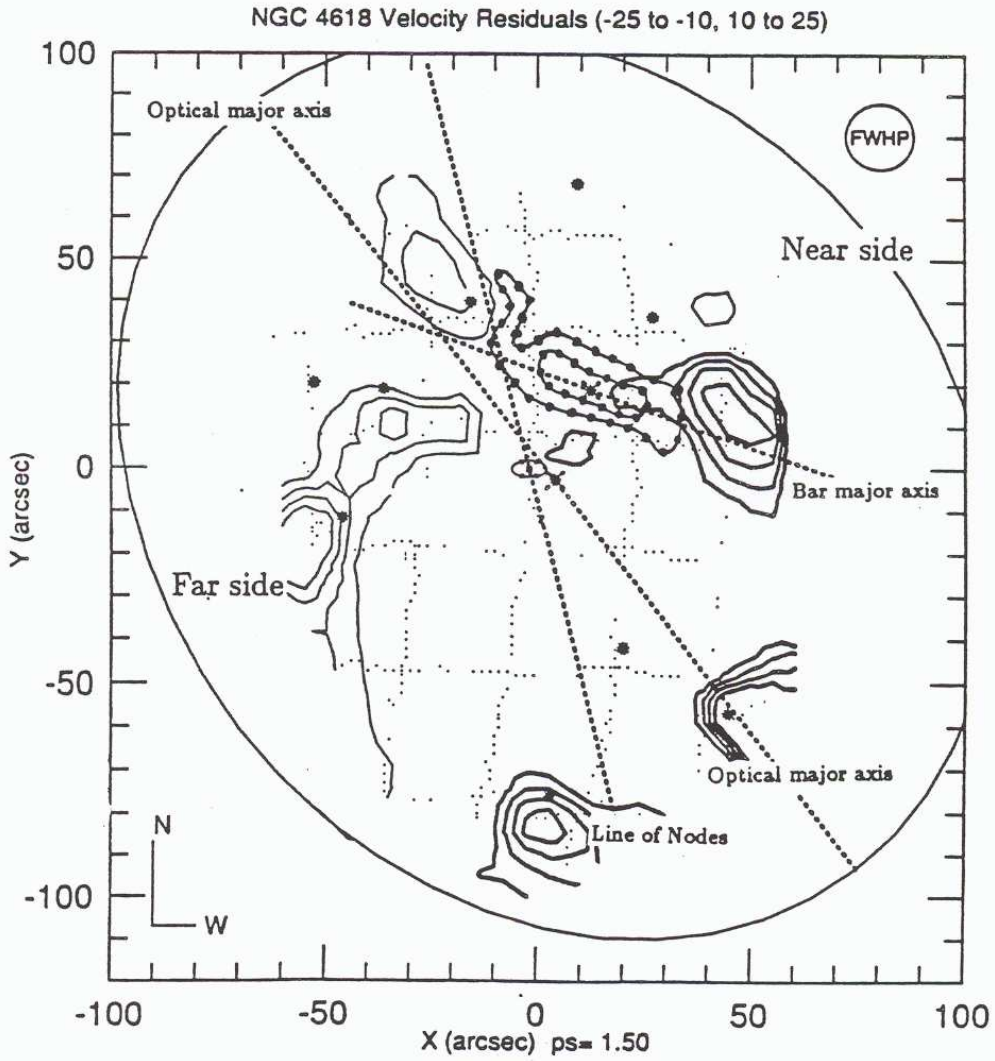

Hα Kinematics in NGC 4618 (Odewahn 1990)

Substantial departures from circular motion in m=1 arms, OFTEN accompanied by large OB associations (SSC?)

Spatially resolved NIRSpec and MIRI integral-field spectra of distant galaxies when compared to the quantitative structure from NIRCam Fourier Decompositions, will directly trace the physical causes of locally enhanced star-formation: infall, bulk velocities in excess of regular rotation, etc.

(5) Details on JWST image simulations:

- All based on HST/WFPC2 F300W images from the HST mid-UV survey of nearby galaxies (Windhorst et al. 2002,ApJ Suppl. 143, 113).
- WMAP COSMOLOGY: H_0=71 km/s/Mpc, Ω_m=0.27, Ω_Λ=0.73.
- INSTRUMENT: 6.0 m effective aperture, diffraction limited at $\lambda \gtrsim 2.0\mu$m, JWST/NIRCam, 0.″034/pix, read-noise=5.0 e^-, dark-current=0.02 e^-/s, NEP-Sky(1.6 μm)=21.7 mag/($''^2$) in L2, Zodi spectrum, t_{exp}=4×900s.

Row	Telesc.	Redshift	λ (μm)	FWHM ($''$)
1	HST	z∼0	0.293μm	0.″04
	JWST	z=1.0	0.586μm	0.″084
	JWST	z=2.0	0.879μm	0.″084
2	JWST	z=3.0	1.17 μm	0.″084
	JWST	z=5.0	1.76 μm	0.″084
	JWST	z=7.0	2.34 μm	0.″098
3	JWST	z=09.0	2.93 μm	0.″122
	JWST	z=12.0	3.81 μm	0.″160
	JWST	z=15.0	4.69 μm	0.″197

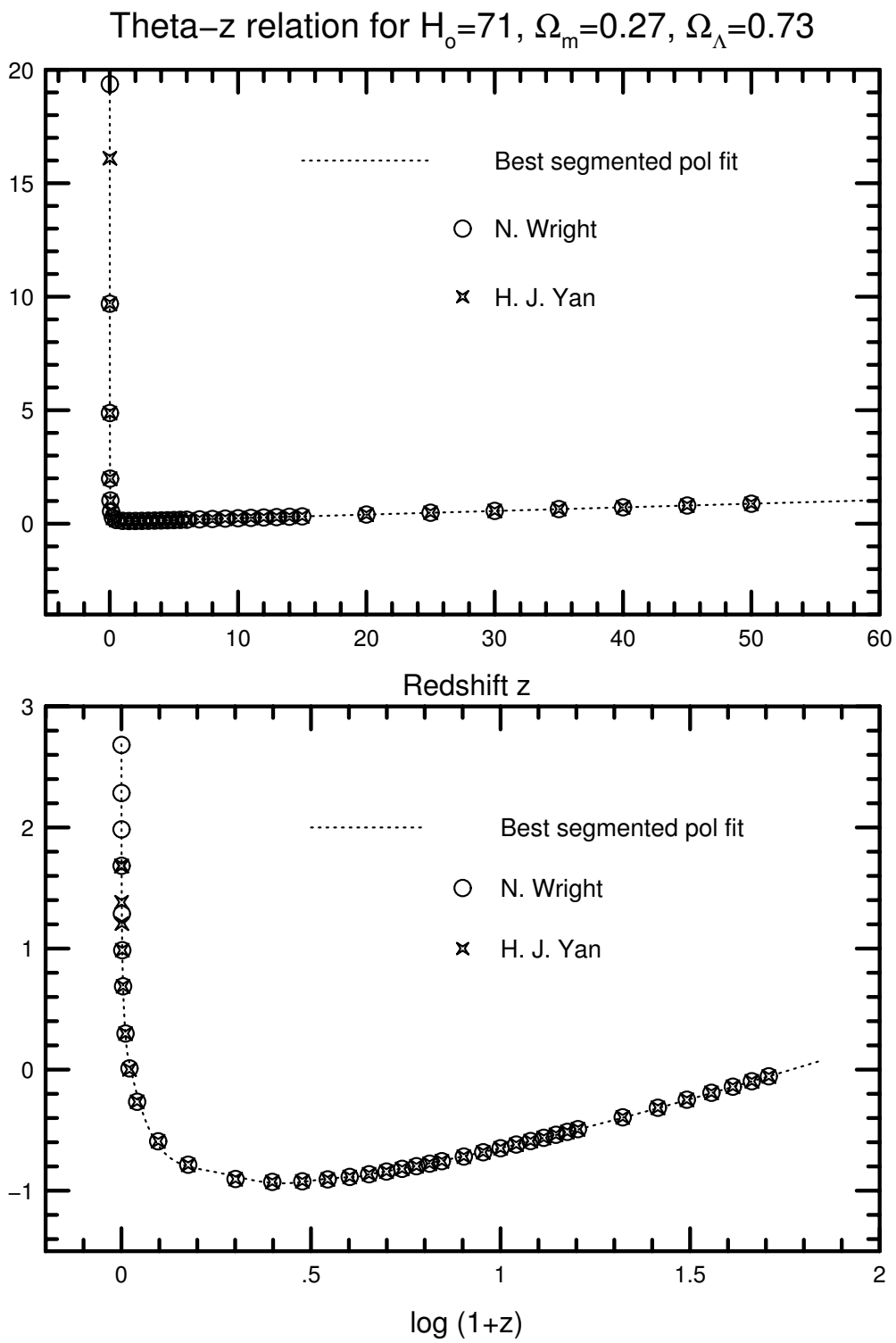

Angular size vs. redshift relation in a Lambda dominated cosmology of H_0 =71 $km\ s^{-1}\ Mpc^{-1}$, Ω_m=0.27, Ω_Λ=0.73.

In the top panel the relation is nearly linear in 1/z for z$\lesssim$0.05 (the small angle approximation) and linear in z for z$\gtrsim$3 (the Lambda dominated universe).

All curvature occurs in the range 0.05$\lesssim$z$\lesssim$3, which is coded up in the IRAF script that does the JWST simulations.

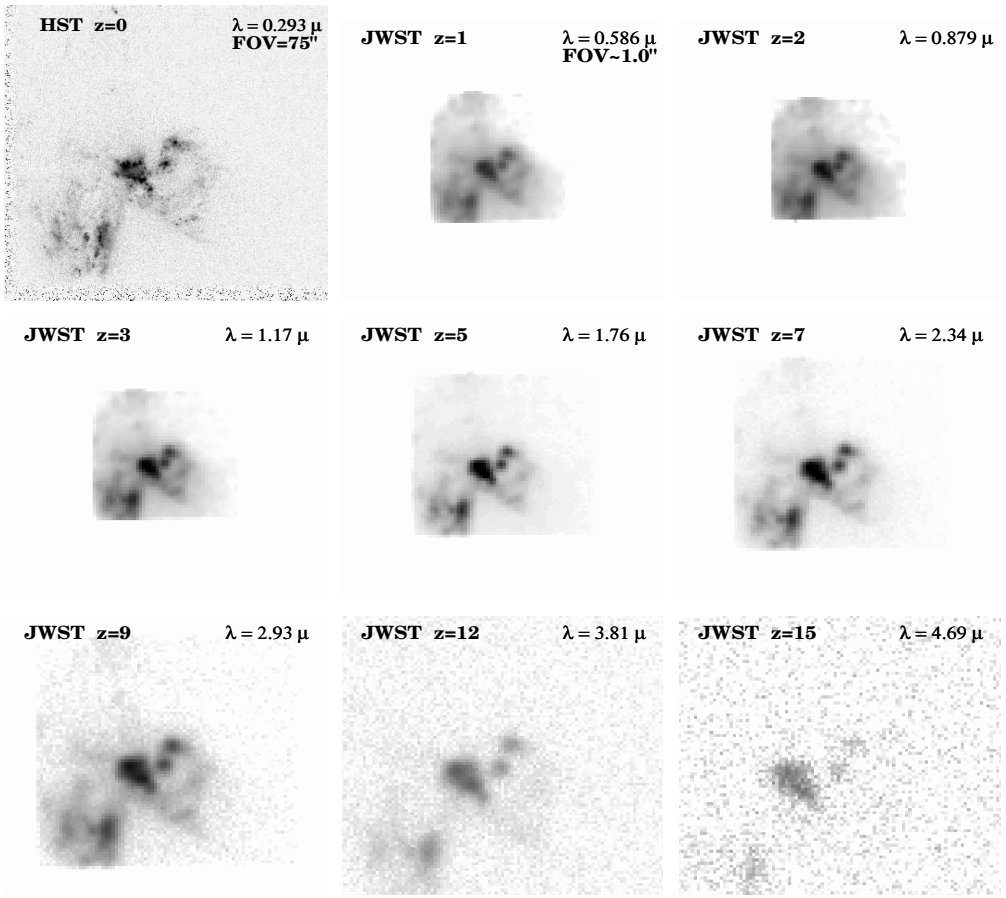

Fig. 4.06.a. JWST simulations based on HST/WFPC2 F300W images of the merger UGC06471-2 (z=0.0104). Note that the two unresolved star-bursting knots in the center remain visible until z∼12, beyond which the SB-dimming also kills their flux. This is the NOMINAL JWST [= (GOALS+REQUIREMENTS)/2].

ASSUMPTIONS: COSMOLOGY: H_0=71 km/s/Mpc, Ω_m=0.27, and Ω_Λ=0.73.

INSTRUMENT: 6.0 m effective aperture, JWST/NIRCam, 0.034″ /pix, RN=5.0 e^-, Dark=0.020 e^-/sec, NEP H-band Sky=21.7 mag/arcsec^2 in L2, Zodiacal spectrum, t_{exp}=1.0 hrs, read-out every 900 sec ("NOMINAL").

Row 1: z=0.0 (HST λ=0.293μm, FWHM=0.04″), z=1.0 (JWST λ=0.586μm, FWHM=0.084″), and z=2.0 (JWST λ=0.879μm, FWHM=0.084″). **Row 2:** z=3.0 (JWST λ=1.17μm, FWHM=0.084″), z=5.0 (JWST λ=1.76μm, FWHM=0.084″), and z=7.0 (JWST λ=2.34μm, FWHM=0.098″). **Row 3:** z=9.0 (JWST λ=2.93μm, FWHM=0.122″), z=12.0 (JWST λ=3.81μm, FWHM=0.160″), and z=15.0 (JWST λ=4.69μm, FWHM=0.197″)

The galaxy merger UGC06471-2 (z=0.0104) is a major and very dusty collision of two massive disk galaxies.

It shows two bright unresolved star-bursting knots to the upper-right of the center, which remain visible until z≃12, beyond which the cosmic SB-dimming kills their flux. These are more typical for the small star-forming objects expected at z≃10–15.

This is the NOMINAL JWST = (GOALS+REQUIREMENTS)/2.

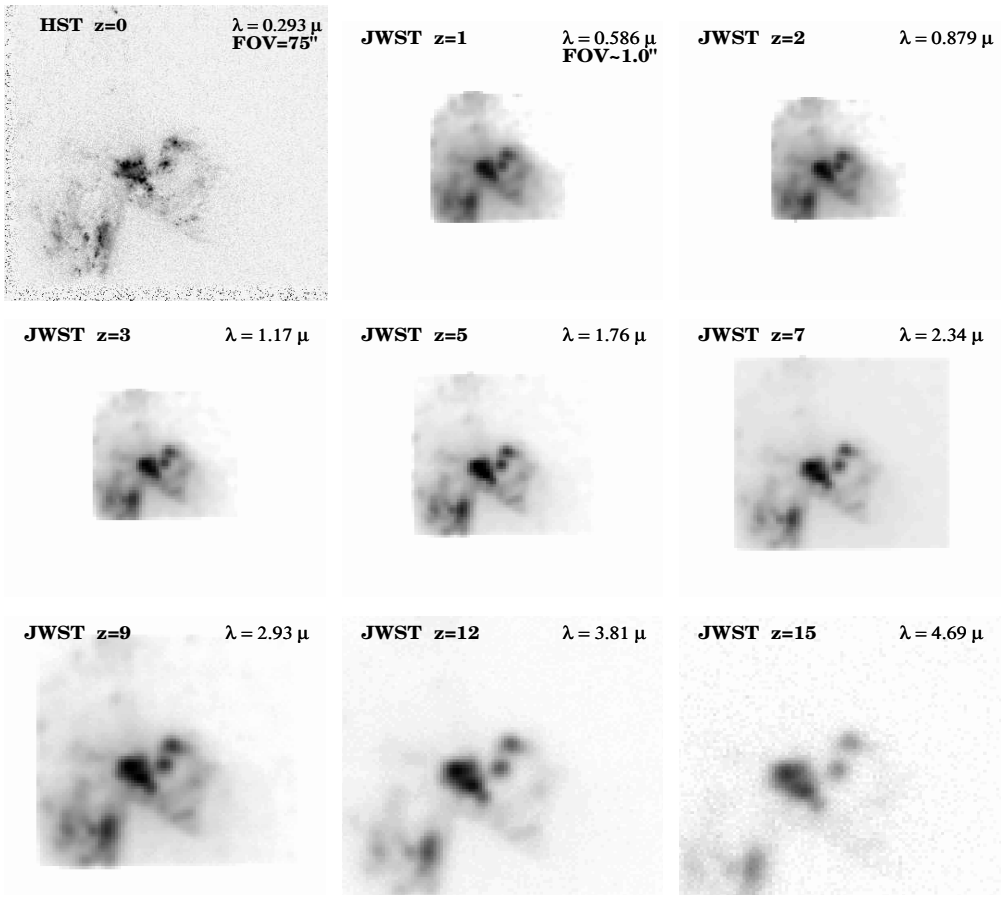

Fig. 4.06.c. JWST simulations based on HST/WFPC2 F300W images of the merger UGC06471-2 (z=0.0104). This is the BEST CASE JWST [meeting all GOALS, and t_{exp}=100 hrs]. The object is recognizable to z≃15.

ASSUMPTIONS: COSMOLOGY: H_0=71 km/s/Mpc, Ω_m=0.27, and Ω_Λ=0.73.

INSTRUMENT: 6.0 m effective aperture, JWST/NIR camera, 0.034″ /pix, RN=3.0 e^-, Dark=0.010 e^-/sec, NEP H-band Sky=21.7 mag/arcsec^2 in L2, Zodi spectrum, t_{exp}=100.0 hrs, read-out every 900 sec ("GOALS").

Row 1: z=0.0 (HST λ=0.293μm, FWHM=0.04″), z=1.0 (JWST λ=0.586μm, FWHM=0.084″), and z=2.0 (JWST λ=0.879μm, FWHM=0.084″). **Row 2:** z=3.0 (JWST λ=1.17μm, FWHM=0.084″), z=5.0 (JWST λ=1.76μm, FWHM=0.084″), and z=7.0 (JWST λ=2.34μm, FWHM=0.098″). **Row 3:** z=9.0 (JWST λ=2.93μm, FWHM=0.122″), z=12.0 (JWST λ=3.81μm, FWHM=0.160″), and z=15.0 (JWST λ=4.69μm, FWHM=0.197″)

The galaxy merger UGC06471-2 (z=0.0104).

This is the BEST CASE JWST. It assumes that all GOALS are met, and that t_{exp}=100 hrs. The whole object (including the two star-forming knots) is recognizable to z≃15.

This does not imply that observing galaxies at z=15 with JWST will be easy. On the contrary, since galaxies formed through hierarchical merging, many objects at z≃10–15 will be 10^1–$10^4\times$ less luminous, requiring to push JWST to its limits.

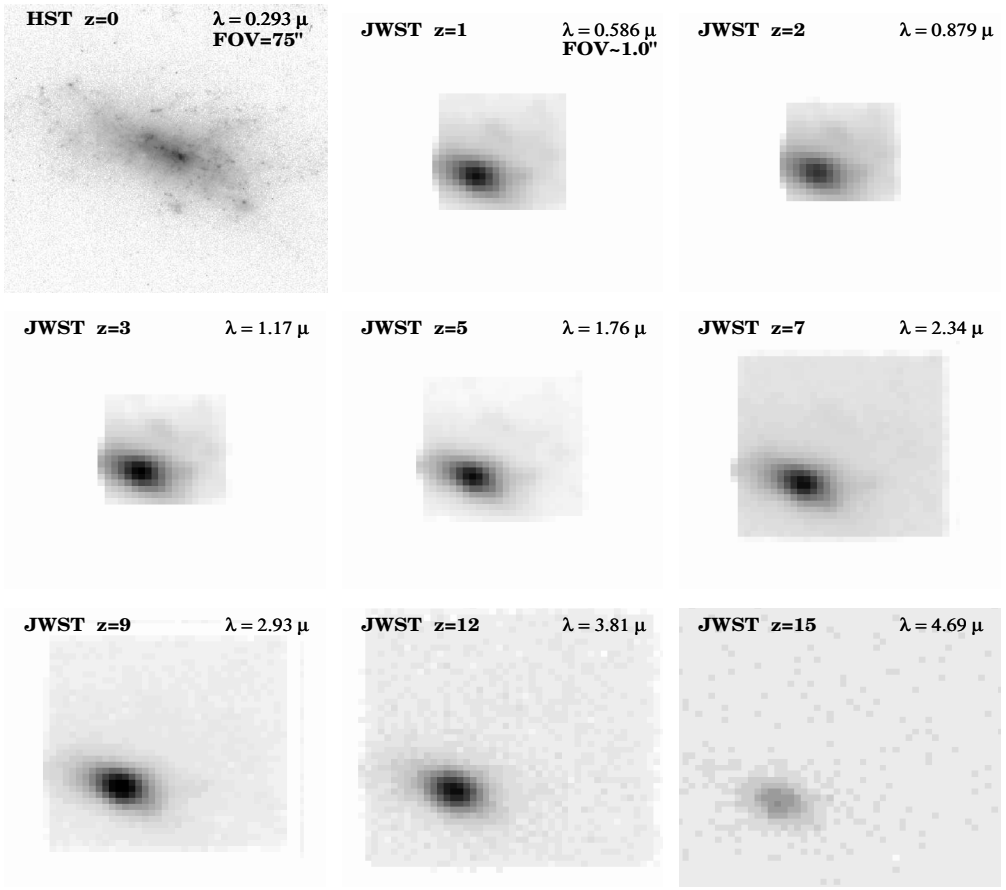

Fig. 4.01. JWST simulations based on HST/WFPC2 F300W images of the dwarf irregular NGC1140 (z=0.0050). This compact high SB object would be visible to z≃15, but hard to classify at all z≥1.

ASSUMPTIONS: COSMOLOGY: H_0=71 km/s/Mpc, Ω_m=0.27, and Ω_Λ=0.73.

INSTRUMENT: 6.0 m effective aperture, JWST/NIRCam, 0.034″ /pix, RN=5.0 e^-, Dark=0.020 e^-/sec, NEP H-band Sky=21.7 mag/arcsec^2 in L2, Zodiacal spectrum, t_{exp}=1.0 hrs, read-out every 900 sec.

Row 1: z=0.0 (HST λ=0.293μm, FWHM=0.04″), z=1.0 (JWST λ=0.586μm, FWHM=0.084″), and z=2.0 (JWST λ=0.879μm, FWHM=0.084″).

Row 2: z=3.0 (JWST λ=1.17μm, FWHM=0.084″), z=5.0 (JWST λ=1.76μm, FWHM=0.084″), and z=7.0 (JWST λ=2.34μm, FWHM=0.098″).

Row 3: z=9.0 (JWST λ=2.93μm, FWHM=0.122″), z=12.0 (JWST λ=3.81μm, FWHM=0.160″), and z=15.0 (JWST λ=4.69μm, FWHM=0.197″)

The compact high-SB dwarf irregular galaxy NGC1140 (z=0.0050).

With JWST, this object would be visible to z≃15, but it will be hard to classify at all redshifts z≥1.

Note that the object indeed reaches a minimum angular size at z≃1.7.

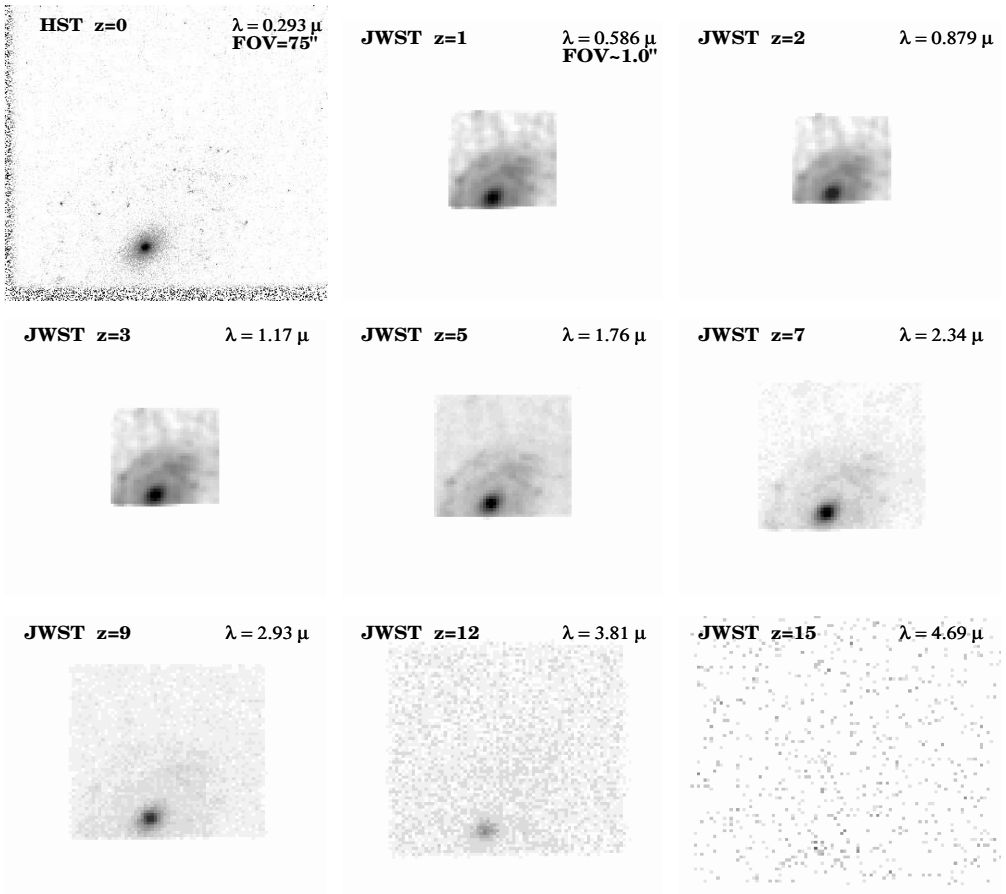

Fig. 4.02. JWST simulations based on HST/WFPC2 F300W images of the mid-type spiral NGC2551 (0.0078). Such an object would be visible to z≃10, but only recognizable to z≃7.

ASSUMPTIONS: COSMOLOGY: H_0=71 km/s/Mpc, Ω_m=0.27, and Ω_Λ=0.73.

INSTRUMENT: 6.0 m effective aperture, JWST/NIRCam, 0.034″ /pix, RN=5.0 e^-, Dark=0.020 e^-/sec, NEP H-band Sky=21.7 mag/arcsec^2 in L2, Zodiacal spectrum, t_{exp}=1.0 hrs, read-out every 900 sec.

Row 1: z=0.0 (HST λ=0.293μm, FWHM=0.04″), z=1.0 (JWST λ=0.586μm, FWHM=0.084″), and z=2.0 (JWST λ=0.879μm, FWHM=0.084″).

Row 2: z=3.0 (JWST λ=1.17μm, FWHM=0.084″), z=5.0 (JWST λ=1.76μm, FWHM=0.084″), and z=7.0 (JWST λ=2.34μm, FWHM=0.098″).

Row 3: z=9.0 (JWST λ=2.93μm, FWHM=0.122″), z=12.0 (JWST λ=3.81μm, FWHM=0.160″), and z=15.0 (JWST λ=4.69μm, FWHM=0.197″)

The mid-type spiral NGC2551 (z=0.0078) would be visible out to z≃10, but only recognizable out to z≃7.

Its disk is in principle visible to z$\gtrsim$5–7. Hence, if such objects are not seen by JWST at z$\lesssim$3, then disks likely form at z$\lesssim$3.

With HST we have seen glimpses of this, but with JWST these will become robust conclusions.

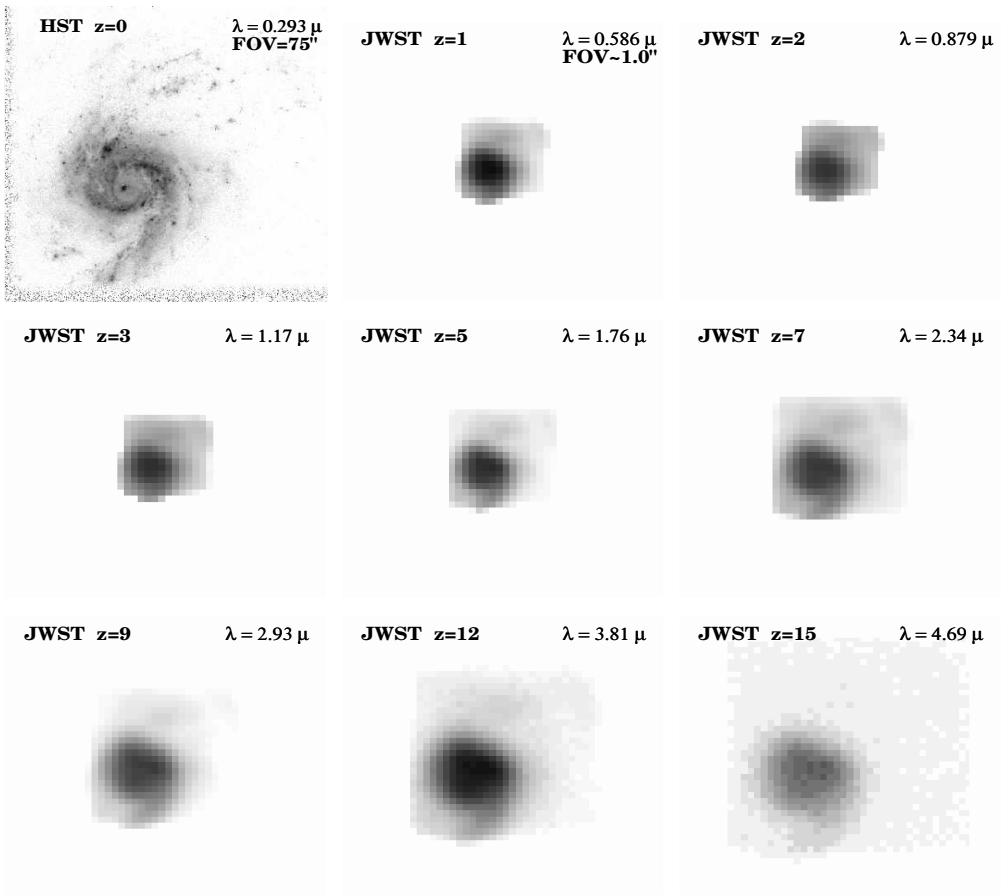

Fig. 4.03. JWST simulations based on HST/WFPC2 F300W images of the high-SB starbursting dwarf spiral galaxy NGC3310 (0.0033). The minimum in the Θ-z relation at z$\simeq$1.7 and the JWST diffraction limit at $\lambda \geq 2.2\mu$m — combined with the object's very high rest-frame UV SB — conspire to improve the effective JWST resolution on the mid-UV morphology of this object from z$\simeq$2 to z$\simeq$7.

ASSUMPTIONS: COSMOLOGY: H_0=71 km/s/Mpc, Ω_m=0.27, and Ω_Λ=0.73. INSTRUMENT: 6.0 m effective aperture, JWST/NIRCam, 0.034″ /pix, RN=5.0 e^-, Dark=0.020 e^-/sec, NEP H-band Sky=21.7 mag/arcsec^2 in L2, Zodiacal spectrum, t_{exp}=1.0 hrs, read-out every 900 sec.

Row 1: z=0.0 (HST λ=0.293μm, FWHM=0.04″), z=1.0 (JWST λ=0.586μm, FWHM=0.084″), and z=2.0 (JWST λ=0.879μm, FWHM=0.084″). **Row 2:** z=3.0 (JWST λ=1.17μm, FWHM=0.084″), z=5.0 (JWST λ=1.76μm, FWHM=0.084″), and z=7.0 (JWST λ=2.34μm, FWHM=0.098″). **Row 3:** z=9.0 (JWST λ=2.93μm, FWHM=0.122″), z=12.0 (JWST λ=3.81μm, FWHM=0.160″), and z=15.0 (JWST λ=4.69μm, FWHM=0.197″)

The very high-SB, compact starbursting dwarf spiral galaxy NGC3310 (z=0.0033).

The minimum in the Θ-z relation at z$\simeq$1.7 and the JWST diffraction limit at $\lambda \geq 2.2\ \mu$m — combined with the object's very high rest-frame UV-SB — conspire to improve the effective JWST resolution on the mid-UV morphology of this object from z$\simeq$2 to z$\simeq$7.

A rather exceptional case of where nasty cosmology doesn't appear to cost you prohibitive sensitivity, but gains you resolution!

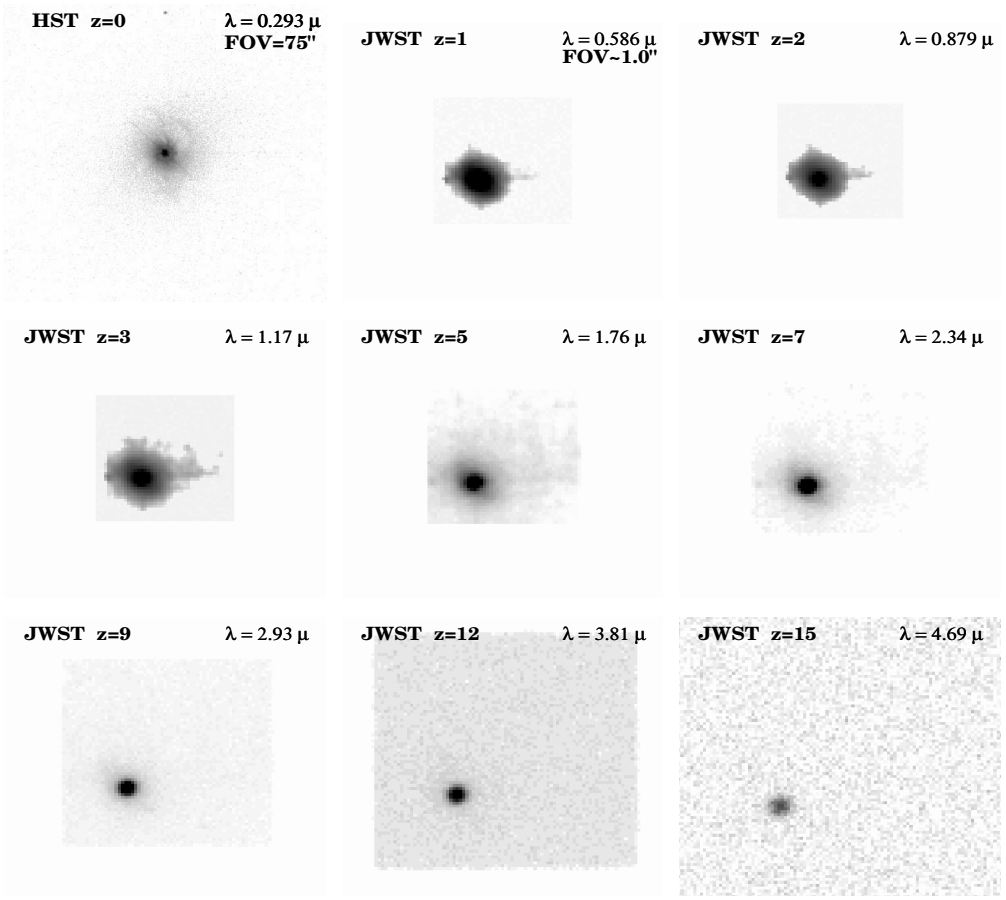

Fig. 4.04. JWST simulations based on HST/WFPC2 F300W images of the Seyfert galaxy NGC3516 (0.0088). Note that the faint nebulosity surrounding the AGN in the mid-UV at z=0 essentially disappears at z≥7, so that at high redshifts such objects would look like a pure AGN.

ASSUMPTIONS: COSMOLOGY: H_0=71 km/s/Mpc, Ω_m=0.27, and Ω_Λ=0.73.

INSTRUMENT: 6.0 m effective aperture, JWST/NIRCam, 0.034″ /pix, RN=5.0 e^-, Dark=0.020 e^-/sec, NEP H-band Sky=21.7 mag/arcsec^2 in L2, Zodiacal spectrum, t_{exp}=1.0 hrs, read-out every 900 sec.

Row 1: z=0.0 (HST λ=0.293μm, FWHM=0.04″), z=1.0 (JWST λ=0.586μm, FWHM=0.084″), and z=2.0 (JWST λ=0.879μm, FWHM=0.084″). **Row 2:** z=3.0 (JWST λ=1.17μm, FWHM=0.084″), z=5.0 (JWST λ=1.76μm, FWHM=0.084″), and z=7.0 (JWST λ=2.34μm, FWHM=0.098″). **Row 3:** z=9.0 (JWST λ=2.93μm, FWHM=0.122″), z=12.0 (JWST λ=3.81μm, FWHM=0.160″), and z=15.0 (JWST λ=4.69μm, FWHM=0.197″)

The Seyfert galaxy NGC3516 (z=0.0088) has a faint nebulosity surrounding its AGN in the mid-UV, while at longer wavelengths the surrounding elliptical galaxy is present (not shown here).

The nebulosity surrounding the AGN is essentially SB-dimmed away at z≥7, so that at high redshifts these objects would look like purely stellar objects ("quasars").

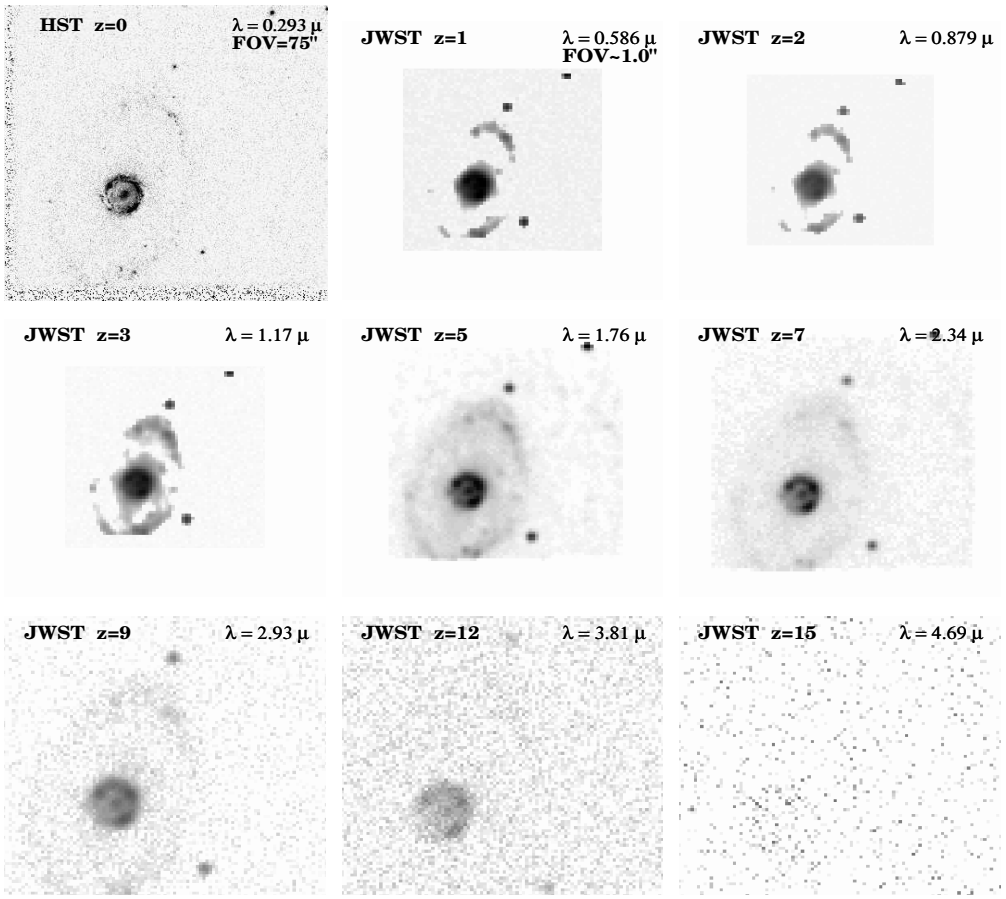

Fig. 4.05. JWST simulations based on HST/WFPC2 F300W images of the barred ring galaxy NGC6782 (0.0125). Note again that for z≃2–7, the effective resolution on the bright star-forming ring improves with increasing redshift, until the $(1+z)^4$-dimming completely kills it for z≳10.

ASSUMPTIONS: COSMOLOGY: H_0=71 km/s/Mpc, Ω_m=0.27, and Ω_Λ=0.73.

INSTRUMENT: 6.0 m effective aperture, JWST/NIRCam, 0.034″ /pix, RN=5.0 e^-, Dark=0.020 e^-/sec, NEP H-band Sky=21.7 mag/arcsec^2 in L2, Zodiacal spectrum, t_{exp}=1.0 hrs, read-out every 900 sec.

Row 1: z=0.0 (HST λ=0.293μm, FWHM=0.04″), z=1.0 (JWST λ=0.586μm, FWHM=0.084″), and z=2.0 (JWST λ=0.879μm, FWHM=0.084″). **Row 2:** z=3.0 (JWST λ=1.17μm, FWHM=0.084″), z=5.0 (JWST λ=1.76μm, FWHM=0.084″), and z=7.0 (JWST λ=2.34μm, FWHM=0.098″). **Row 3:** z=9.0 (JWST λ=2.93μm, FWHM=0.122″), z=12.0 (JWST λ=3.81μm, FWHM=0.160″), and z=15.0 (JWST λ=4.69μm, FWHM=0.197″)

The barred ring galaxy NGC6782 (0.0125) shows that at z≃2 to z≃7, the effective resolution on its high-SB bright star-forming ring improves with increasing redshift, until the $(1+z)^4$-dimming completely kills it for z≳10–12.

Another good case showing why cosmology is not "WYSIWYG".

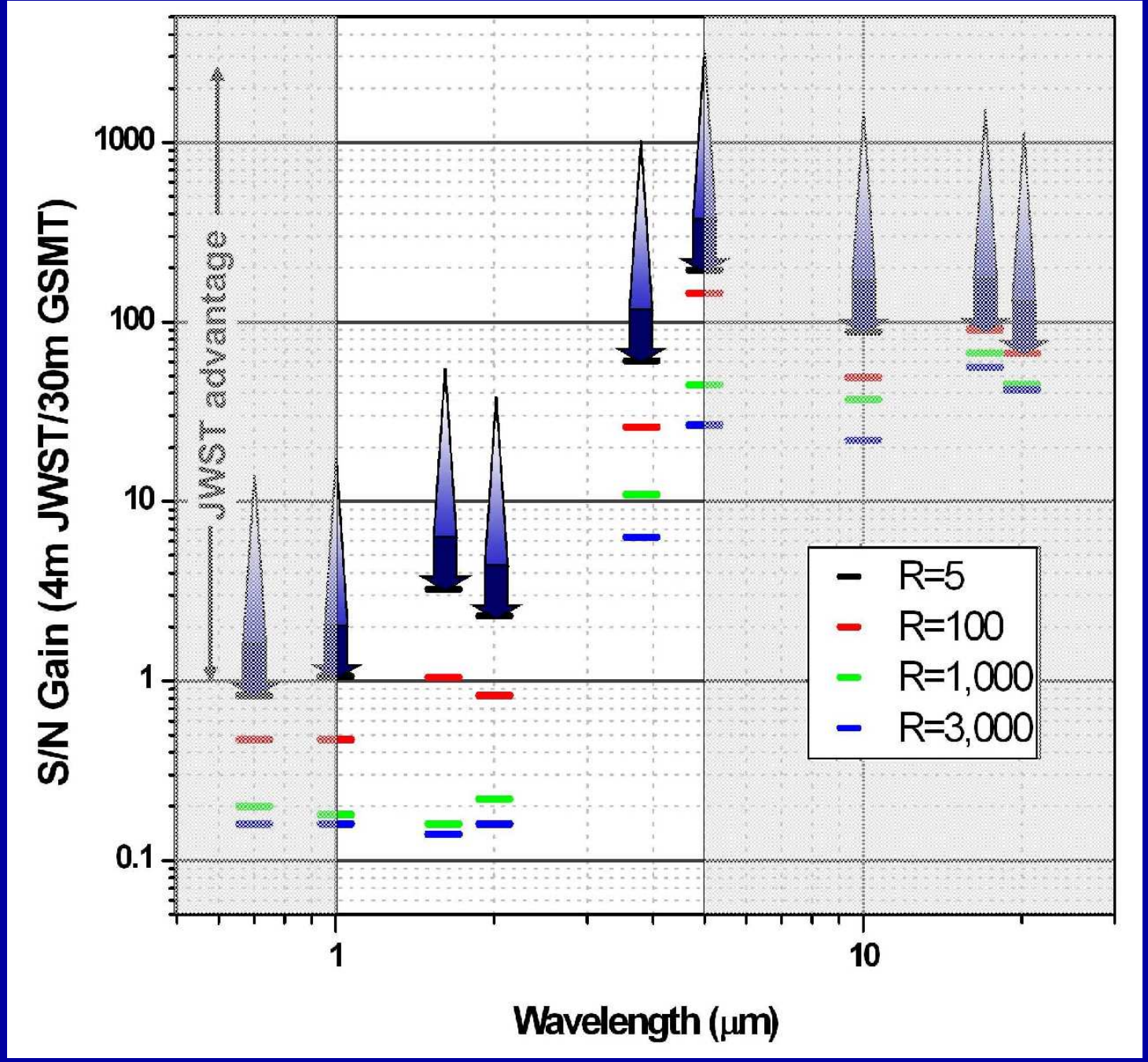

Conclusion: JWST must not be descoped to a 4 meter Arrows indicate:

Top: 6m JWST/Keck; Middle: 6m JWST/30m gb; Bottom: 4m JWST/30m gb

(7) Lessons to be learned from new NASA Vision

- In the New NASA Vision: Moon/Mars/Beyond, we must keep in mind:

Earth/Moon/Mars/Beyond $\simeq 10^{51}/10^{49}/10^{50}/10^{80}$ baryons.

(and 96% of the Universe's energy density is not listed here!)

Funding doesn't have be proportional to these numbers! :)

But, for this new Vision to succeed, we must not forget to:

- (1) Build a balanced program that covers all relevant areas.
- (2) Build strong interdisciplinary ties between fields.
- (3) Use L2 and the Moon to deploy the next generation of telescopes.